

## ABSTRACT

Title of Dissertation: MESOPOROUS SILICA NANOPARTICLES AS DRUG DELIVERY SYSTEMS AND DIAGNOSTIC TOOLS

Matthew Thomas Hurley, Doctor of Philosophy, 2012

Dissertation directed by: Professor Philip DeShong  
Department of Chemistry and Biochemistry

Micro- and nano-scale silica materials have recently gained attention due to their potential as biosensors, site-specific drug delivery systems and diagnostic tools. Accordingly, examples of the preparation and use of silica materials for such applications are highlighted throughout this dissertation.

A significant portion of developing materials used for targeting, detection, or sensing applications is functionalizing the surface of the material with biomolecules (i.e. proteins, nucleotides, carbohydrates) that function as targeting or receptor moieties. N-linked pentenyl glycoside derivatives, prepared via a modified Staudinger ligation method, proved to be key intermediates in developing a methodology to efficiently prepare carbohydrate derivatives capable of functionalizing a variety of different materials. Glucosyl and lactosyl siloxane derivatives, synthesized from the hydrosilation of the corresponding pentenyl glycoside intermediate, were used to prepare glucose- and lactose-functionalized evanescent wave fiber Bragg gratings. The carbohydrate-

functionalized fibers were subsequently used to detect the specific binding of lectins to the carbohydrates attached to the surface of the fiber, demonstrating their potential as biosensors. In addition, olefin cross metathesis was used to couple N-linked pentenyl glycoside intermediates with terminal alkene derivatives containing moieties used to functionalize a range of inorganic material, thus yielding glycoconjugates capable of functionalizing material of various composition. The advantage of this synthetic strategy is the ability to create a series of carbohydrate derivatives capable of functionalizing a variety of different material from a common N-linked pentenyl glycoside intermediate.

Mesoporous silica nanoparticles (MSN) have potential as drug delivery and controlled release devices due to their high surface area and large payload capacity. The effect of surface charge and pH on the release of the fluorescent dye rhodamine 6G from MSN prepared via an aerosol methodology has been studied. Release profiles of rhodamine 6G from bare and amine-coated MSN at pH 5.0 and 7.4 are very different and demonstrate that electrostatic interactions between entrapped rhodamine 6G molecules and the charged surface of the MSN have a significant effect on release kinetics. Release of rhodamine 6G from amine-coated MSN can be fit to a single exponential function, while release from bare MSN can be fit to a double exponential function—indicating that the release of rhodamine 6G from bare MSN is a two-phase process. In addition, it was determined that MSN need to be sonicated in dye solution to maximize their loading capacity.

Fluorescent silica nanoparticles (FSN) are being studied for their potential in diagnostic imaging techniques and immunoassays. Fluorescent silica nanoparticles were prepared by incorporating a hydrophobically modified dye into a mesoporous silica

nanoparticle synthesis procedure. The MSN-based FSN do not leach dye and have strong, stable fluorescence that is 5 times more intense than that of CdSe quantum dots. For diagnostic applications, a method to selectively and covalently bind antibodies to the surface of the FSN was devised. It was found that the triblock copolymer, Pluronic F127, is effective in preventing nonspecific binding of proteins to FSN. Antibodies were selectively and covalently attached to FSN that were functionalized with a mixed PEG/epoxide coating in the presence of Pluronic F127.

MESOPOROUS SILICA NANOPARTICLES AS DRUG DELIVERY SYSTEMS AND  
DIAGNOSTIC TOOLS

By

Matthew Thomas Hurley

Dissertation submitted to the Faculty of the Graduate School of the  
University of Maryland, College Park in partial fulfillment  
of the requirements for the degree of  
Doctor of Philosophy  
2012

Advisory Committee:

Professor Philip DeShong, Chair

Professor Daniel Falvey

Professor Sang Bok Lee

Professor David Mosser

Professor Steven Rokita



© Copyright by  
Matthew T. Hurley  
2012

## DEDICATIONS

To my grandmother, Hazel Hofe, for reminding me to be patient and that God is good.

## ACKNOWLEDGEMENTS

I take this opportunity to recognize and thank the individuals that have been instrumental to my success throughout my graduate career.

I thank my mentor and advisor, Dr. Philip DeShong, for his wisdom and guidance that have shaped me into the person and chemist I am today. I am certain the skills and knowledge that I gained while under his tutelage will help me excel in my future professional endeavors. Dr. DeShong is an exceptional teacher and the best motivator I have ever met. I am lucky to have had the opportunity to conduct my graduate research under his supervision.

I thank the past and current DeShong lab group members for sharing their knowledge and friendship. I especially thank Juhee Park for guiding me through the early stages of my graduate career.

I thank my family and friends for their continuous love, support, and encouragement. I especially thank my parents for helping to instilling within me the self-confidence and work ethic necessary to complete this task.

I thank the members and congregation of University Baptist Church for their prayers and support. UBC is a blessing to my life and an answer to my father's prayers.

Finally, I thank God for his love and the strength I have found through Him. "I have brought you glory on earth by completing the work you gave me to do."—John 17:4

## TABLE OF CONTENTS

List of Tables.....	vii
List of Figures .....	viii
List of Abbreviations.....	xi
Chapter 1: Surface Functionalization and the Preparation of Protein- and Carbohydrate- Functionalized Materials.....	1
Introduction .....	1
Surface Functionalization.....	1
Protein-Functionalized Materials .....	4
Carbohydrate-Functionalized Materials.....	8
Results and Discussion.....	11
Preparation of Carbohydrate-Siloxane Derivatives via Hydrosilation.....	11
Preparation of Carbohydrate Derivatives via Grubbs' Cross-Metathesis .....	17
Attachment of Reducing Sugars to Amine-Functionalized Surfaces via Reductive Amination.....	22
Conclusions .....	24
Experimental .....	25
General .....	25
Synthesis of Compounds .....	26
Preparation of Glucose-Functionalized Glass .....	40
XPS Analysis of Bare and Glucose-Functionalized Glass Slides .....	40
Preparation of Glucose-Functionalized Bragg Fiber.....	41
Preparation of APTES-Functionalized Fluorescent Silica Nanoparticles.....	41

Preparation of Lactose-Functionalized Fluorescent Silica Nanoparticles via Reductive Amination.....	42
Phenol/Sulfuric Acid Colorimetric Assay.....	42
Acknowledgements .....	42
References .....	43
Chapter 2: Mesoporous Silica as Controlled Release Devices: Synthesis, Characterization, and pH-Sensitive Release.....	50
Introduction .....	50
Preparation of Mesoporous Silica .....	51
Mesoporous Silica Nanoparticles.....	55
MSN as Controlled Release, Drug Delivery Systems.....	56
Results and Discussion.....	58
Characterization of MSN .....	59
Loading and Release Studies.....	62
Conclusions .....	72
Experimental .....	73
General .....	73
Fabrication of MSN.....	74
Gravity Filtration.....	75
Rhodamine 6G Loading .....	75
MSN Functionalization .....	75
Rhodamine 6G Release Quantification using UV-Vis Spectroscopy .....	76
Mathematical Modeling of Release from MSN .....	76
Acknowledgements .....	77

References .....	77
Chapter 3: MSN-Based Fluorescent Silica Nanoparticles for Application in Diagnostics .....	85
Introduction .....	85
Fluorescent Silica Nanoparticle Synthesis .....	86
Results and Discussion .....	87
MSN-Based FSN Synthesis .....	87
Fluorescence Microscopy Analysis of FSN .....	91
Dye Release Experiments .....	92
Protein Functionalization of MSN-Based FSN .....	93
Conclusions .....	99
Experimental .....	100
General .....	100
MSN-Based Fluorescent Silica Nanoparticle Preparation .....	100
Fluorescence Imaging .....	101
PEG Functionalized FSN .....	101
PEG/Epoxide Functionalized FSN .....	102
Conjugation of Goat Anti-Gonococcus IgG Antibody to PEG/Epoxide Functionalized FSN .....	102
BCA Assay Protocol .....	103
Acknowledgements .....	104
References .....	104
List of References by Chapter .....	109

## LIST OF TABLES

### Chapter 1

Table 1: List of materials and the functional groups used to functionalize their surface .....	2
Table 2: Hydrosilation results .....	13
Table 3: Olefin cross-metathesis results.....	20

### Chapter 2

Table 4: Mesoporous silica materials.....	55
Table 5: Zeta potential measurements of APTES-coated and bare MSN at pH 7.4 and 5.0 ..	62
Table 6: Fit parameters for release of rhodamine 6G from sonicated and unsonicated MSN at pH 7.4 .....	64
Table 7: Two-phase fit parameters for release of rhodamine 6G from bare MSN .....	67
Table 8: One-phase fit parameters and half-life for release of rhodamine 6G from APTES-coated MSN .....	71

## LIST OF FIGURES

### Chapter 1

Figure 1: Schematic representation of monolayer formation of thiols on gold, siloxanes on silica, and organophosphonates on titanium oxide .....	3
Figure 2: Examples of common bifunctional linker molecules .....	5
Figure 3: Common methods used to covalently attach proteins to functionalized surfaces ...	7
Figure 4: Attachment of unmodified carbohydrates to a hydrazine-functionalized surface ...	8
Figure 5: Popular glycosylation techniques .....	10
Figure 6: General Staudinger ligation method used by DeShong to prepare glycoconjugates .....	11
Figure 7: Synthesis of glucose-siloxane conjugate .....	12
Figure 8: Synthesis of mannose-alkene conjugate .....	13
Figure 9: C 1s and N 1s high-resolution X-ray photoelectron spectra of the bare, unfunctionalized glass slide and the glucose-functionalized glass slide .....	14
Figure 10: Preparation of a glucose-functionalized Bragg fiber .....	16
Figure 11: General olefin cross-metathesis reaction .....	17
Figure 12: Popular Grubbs' metathesis catalysts .....	18
Figure 13: Cross-coupling partners used to prepare glycoconjugates.....	19
Figure 14: Olefin cross-metathesis of N-linked pentenyl glycoconjugates .....	19
Figure 15: Preparation of lactose-functionalized fluorescent silica nanoparticles via reductive amination .....	23
Figure 16: Absorbance spectra from the phenol/sulfuric acid colorimetric assay of lactose-functionalized fluorescent silica nanoparticles, and sucrose treated, amine-functionalized fluorescent silica nanoparticles.....	24



## Chapter 2

Figure 17: Templated MCM-41 synthesis .....	54
Figure 18: Schematic representation of a pH driven controlled release device .....	59
Figure 19: TEM images of MSN used in release studies .....	60
Figure 20: Nitrogen adsorption/desorption BET isotherms of MSN .....	61
Figure 21: Release profiles of rhodamine 6G from MSN with and without sonication .....	63
Figure 22: Schematic representation of the effect of sonication on MSN loading. ....	64
Figure 23: Release profiles of rhodamine 6G from bare MSN at pH 7.4 and 5.0 .....	66
Figure 24: Schematic representation of release of rhodamine 6G from bare MSN at pH 7.4 and 5.0 .....	67
Figure 25: Release profiles of rhodamine 6G from amine-coated MSN at pH 7.4 and 5.0 ....	70
Figure 26: Schematic representation of release of rhodamine 6G from APTES-coated MSN at pH 7.4 and 5.0 .....	71

## Chapter 3

Figure 27: Common strategies used to prepare fluorescent silica nanoparticles .....	87
Figure 28: Schematic illustration of MCM-41 type mesoporous silica nanoparticle synthesis.....	89
Figure 29: Schematic illustration of MSN-based fluorescent silica nanoparticle synthesis ...	89
Figure 30: Structure of the hydrophobically modified rhodamine B derivative used to prepare FSN .....	90
Figure 31: TEM images of prepared MSN-based FSN.....	90
Figure 32: Fluorescent, z-scan confocal images of MSN-based FSN.....	91
Figure 33: Comparison of fluorescence intensity of MSN-based FSN and CdSe quantum dots.....	92
Figure 34: Absorbance spectra from the BCA assay of mouse anti-goat IgG functionalized FSN prepared using Guo's method.....	94

Figure 35: Absorbance spectra from the BCA assay of BSA treated PEGylated FSN with no additional PEG additive, Tween 20, and Pluronic F127.....	96
Figure 36: Absorbance spectra from the BCA assay of goat anti-listeria IgG antibody treated PEGylated FSN with and without Pluronic F127 .....	96
Figure 37: Strategy used to prepare IgG-functionalized FSN.....	98
Figure 38: Proposed mixed-multilayer formed on PEGTMS/GPTES functionalized FSN....	98
Figure 39: Absorbance spectra from the BCA assay of goat anti-gonococcus IgG antibody functionalized FSN, PEG/epoxide functionalized FSN, and ethanolamine pretreated PEG/epoxide FSN .....	99

## LIST OF ABBREVIATIONS

BET	Brunauer, Emmett, Teller
BJH	Barrett, Joyner, Halenda
cald.	Calculated
ESI	electrospray ionization
FSN	fluorescent silica nanoparticles
Hz	hertz
I	ionic strength
IR	infrared
<i>J</i>	coupling constant
M	Molarity
M <sup>+</sup>	molecular ion
MHz	megahertz
min	minute
mL	milliliter
MS	mass spectrometry
MSN	mesoporous silica nanoparticles
nm	nanometer
NMR	nuclear magnetic resonance
PBS	phosphate buffered saline
R6G	rhodamine 6G
TEM	transmission electron microscopy

TEOS	tetraethyl orthosilicate
UV	ultraviolet
Vis	visible
XPS	X-ray photoelectron spectroscopy

# **Chapter 1: Surface Functionalization and the Preparation of Protein- and Carbohydrate-Functionalized Materials**

## **1 Introduction**

Recently, micro- and nano-scale inorganic materials functionalized with proteins and carbohydrates have gained much attention due to their potential as biosensors and diagnostic tools, site-specific drug delivery systems, and vaccines.<sup>1-4</sup> In addition, these hybrid materials (known as microarrays and functionalized nanoparticles) have also been used to study and gain a better understanding of biological processes, such as specific carbohydrate-protein binding, carbohydrate antigen adhesion, and carbohydrate-carbohydrate interactions.<sup>1-2</sup> This chapter will review the methodologies used to prepare carbohydrate- and protein-functionalized materials found throughout the literature and highlight the work that has been done within the DeShong lab to prepare carbohydrate-functionalized materials.

### *1.1 Surface Functionalization*

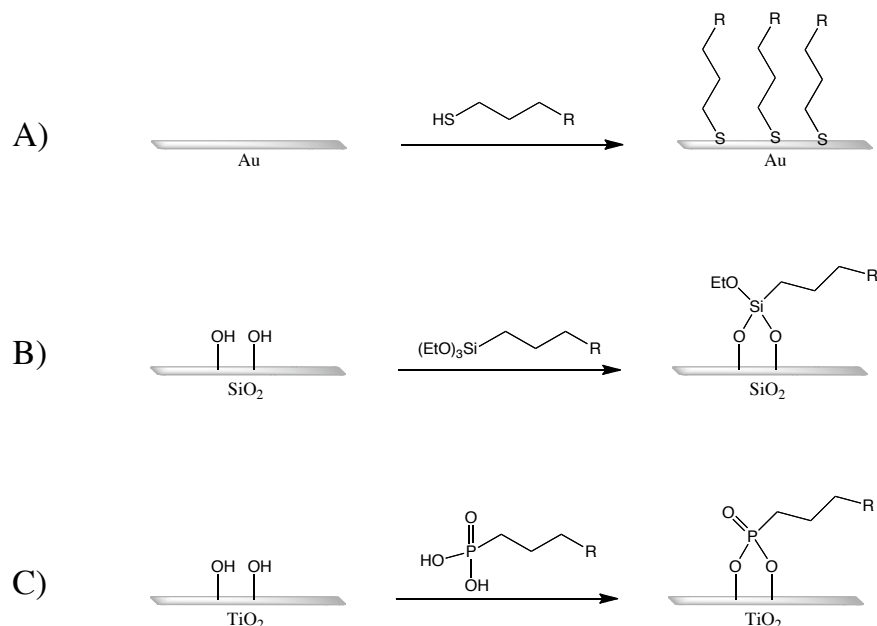
In the early to mid twentieth century, Blodgett<sup>5-6</sup> and then Bigelow<sup>7</sup> demonstrated that organic monolayers could be formed on solid surfaces. Since their initial discoveries, the formation of organic films on solid surfaces has grown into a significant area of research. Throughout the literature, one will find numerous examples of siloxanes, organophosphonates, and carboxylic acids immobilized on hydroxalated surfaces and metal oxides, as well as organothiols absorbed onto gold and silver.<sup>8-29</sup> Notable is the work done by Whitesides, Nuzzo, and Allara that has greatly contributed to

the understanding and characterization of self-assembled monolayers of organothiols absorbed onto gold surfaces.<sup>10-13</sup> In addition, Lee, Zisman, and Sagiv conducted seminal research investigating the formation of silane films on glass surfaces using siloxanes and chlorosilanes.<sup>9, 14-17</sup> Others have built upon their work and have made significant progress in developing and understanding silane SAMs.<sup>9</sup> Accounts by Allara, Nuzzo and Ogawa describe n-alkanoic acids forming monolayers on aluminum oxide.<sup>9, 23-24</sup> The formation of n-alkanoic acids on silver surfaces was also reported by Schlotter et al.<sup>9, 25</sup>, while Tao and coworkers have studied and characterized n-alkanoic acid SAMs on copper and other metal oxides.<sup>9, 26</sup> Table 1 lists different materials and the functional groups that are commonly used to functionalize them.

**Table 1:** List of materials and the functional groups used to functionalize their surface.

<b>Material</b>	<b>Functional group(s) used to functionalize the surface</b>
Gold	Thiols <sup>9-10</sup> , disulfides <sup>28</sup>
Silver	Thiols <sup>9</sup> , disulfides
Silica (SiO <sub>2</sub> )	Siloxanes <sup>15, 18, 27</sup> , halosilanes <sup>9, 17, 21</sup> , organophosphonates <sup>20</sup> , carboxylic acids <sup>5-6</sup>
Titanium oxide (TiO <sub>2</sub> )	Siloxanes <sup>19, 21</sup> , halosilanes <sup>21</sup> , organophosphonates <sup>19</sup>
Aluminum oxide (Al <sub>2</sub> O <sub>3</sub> )	Siloxanes <sup>21</sup> , halosilanes <sup>21</sup> , carboxylic acids <sup>9, 23-24</sup>
Iron oxide (Fe <sub>3</sub> O <sub>4</sub> )	Siloxanes <sup>29</sup> , halosilanes <sup>29</sup> , carboxylic acids <sup>29</sup>
Silver oxide (AgO)	Carboxylic acids <sup>9, 25</sup>

**Figure 1:** Schematic representation of monolayer formation of (A) thiols on gold, (B) siloxanes on silica, and (C) organophosphonates on titanium oxide.



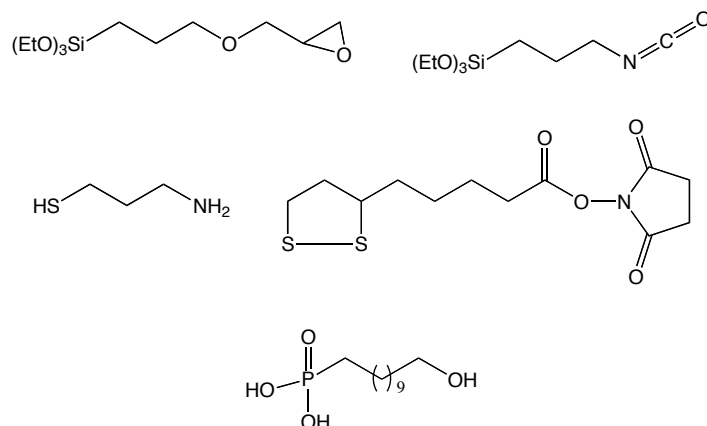
The principles of surface functionalization are used to prepare nucleotide-, protein-, and carbohydrate-functionalized materials. It is appreciated that biomolecule-functionalized nanoparticles have been prepared by passive (non-covalent) absorption, such as ionic bonding and electrostatic absorption.<sup>3, 30</sup> However, these systems are not as robust and reproducible as systems created through covalent linkages.<sup>30</sup> Biomolecules passively absorbed onto a surface can fall off, denature, and lose their biological activity.<sup>3, 30</sup> By covalently linking biomolecules to the surface, these issues of instability are bypassed.<sup>30</sup> Thus, significant research has been done to develop methodologies for specific, covalent attachment of proteins and carbohydrates to solid surfaces.<sup>3-4, 31-32</sup> These surface functionalization methodologies will be highlighted in the next two sections of this chapter.

## 1.2 *Protein-Functionalized Materials*

Many strategies that are used to prepare protein-functionalized materials are predicated on the use of bifunctional “linker” molecules, where one functional group is used to make a covalent bond to a protein or carbohydrate and the other functional group is used to anchor the complex to a surface of interest (Figure 2).<sup>4</sup> The bifunctional linker molecule can first be attached to a surface and then the protein or carbohydrate can react to form a covalent bond with the functionalized surface, or the bifunctional linker can first be reacted with a protein or carbohydrate to produce protein derivatives and glycoconjugates containing a terminal functional group that can then be covalently attached to the desired material. The composition of the material being functionalized dictates what functional group is used as the anchor moiety. As highlighted above, thiols and disulfides are used to immobilized molecules to the surface of gold and silver, while siloxanes and organophosphonates are used to functionalize silica and other hydroxylated surfaces. The functional group used to couple the protein to the bifunctional linker or to a functionalized surface is dependent upon the protein conjugation methodology that is employed.



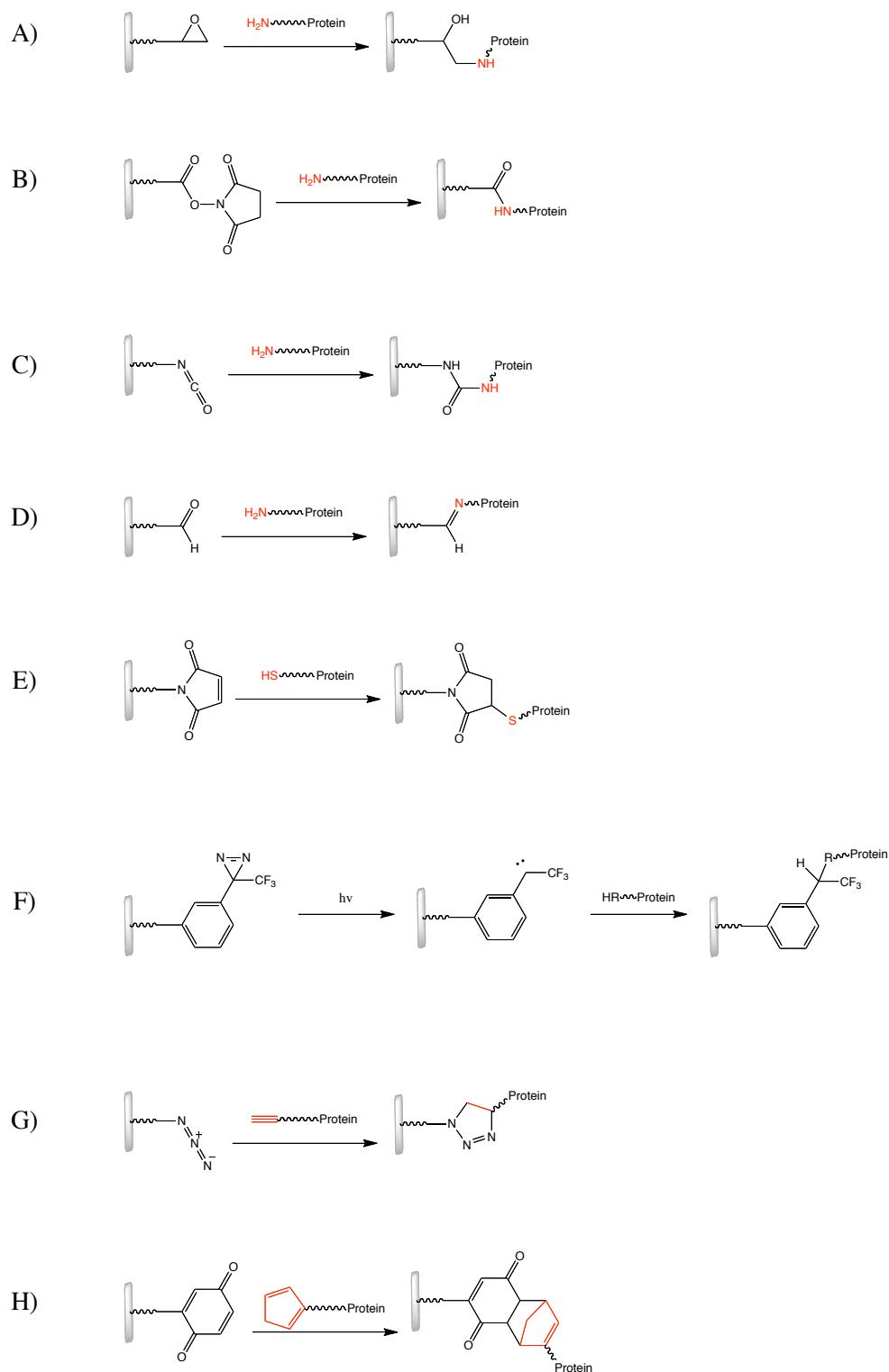
**Figure 2:** Examples of common bifunctional linker molecules.



Most protein coupling methodologies utilize chemistry common to functional groups found within the native protein, such as amines, thiols and carboxylic acids. Lysine and cysteine residues found within the protein are commonly used to conjugate the protein to epoxide-<sup>34-36</sup>, NHS ester-<sup>37-38</sup>, malaimide-<sup>33</sup>, isocyanate-<sup>39</sup>, or aldehyde-functionalized<sup>39-44</sup> surfaces (Figure 3, A-E). However, others have demonstrated that peptides and proteins can be immobilized onto surfaces modified with photoactivatable groups. Angeloni and co-workers prepared glass slides with a dextran polymer derivatized with aryltrifluoromethyl-diazirine groups.<sup>45</sup> Upon exposure to ultraviolet light (350 nm) the aryltrifluoromethyl-diazirine groups decompose to generate molecular nitrogen and highly reactive carbenes. The carbenes then undergo insertion reactions with proteins, covalently linking the protein or peptide to the surface (Figure 3, F).<sup>45</sup> Similarly, irradiating surfaces functionalized with arylazides, and benzophenone derivatives result in the formation of nitrene and ketyl radical intermediates that can further react to form covalent linkages with proteins.<sup>46</sup>

Others have prepared protein derivatives that contain a terminal functionality designed to react specifically with a complementary moiety immobilized onto a surface (Figure 3, F-G). For example, Maltzahn et al prepared peptides bearing heptynoic acid or parparylglycine at the N-terminus.<sup>47</sup> The terminal alkynes of the peptide derivatives were then coupled to azides exposed on the surface of iron oxide nanoparticles via “click” chemistry.<sup>47</sup> Additionally, Houseman and coworkers utilize the Diels-Alder reaction to couple peptide-cyclopentadiene derivatives with quinone groups that are immobilized onto gold-coated glass coverslips, producing peptide-functionalized gold chips.<sup>48</sup>

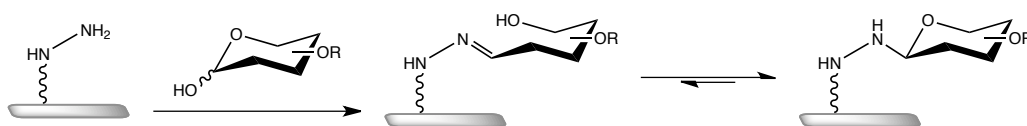
**Figure 3:** Common methods used to covalently attach proteins to functionalized surfaces.<sup>31</sup>



### 1.3 Carbohydrate-Functionalized Materials

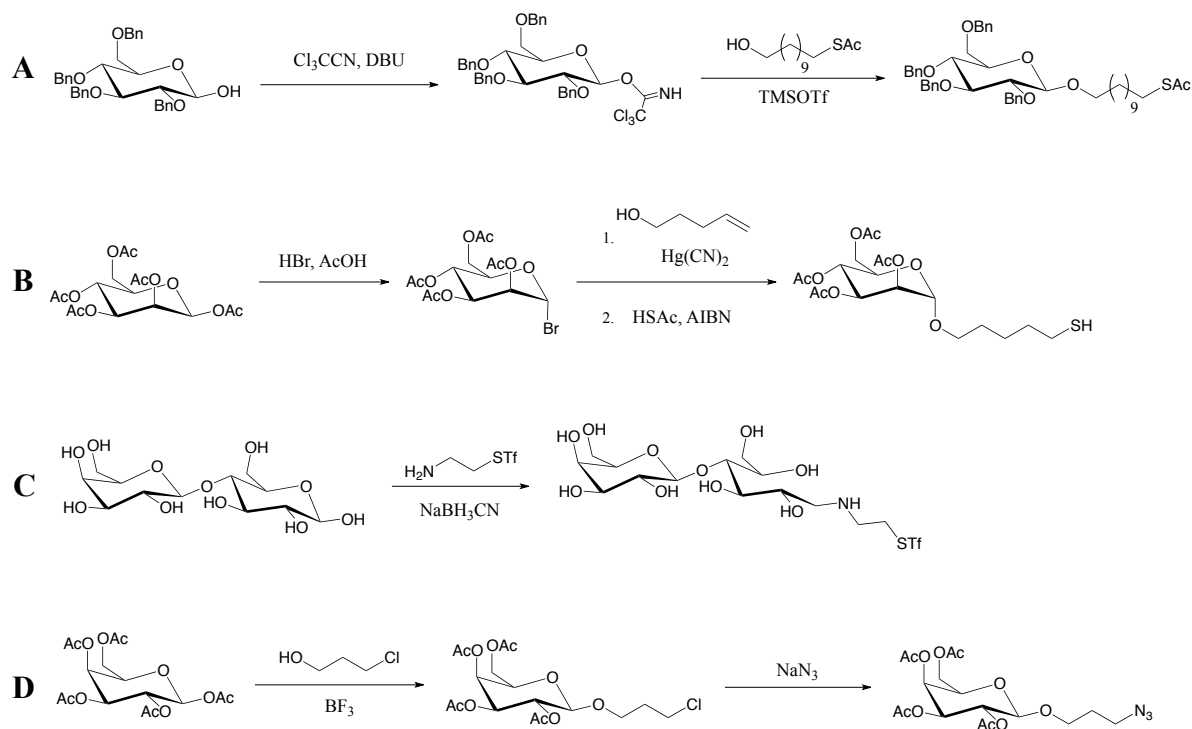
Carbohydrates are not as chemically diverse as proteins, so there are only a few methods known to attach unmodified carbohydrates to functionalized surfaces. A common strategy employed to create glycan arrays from unmodified carbohydrates entails reacting a reducing sugar with surfaces functionalized with hydrazide or alkylaminoxy groups (Figure 4).<sup>49-54</sup> For example, Zhi et al. prepared oligosaccharide microarrays by coupling nonderivatized oligosaccharides to hydrazine modified gold films.<sup>50</sup> More recently, Bertozzi reported conjugating a range of reducing sugars to a poly(acryloyl hydrazide) scaffold in the presence of aniline.<sup>49</sup> Alternatively, in the same way they attached proteins to photoactivatable surfaces, Angeloni et al. prepared glycan microarrays by covalently attaching bacterial exopolysaccharides to carbenes generated from aryltrifluoromethyl-diazirine groups attached to glass slides.<sup>45</sup>

**Figure 4:** Attachment of unmodified carbohydrates to a hydrazine-functionalized surface.



Carbohydrate-functionalized materials are typically prepared from glycoconjugates containing a terminal functional group that can be covalently attached to the surface of the material. These glycoconjugates are prepared using standard glycosylation strategies.<sup>55-56</sup> Penades et al employed the trichloroacetimidate method to produce a series of carbohydrate derivatives bearing a terminal thiol at the anomeric carbon (Figure 5, A).<sup>57</sup> Nishimura et al used the same approach to develop a novel solid phase oligosaccharide synthesis technique using gold nanoparticles.<sup>58</sup> Using the traditional Koenigs-Knorr method, Lin and coworkers also prepared thiol terminated glycoconjugates by glycosylating carbohydrate-bromide derivatives using 4-pentenyl alcohol (Figure 5, B).<sup>59</sup> The alkene-terminated glycoconjugates were then converted into thiol conjugates via radical elongation methods.<sup>59</sup> Additionally, Kamerling et al describe a reductive amination procedure that expediently introduces a thiol-containing spacer at the reducing end of a free oligosaccharide (Figure 5, C).<sup>60</sup> Both Wang<sup>61</sup> and Huang<sup>62</sup> synthesized azide-containing sugars that were subsequently attached to the surface of nanoparticles functionalized with alkynes via “click” chemistry. Wang utilized the trichloroacetimidate method to create the azide derivatives, while Huang used a Lewis acid promoted glycosylation method (Figure 5, D). Huang also synthesized carbohydrate amido-acid derivatives that were then coupled to amine groups present at the surface of silica-coated magnetite nanoparticles.<sup>62</sup> In addition, Ying et al prepared dextran derivatives containing succinimidyl-activated esters, which were then conjugated to amine-coated silica nanoparticles.<sup>63</sup>

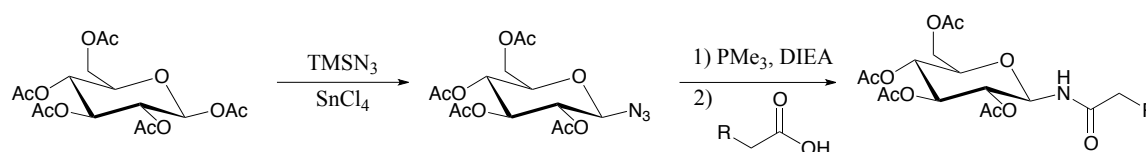
**Figure 5:** Popular glycosylation techniques.



Our lab previously reported the formation of glycosylamide derivatives from glycopyranosyl azides via a modified Staudinger ligation method (Figure 6).<sup>64-65</sup> Using this methodology, several disulfide containing carbohydrate derivatives were synthesized and used to functionalize gold surfaces and nanoparticles.<sup>65</sup> This synthetic strategy is superior to other methods because it is possible to control the stereochemistry at the anomeric center by choosing the “appropriate combination of phosphine and reaction conditions”.<sup>65</sup> The ability to control the stereochemistry at the anomeric center is significant because the two different anomers form monolayers on gold with different surface characteristics.<sup>65</sup> X-Ray photoelectron spectroscopy was used to determine that  $\beta$ -linked glucopyranosylamide derivatives form monolayers with higher surface coverage

than the corresponding  $\alpha$ -linked derivatives. In addition, the glycosylamide derivatives are quite robust. The amide linkage can withstand strongly acidic or basic conditions, which enables a wide range of protecting group strategies to be employed if needed in later chemical transformations.<sup>65</sup>

**Figure 6:** General Staudinger ligation method used by DeShong to prepare glycoconjugates.<sup>64</sup>



## 2 Results and Discussion

### 2.1 Preparation of Carbohydrate-Siloxane Derivatives via Hydrosilylation

Silica materials have gained considerable attention in the biotechnology community due in large part to their biocompatibility and ease of preparation.<sup>66</sup> The preparation of silica biosensors, diagnostic tools and site-specific drug delivery systems requires a need to prepare carbohydrate- and protein-functionalized silica materials in an efficient manner. Thus, the goal of the research presented here was to extend our glycosylation methodology to the preparation of glycoconjugates containing terminal siloxanes that could then be immobilized onto silica surfaces.

In our synthetic strategy, we coupled glucopyranosyl azide **1** with 4-pentenioic acid to yield the glucose-alkene derivative **2**. Hydrosilylation of the terminal alkene using platinum (IV) oxide yielded the desired terminal-siloxane conjugate **3** (Figure 7).

Unfortunately, this methodology is limited by the competing hydrogenation reaction that gives the fully saturated pentanyl derivative **4**. Nevertheless, the same hydrosilation method was also employed to prepare lactose- and mannose-siloxane conjugates **6** and **11**, respectively. Table 1 summarizes the results of these hydrosilation reactions. It is important to note that lactose-alkene **5** was prepared using the same coupling methodology as glucose-alkene **2**. However, because only the  $\alpha$ -form of mannose-azide **8** was produced in the azidation step, a different coupling strategy, which was previously reported by our lab, was needed to create the  $\beta$ -mannose-alkene **10**.<sup>64</sup> In this coupling strategy, the stereochemistry at the anomeric carbon is set by the formation of the isoxazoline intermediate **9**, which is formed *in situ* (Figure 8).

**Figure 7:** Synthesis of glucose-siloxane conjugate.

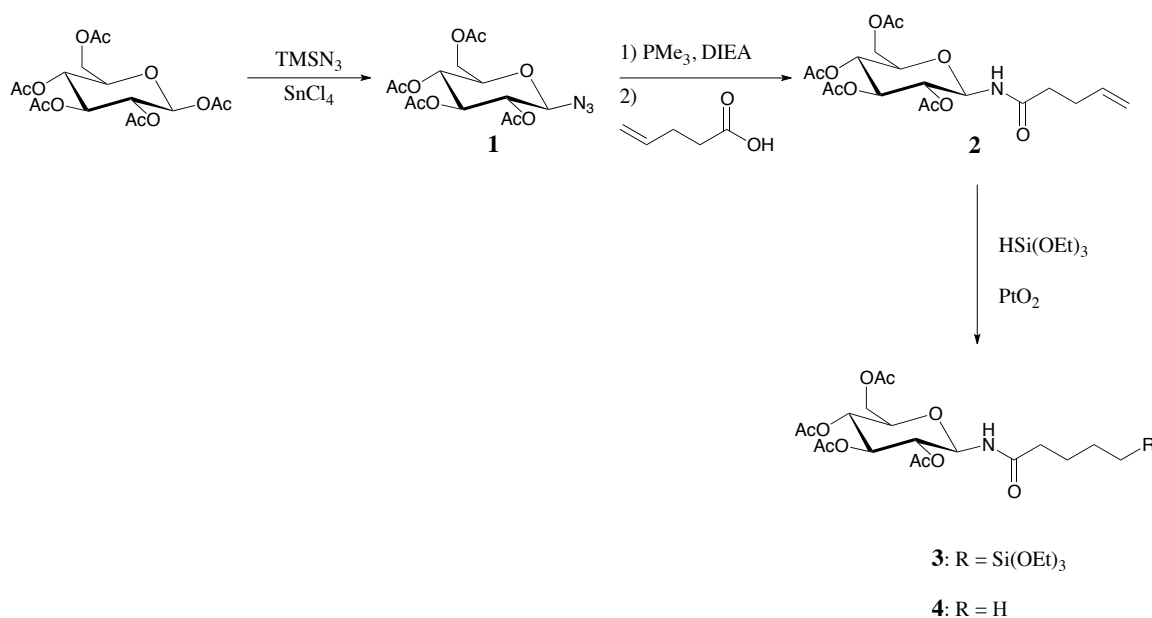




**Figure 8:** Synthesis of mannose-alkene conjugate.

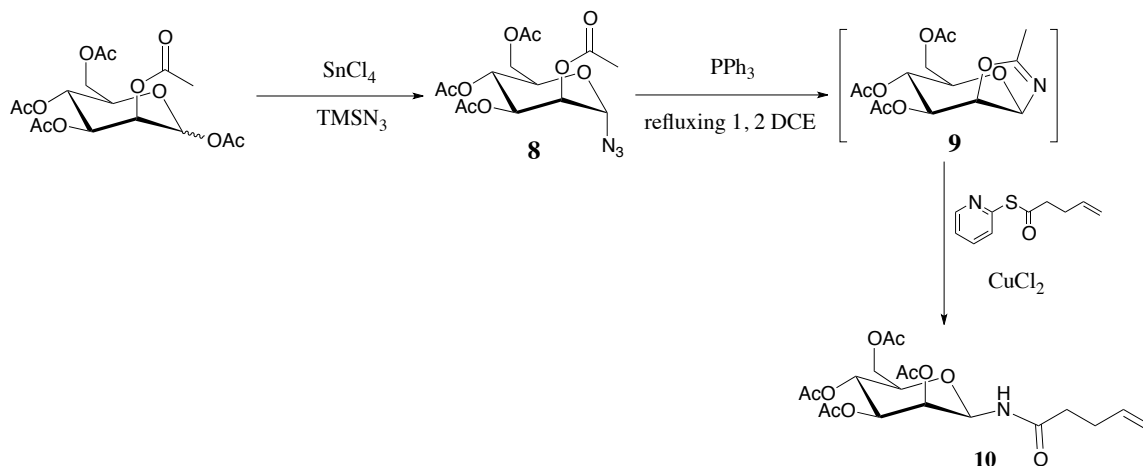


**Table 2:** Hydrosilation results.

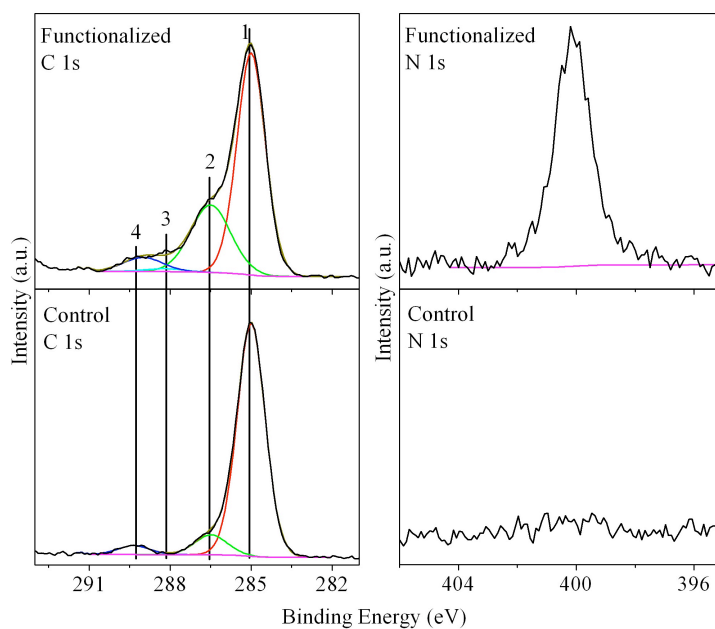
Entry	Starting Carbohydrate-Alkene	Hydrosilation Product	Hydrogenation Product	Siloxane : Alkane Ratio (mol) <sup>1</sup>	% Yield of Siloxane Derivative
1				3 : 1	57
2				2 : 1	52
3				3 : 1	47

<sup>1</sup>Molar ratios were determined by <sup>1</sup>H NMR.

Proof that carbohydrate-siloxane conjugates could be used to functionalize silica surfaces was acquired through X-ray photoelectron spectroscopy (XPS). Glucose-siloxane **3** was immobilized onto a glass cover slip and the functionalized slide was then analyzed using XPS. . The high-resolution X-ray photoelectron spectra for bare and functionalized glass slides are depicted in Figure 9. The C 1s spectrum of the

unfunctionalized glass slide indicates a small amount of carbon on the surface due to hydrocarbon contamination, with some oxidized carbon due to atmospheric exposure. Notably, there is no nitrogen detected on the surface of the bare, unfunctionalized glass slide. However, the XPS spectrum of the glass slide that was treated with glucose-siloxane **1** reveals a well-resolved nitrogen peak at 400.2 eV (~2 atomic % of all elements detected) and increased oxidized carbon species (C=O, C-N, and C-O), which is consistent with the attachment of the protected glucose-siloxane conjugate

**Figure 9:** C 1s and N 1s high-resolution X-ray photoelectron spectra of the bare, unfunctionalized glass slide (control) and the glucose-functionalized glass slide.



Legend: 1 = C-C/C-H, 2 = C-O / C-N, 3 = RC=ON, 4 = OC=OR

Additional confirmation that the carbohydrate-siloxane can be immobilized onto silica surfaces came from studies performed in the Dagenais lab in the Department of

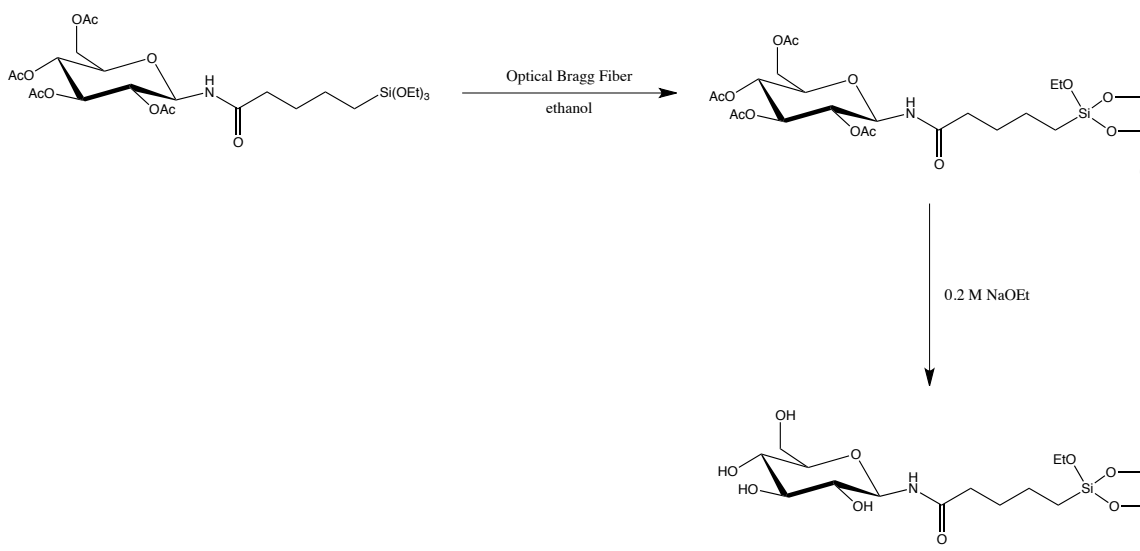
Electrical and Computer Engineering at the University of Maryland, College Park.

Dagenais et al. used the glucose- and lactose-siloxane derivatives (compound **3** and **4**) to create carbohydrate-functionalized evanescent wave fiber Bragg gratings.<sup>67</sup> The fibers used are composed of hydrogen-loaded germanosilicate and were etched to a final diameter of 5  $\mu\text{m}$ . Dagenais and coworkers monitored the attachment of glucosyl siloxane, **3**, to the fiber Bragg grating by measuring the change in the Bragg wavelength over time. The evanescent wave in the fiber sensor senses the change of the index of refraction following the binding of the carbohydrate to the surface of the sensor. This change of index of refraction leads to a change of the Bragg wavelength, which is detected.<sup>67</sup> A final shift of 24 pm was measured after the fiber was incubated in a solution of **3** for one hour. This change in Bragg wavelength corresponds to a change of the surrounding index of  $5.6 \times 10^{-4}$ . If it is assumed that a solid layer of glucose is formed on the fiber of index 1.543, a beam propagation simulation suggests that a layer with a thickness of 1 nm is formed, corresponding to a monolayer of glucose conjugate **3**.<sup>67</sup>

Dagenais and coworkers also provided proof that the surface-immobilized carbohydrate-siloxane conjugates are functional and can be used for sensing applications. Using the same method of detection described above, Ryu was able to detect the specific binding of lectins to carbohydrate-functionalized fibers.<sup>68</sup> The preparation of unprotected glucose-functionalized fibers is outlined in Figure 10. Lactose-functionalized fibers were prepared in an analogous fashion using lactose-siloxane **4**. The acetylated carbohydrate-siloxane conjugates were first immobilized onto the Bragg fiber, and then 0.2M sodium ethoxide solution was used to remove the acetate protecting groups. The functionalized

fibers were then exposed to separate solutions of concanavalin A (Con A) and peanut agglutinin (PNA). Con A is known to bind selectively to glucose and mannose, while PNA is known to be selective for galactose. Exposure of Con A to glucose-functionalized fibers resulted in a Bragg wavelength shift of 60 pm. However, no shift of the Bragg wavelength was observed when the glucose-functionalized fiber was exposed to PNA.<sup>68</sup> Conversely, exposing the lactose-functionalized fiber to PNA caused a shift of 40 pm, while exposing the lactose-functionalized fiber to Con A had no effect on the Bragg wavelength.<sup>68</sup> These results demonstrate that the carbohydrates bound to the surface of the fibers are functional and that carbohydrate functionalized Bragg fiber gratings can be used to detect the selective binding of lectins to the immobilized carbohydrates.

**Figure 10:** Preparation of a glucose-functionalized Bragg fiber.



## 2.2 Preparation of Carbohydrate Derivatives via Grubbs' Cross-Metathesis

While developing the hydrosilation methodology, it was realized that the pentenyl glycoside intermediates (**2**, **5**, and **10**) had the potential to be quite valuable. Fraser-Reid et al have reported the preparation of O-linked pentenyl glycosides and a number of transformations that they can undergo.<sup>69</sup> In addition, olefin cross-metathesis (CM) using Grubbs' ruthenium-based carbene catalysts has emerged as a convenient and popular method to functionalize terminal alkenes (Figures 11-12).<sup>69-78</sup> Importantly, there are numerous examples in which cross-metathesis has been utilized to couple O- and C-linked alkenyl glycosides with other terminal olefins to produce a variety of glycoconjugates.<sup>79-89</sup> For example, Danishefsky et al demonstrated that  $\beta$ -O-pentenyl-glycosides undergo olefin cross-metathesis with amino acid derivatives containing a terminal alkene to yield glycoprotein conjugates.<sup>89</sup> Having stable, alkene-terminated glycoconjugates readily available, we recognized that olefin cross metathesis could be used as a general, practical approach to glycoconjugates with a variety of terminal functionalities that could be used to prepare glycoconjugate functionalized materials..

**Figure 11:** General olefin cross-metathesis reaction.

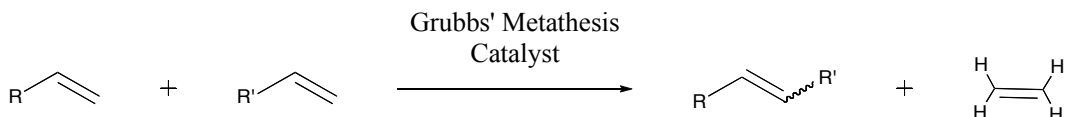
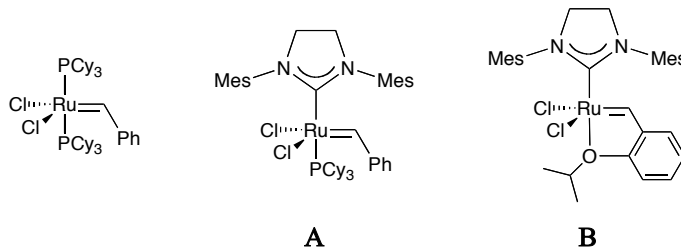
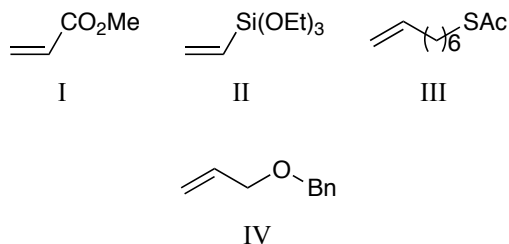


**Figure 12:** Popular Grubbs' metathesis catalysts.



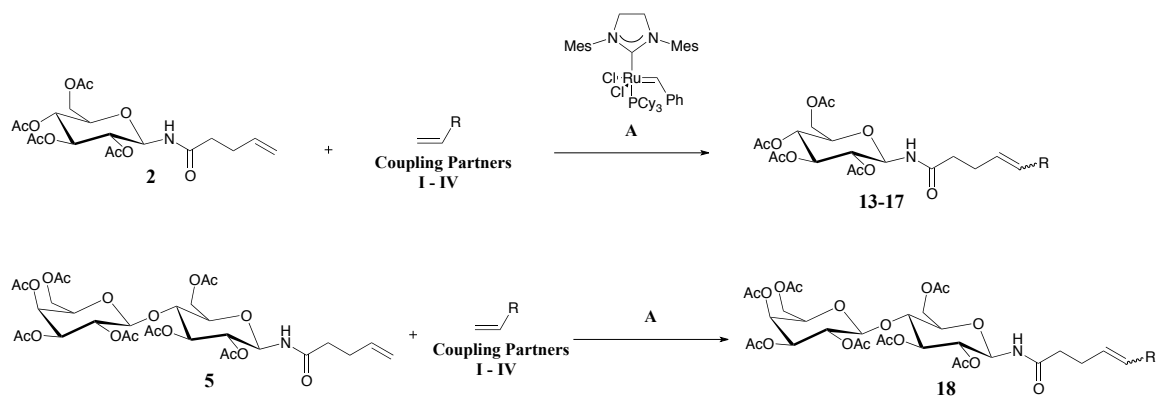
At the onset of this project, a series of commercially available cross-coupling partners were selected that could be used to functionalize a variety of surfaces, and would create monolayers with beneficial features (Figure 13). We were most interested in vinyltriethoxysiloxane, alkenyl thioesters, allylic alcohol derivatives, and methyl acrylate. Cross-coupling products obtained from using vinyltriethoxysiloxane could be used to functionalize silica surfaces, while products formed using alkenyl thioesters could easily be transformed into thiol derivatives for functionalizing gold materials. Allylic alcohols were of interest because they could be used to model allylic polyethylene glycol (PEG) units. PEG moieties are often used to form hybrid monolayers on nanoparticles due to their ability to prevent nanoparticle aggregation in aqueous media.<sup>90</sup> PEG groups have also been shown to prevent nonselective binding in biological screening assays.<sup>91</sup> Finally, methyl acrylate was chosen because the corresponding products can be converted into carboxylic acid derivatives.

**Figure 13:** Cross-coupling partners used to prepare glycoconjugates.

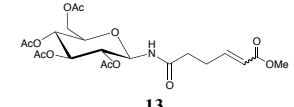
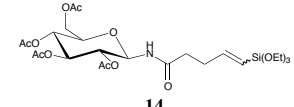
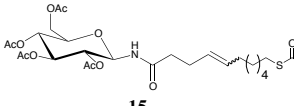
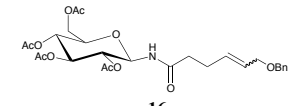
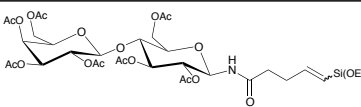


Using Grubbs' ruthenium-based, N-heterocyclic carbene-coordinated catalyst **A**, we were able to link cross coupling partners with glucosyl alkene **2** and lactosyl alkene **5** with varying success (Figure 14). Table 3 documents the results of these metathesis reactions.

**Figure 14:** Olefin cross-metathesis of N-linked pentenyl glycoconjugates.



**Table 3:** Olefin cross-metathesis results.

Entry	Starting Carbohydrate-Alkene	Coupling Partner	Catalyst Mol %	Cross Metathesis Product	% Yield	E/Z Ratio <sup>1</sup>
1	2	I	10	 13	67	*
2	2	II	10	 14	65	5.5/1
3	2	III	10	 15	35	3/1
4	2	IV	10	 16	25	*
5	5	II	15	 18	50	3/1

<sup>1</sup>E/Z ratios were determined by <sup>1</sup>H NMR.

\*Could not be determined based on <sup>1</sup>H NMR.

The carbohydrate-alkene conjugates reacted most efficiently with methyl acrylate **I** and vinyltriethoxysilane **II**, respectively. This was expected based on the work of others.<sup>78</sup> It is known that electron-deficient, sterically hindered alkenes, such as acrylates and vinyl siloxanes, are good cross-coupling candidates.<sup>70, 78</sup> These types of alkenes do not readily homodimerize, and the products formed do not readily undergo secondary metathesis reactions.<sup>78</sup> The yields for products **13** and **14** are consistent with similar systems reported by Bruchner in which C-allyl-glycosides are coupled to  $\alpha,\beta$ -unsaturated amide compounds using catalyst **A**.<sup>87</sup> However, the authors report a 25% increase in yield using Hoveyda-Grubbs' second-generation metathesis catalyst, **B**.<sup>87</sup> Thus, it may



be of interest to retry the metathesis between our glycoconjugates and couplings partners **I** and **II** using catalyst **B**.

The inefficiency of the cross metathesis reactions using octenyl thioester **III** and the allylic ether **IV** can be attributed to the propensity of the coupling partners and the alkene-glycoconjugates to homodimerize. It is well established that electron-rich, sterically unhindered alkenes readily homodimerize.<sup>78</sup> Metathesis between two alkenes that have the tendency to homodimerize will result in a statistical distribution of homodimerized products and the desired cross-coupled product.<sup>78</sup> However, it has been shown that the efficiency of cross-metathesis between glycosyl-alkenes and coupling partners that readily homodimerize can be increased by placing a methyl “cap” on the coupling partner<sup>89</sup> or by using the homodimer of the coupling partner in place of the terminal alkene compound.<sup>79-80</sup>

The E-isomer of the cross metathesis products was favored in all of the metathesis reactions reported here, which is consistent with the findings of others.<sup>70, 72, 78, 88</sup> The stereoselective formation of the E-isomer is important for our purposes, because it is known that monolayers formed from Z-alkenes have different characteristics than monolayers formed using the trans-isomer. For example, E-unsaturated fatty acids form monolayers that are packed more densely than monolayers formed from the corresponding Z-isomer.<sup>92</sup> Thus, the properties of the monolayers formed using the metathesis products may be affected by their E/Z ratio. Notably, Wong has reported that perbenzylated allyl glycosides undergo metathesis with non-functionalized alkenes to yield the E-isomer stereospecifically.<sup>86</sup>

### 2.3 *Attachment of Reducing Sugars to Amine-Functionalized Surfaces via Reductive Amination*

Though the Staudinger ligation and olefin cross metathesis methodologies were effective in the preparation of simple glycan derivatives, extending these methodologies to the synthesis of complex oligosaccharides was a concern due to foreseen difficulty with substrate solubility and the complex protecting group strategies that would be required. Thus, a method that could be used to directly immobilize natural, unprotected oligosaccharides to a surface was sought. As mentioned above, others have accomplished this goal by coupling reducing sugars to surfaces decorated with hydrazine derivatives. However, preparing a hydrazine-functionalized surface is a multistep process. Conversely, aminated surfaces can be achieved in one step using commercially available amine-thiols or amino-siloxane compounds. In addition, it is well known that reductive amination is a facile method used to conjugate reducing carbohydrates with proteins. Thus, we rationalized that coupling natural, unmodified carbohydrates to amine-coated surfaces could be achieved through reductive amination.

In the following studies, fluorescent silica nanoparticles (FSN) were used. Refer to chapter 3 of this dissertation for details in regard to the preparation and characterization of these materials. Amine-coated fluorescent silica nanoparticles were prepared by reacting bare FSN with 3-aminopropyltriethoxysilane (APTES). Initially, an attempt to conjugate lactose to APTES-functionalized FSN under standard reductive amination conditions using  $\text{NaCNBH}_3$  in acetate buffer (pH = 5.0) was made.<sup>93</sup> After being thoroughly washed, the particles were analyzed for carbohydrates using the phenol/sulfuric acid colorimetric assay.<sup>94</sup> This assay is able to detect carbohydrates in

concentrations as low as micrograms per milliliter.<sup>94</sup> The conjugate that is produced in the reaction has a distinctive light-brown color and a strong absorbance at 490 nm.<sup>94</sup> Unfortunately, the particles tested negative for carbohydrates, indicating that lactose had not been coupled to the amine-functionalized surface. Therefore, an alternative method using borate buffer (pH = 8.0) and high salt concentrations described by Gildersleeve et al. was attempted (Figure 15).<sup>95</sup> The colorimetric assay of the resulting material was positive for carbohydrates, indicating that lactose was bound to the surface of the nanoparticles (Figure 16). As a control, amine-functionalized fluorescent silica nanoparticles were treated with sucrose under identical reaction conditions. Sucrose is a non-reducing sugar, and the glycosidic bonds of sucrose are not expected to hydrolyze under mildly basic reaction conditions. Thus, under the reaction conditions described by Gildersleeve, sucrose should be incapable of undergoing reductive amination. The amine-functionalized fluorescent silica nanoparticles that were treated with sucrose under the reductive amination reaction conditions tested negative for carbohydrates (Figure 16). This result indicates that lactose is bound to the surface of the nanoparticles through covalent linkages and not by hydrophobic or electrostatic interactions.

**Figure 15:** Preparation of lactose-functionalized fluorescent silica nanoparticles via reductive amination.

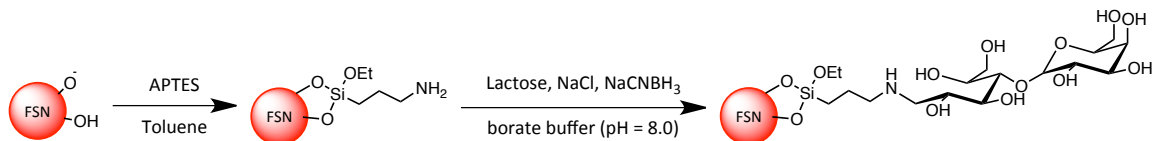
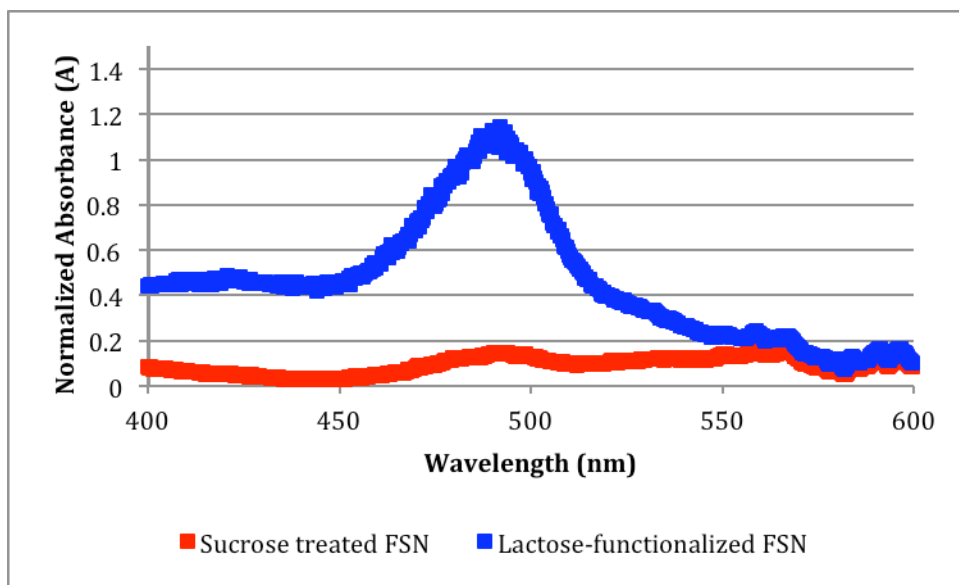


**Figure 16:** Absorbance spectra from the phenol/sulfuric acid colorimetric assay of lactose-functionalized fluorescent silica nanoparticles (blue) and sucrose treated, amine-functionalized fluorescent silica nanoparticles (red). Absorbance at 490 nm indicates the presence of carbohydrates within the sample.



The absorbance spectra shown are from the phenol/sulfuric acid colorimetric assay of one trial. The results are representative of the results from two individual trials. In both cases, a stronger absorbance at 490 nm was observed for lactose-functionalized FSN than for sucrose treated, amine-functionalized FSN.

### 3 Conclusions

Methods used to prepare protein- and carbohydrate-functionalized materials have been reviewed. In general, protein- and carbohydrate-functionalized materials are prepared by one of two ways: (1) by synthetically introducing an anchor moiety into the protein or carbohydrate, which is used to covalently attach the biomolecule to the surface of a specific material; or, (2) by functionalizing the surface of a material with a functional group that will react to covalently attach a protein or carbohydrate to the material. Bifunctional linker molecules are commonly used to prepare protein-

functionalized materials, while a variety of glycosylation methodologies are used to prepare carbohydrate-functionalized materials.

From the work presented here, there are several significant findings. N-linked glycosyl siloxane derivatives, prepared via a modified Staudinger ligation method, were used to create carbohydrate-functionalized evanescent wave fiber Bragg gratings. The carbohydrate-functionalized fibers were subsequently used to detect the specific binding of lectins to the carbohydrates attached to the surface of the fiber. In addition, it was found that N-linked pentenyl glycoside intermediates could undergo cross metathesis with terminal alkene derivatives containing a variety of anchor moieties. The advantage of this synthetic strategy is the ability to create a series of carbohydrate derivatives capable of functionalizing a variety of different material from a common pentenyl glycoside intermediate. Also, reductive amination proved to be a facile method to conjugate natural, unmodified carbohydrates to amine-functionalized fluorescent silica nanoparticles.

## **4 Experimental**

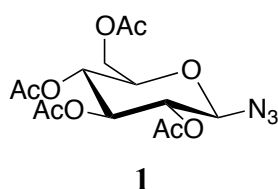
### *4.1 General*

All compounds were used as received from the supplier unless otherwise stated.

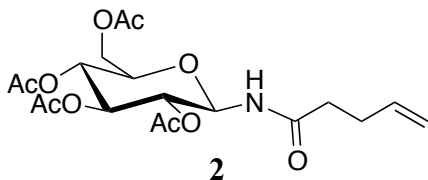
Methylene chloride ( $\text{CH}_2\text{Cl}_2$ ), dimethyl formamide (DMF) and 1, 2-dichloroethane were distilled from calcium hydride. Infrared spectra were obtained on a Nicolet 5DXC FT-IR spectrophotometer. Band positions are given in reciprocal centimeters ( $\text{cm}^{-1}$ ) and relative intensities are listed as br (broad), s (strong), m (medium), w (weak).  $^1\text{H}$  and  $^{13}\text{C}$  NMR spectra were obtained on a Bruker DRX-400 MHz spectrometer. Chemical shifts are

reported in parts per million (ppm) relative to  $\text{CHCl}_3$  ( $\delta$  7.24). Coupling constants ( $J$  values) are given in hertz (Hz). Spin multiplicities are indicated by the following symbols: s (singlet), d (doublet), t (triplet), q (quartet), m (multiplet). High resolution mass spectra (HRMS) were obtained on a JEOL Accu TOF-CS mass spectrometer using electrospray ionization (ESI). An Ocean Optics USB 2000 Spectrometer was used to obtain absorbance spectra. Room temperature (RT) is defined as 20°C. All glassware was dried in an oven set to 120 °C for at least 12 hours before use.

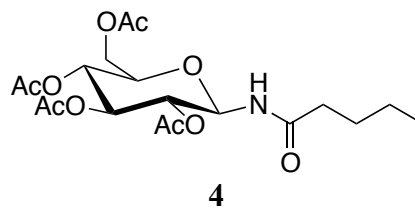
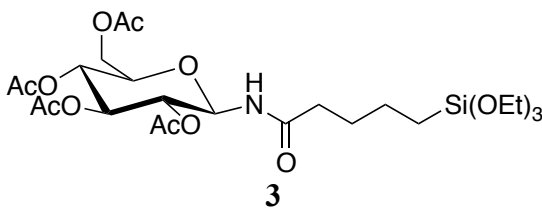
## 4.2 Synthesis of Compounds



$\beta$ -Glucose pentaacetate (2.4 g, 6.2 mmol) was dissolved in 25 mL of freshly distilled  $\text{CH}_2\text{Cl}_2$  under an argon atmosphere. Trimethylsilyl azide (1.2 mL, 9.3 mmol) was added via syringe followed by a 1.0 M solution of  $\text{SnCl}_4$  (3.1 mL, 3.1 mmol) via syringe. The reaction mixture stirred at RT for 21.5 hours. The reaction mixture was then diluted with 100 mL of  $\text{CH}_2\text{Cl}_2$  and washed twice with saturated  $\text{NaHCO}_3$  solution and then four times with  $\text{H}_2\text{O}$ . The organic layer was collected, dried over  $\text{MgSO}_4$ , and concentrated *in vacuo* to yield a colorless oil. The oil was recrystallized from EtOAc and hexanes to yield 1.9 g (85%) of azide **1** as white crystals. Spectral data were identical to the data reported by Damkaci.<sup>96</sup>

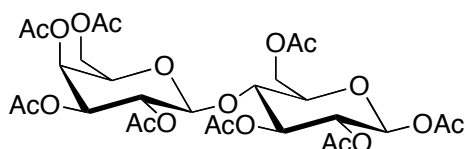


Glucose azide **1** (1.0 g, 2.7 mmol) was dissolved in 25 mL of freshly distilled  $\text{CH}_2\text{Cl}_2$ . Diisopropylethylamine (1.0 mL) was added via syringe followed by a 1.0 M solution of trimethylphosphine (3.5 mL, 3.5 mmol) via syringe. Evolution of gas was observed. The reaction mixture stirred at RT for 30 minutes. 4-Pentenoic acid (0.6 mL, 5 mmol) was added via syringe in one aliquot. The reaction mixture stirred at RT for 22 hours. The reaction mixture was then diluted with 125 mL of EtOAc and washed three times with  $\text{H}_2\text{O}$ . The organic layer was collected, dried over  $\text{MgSO}_4$  and concentrated *in vacuo* to yield a colorless oil. Purification of the oil by flash chromatography (hexanes: EtOAc, 1:1) gave 0.62 g (54%) of alkene **2** as a colorless oil. Spectral data were identical to the data reported by Park.<sup>97</sup>



Glucose alkene **2** (0.43 g, 1.0 mmol) and  $\text{PtO}_2$  (0.01 g, 0.05 mmol) were added into a vial and dissolved with 1.5 mL of freshly distilled THF. Triethoxysilane (0.9 mL, 5 mmol) was added via syringe in one portion. The vial was flushed with argon and sealed. The reaction mixture stirred at 95 °C for 3 hours. The reaction mixture was diluted with 20 mL of EtOH and filtered through a Celite plug. Concentration *in vacuo* yielded a colorless oil. Purification by flash chromatography (hexanes : EtOAc, 1:1) gave 0.42 g

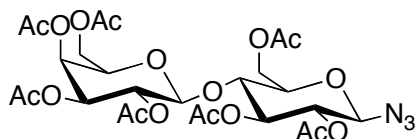
of an inseparable mixture of siloxane **3** and amide **4**. The mol ratio of **3**: **4** (3:1) and percent yields (57% for **3** and 18% for **4**) were determined by integration of the  $^1\text{H}$ -NMR signals at 0.60 ppm (corresponding to the protons on the carbon adjacent to the siloxane group in **3**) and 0.88 ppm (corresponding to the protons on the terminal carbon in **4**). Spectral data were identical to the data reported by Park.<sup>97</sup>



### Peracetylated Lactose

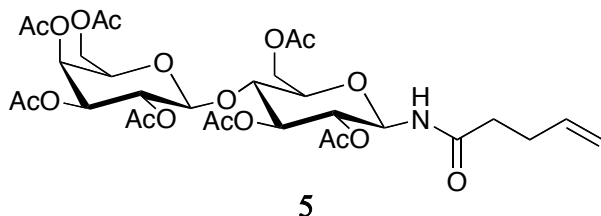
To a refluxing mixture of NaOAc (2.7 g, 33 mmol) in acetic anhydride (24 mL) was added  $\alpha$ -D-lactose (3.0 g, 8.3 mmol) in three equal portions over 30 minutes. The mixture stirred at reflux (150 °C) for 3 hours. After 3 hours, the reaction mixture had turned dark brown. The mixture was cooled to 100 °C and added to 200 mL of an ice/water mixture. This heterogeneous mixture was vigorously stirred at RT for 18 h. After 18 hours, a precipitate had formed. The water was decanted and the precipitate was dissolved in 75 mL of  $\text{CH}_2\text{Cl}_2$ . The organic layer was washed twice with saturated  $\text{NaHCO}_3$  and then three times with  $\text{H}_2\text{O}$ . The organic layer was collected, dried over  $\text{MgSO}_4$ , and concentrated *in vacuo* to yield an orange/brown colored oil. Recrystallization from  $\text{CH}_2\text{Cl}_2$  and diethyl ether yielded 3.2 g (60%) of peracetylated lactose as a white powder. Spectral data were identical to the data reported by Damkaci.<sup>96</sup>





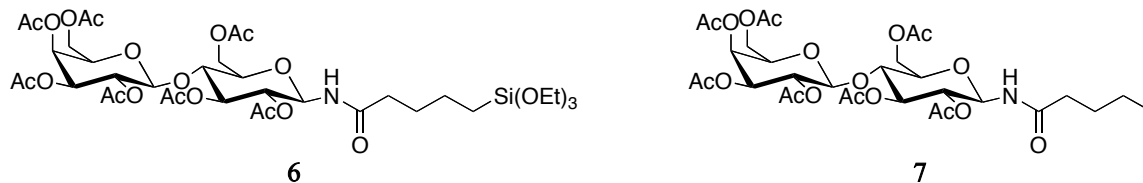
### Lactose azide

Peracetylated lactose (1.6 g, 2.4 mmol) was dissolved in 15 mL of freshly distilled  $\text{CH}_2\text{Cl}_2$ . Trimethylsilyl azide (1.2 mL, 9.3 mmol) was added via syringe followed by a 1.0 M solution of  $\text{SnCl}_4$  (3.1 mL, 3.1 mmol) via syringe. The mixture was stirred at RT for 40 hours under argon atmosphere. The mixture was then diluted with 50 mL of  $\text{CH}_2\text{Cl}_2$  and washed three times with saturated  $\text{NaHCO}_3$  and then three times with  $\text{H}_2\text{O}$ . The organic layer was collected and dried over  $\text{MgSO}_4$  and concentrated *in vacuo* to yield a colorless oil. Purification by flash chromatography (hexanes : EtOAc, 3:7) gave 1.34 g (85%) of the lactose azide conjugate as a colorless oil. Spectral data were identical to the data reported by Damkaci.<sup>96</sup>

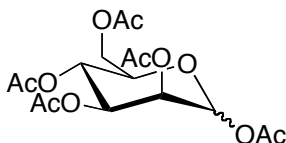


Lactose azide conjugate (0.6 g, 0.9 mmol) was dissolved in 25 mL of freshly distilled  $\text{CH}_2\text{Cl}_2$ . Diisopropylethylamine (0.3 mL) was added via syringe followed by a 1.0 M solution of trimethylphosphine (1.4 mL, 1.4 mmol) via syringe. Evolution of gas was observed. After the reaction mixture stirred at RT for 0.5 h, 4-pentenoic acid (0.2 mL, 1.8 mmol) was added via syringe. The reaction mixture stirred at RT for 20 hours. The reaction mixture was then diluted with 70 mL of EtOAc and washed three times with  $\text{H}_2\text{O}$ . Organic layer was collected and dried over  $\text{MgSO}_4$  and concentrated *in vacuo* to

yield a colorless oil. Purification of the oil by flash chromatography (hexanes : EtOAc, 1:9) gave 0.3 g (48%) of alkene **5** as a colorless oil. Spectral data were identical to the data reported by Park.<sup>97</sup>

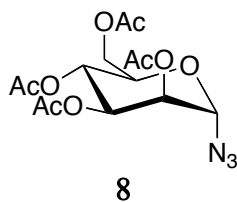


Alkene **5** (0.140 g, 0.19 mmol) and PtO<sub>2</sub> (0.003 g, 0.01 mmol) were weighed into a vial and dissolved with 0.3 mL of freshly distilled THF. Triethoxysilane (0.2 mL, 1.0 mmol) was added via syringe. The vial was flushed with argon and tightly capped. Reaction mixture stirred at 95 °C for 3 hours. The reaction mixture was diluted with 20 mL of EtOH and filtered through a Celite plug. Concentration *in vacuo* yielded a colorless oil. Purification by flash chromatography (hexanes : EtOAc, 2:8) gave 0.128 g of an inseparable mixture of siloxane **6** and amide **7**. The mol ratio of **6**:**7** (2:1) and percent yields (52% for **6** and 30% for **7**) were determined by integration of the <sup>1</sup>H-NMR signals at 0.60 ppm (corresponding to the protons on the carbon adjacent to the siloxane group in **6**) and 0.88 ppm (corresponding to the protons on the terminal carbon in **7**). Spectral data were identical to the data reported by Park.<sup>97</sup>



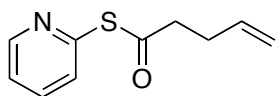
### Peracetylated Mannose

To a refluxing mixture of NaOAc (1.8 g, 23 mmol) in acetic anhydride (20 mL) was added mannose (1.0 g, 5.5 mmol) in three equal portions over 30 minutes. The mixture stirred at reflux for 3 hours. After 3 hours, the reaction mixture had turned a dark brown color. The mixture was cooled to 100 °C and added to 200 mL of an ice/water mixture. This heterogeneous mixture vigorously stirred at RT for 18 hours. The reaction mixture was transferred to a separatory funnel and 75 mL of CH<sub>2</sub>Cl<sub>2</sub> was added. The organic layer was washed with saturated NaHCO<sub>3</sub> (2 x 50 mL) and H<sub>2</sub>O (2 x 50 mL). The organic layer was collected, dried over MgSO<sub>4</sub> and concentrated *in vacuo* to yield a crude oil. Purification by flash chromatography (hexanes: EtOAc, 1:1) gave 2.1 g (99%) of peracetylated mannose ( $\alpha$  :  $\beta$ , 2.3 : 1) as a colorless, viscous oil. Spectral data were identical to the data reported by Park.<sup>97</sup> The  $\alpha$  :  $\beta$  ratio was determined by integration of the <sup>1</sup>H-NMR signals at 5.84 ppm (corresponding to the anomeric proton of the  $\beta$ -anomer) and 6.07 ppm (corresponding to the anomeric proton of the  $\alpha$ -anomer).



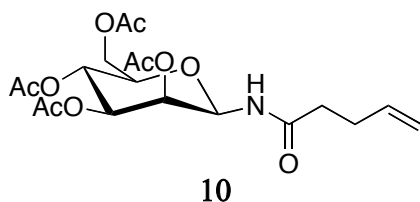
Peracetylated mannose (1.6 g, 4.2 mmol) was dissolved in 20 mL of freshly distilled CH<sub>2</sub>Cl<sub>2</sub>. Trimethylsilyl azide (0.8 mL, 6.3 mmol) was added via syringe followed by 1.0

M SnCl<sub>4</sub> (2.1 mL, 2.1 mmol) via syringe. The mixture was stirred at RT for 40 hours under argon atmosphere. The mixture was diluted with 50 mL of CH<sub>2</sub>Cl<sub>2</sub> and washed three times with saturated NaHCO<sub>3</sub> and then three times with H<sub>2</sub>O. The organic layer was collected and dried over MgSO<sub>4</sub> and concentrated *in vacuo* to yield 1.4 g (88%) of crude azide **8** as a colorless oil. This crude product was taken to the next synthetic step without further purification. Spectral data were identical with the data reported by Damkaci.<sup>96</sup>

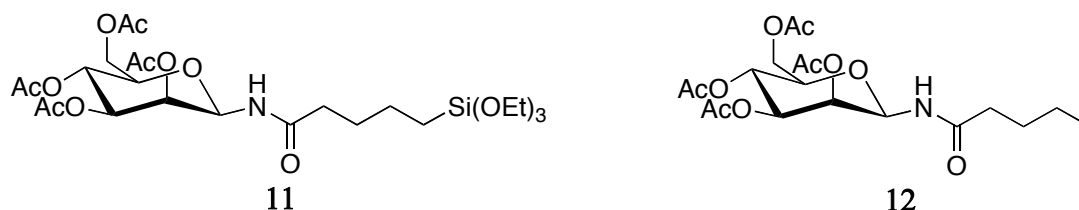


### 2-Pyridyl thioester of pentenoic acid

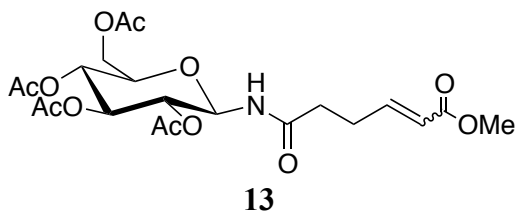
2, 2'-Dipyridyl disulfide (2.6 g, 12 mmol) and triphenylphosphine (3.2 g, 12 mmol) were dissolved in freshly distilled THF (15 mL). 4-Pentenoic acid (0.8 mL, 8 mmol) was added to the reaction mixture via syringe in one aliquot. Reaction mixture stirred under argon atmosphere at RT for 20 hours. Reaction mixture was concentrated *in vacuo*. Purification by flash chromatography (hexanes:EtOAc, 2:1) gave 1.7 g (100%) of the thioester. IR (CCl<sub>4</sub>) 3084 (m), 3068 (m), 3056 (m), 2986 (m), 2921 (m), 2851 (m), 1711 (s), 1572 (s), 1421 (s); <sup>1</sup>H NMR (CDCl<sub>3</sub>) δ 2.42-2.48 (m, 2H), 2.79 (t, *J* = 7.6, 2H), 5.01-5.11 (m, 2H), 5.76-5.86 (m, 1H), 7.24-7.29 (m, 1H), 7.59 (d, *J* = 8.0, 1H), 7.72 (dt, *J* = 2.0, 8.0, 1H), 8.60-8.61 (m, 1H).



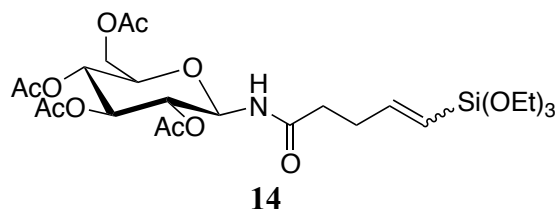
A solution of azide **8** (0.7 g, 2 mmol) dissolved in freshly distilled 1, 2-dichloroethane (20 mL) was transferred to a flask under argon atmosphere containing 4 Å molecular sieves and triphenylphosphine (0.58 g, 2.2 mmol) via syringe in one aliquot. The reaction mixture was heated to reflux under argon atmosphere for 19 hours without stirring and then cooled to RT. The 2-pyridyl thioester of pentenoic acid (0.48 g, 2.5 mmol) was added to the reaction mixture via syringe. Cupric chloride ( $\text{CuCl}_2$ ) (0.35 g, 2.6 mmol) was added to the reaction mixture under argon flow. Reaction mixture stirred at RT for 60 hours. The reaction mixture was filtered and the molecular sieves were washed with  $\text{CH}_2\text{Cl}_2$  (3 x 15 mL). The organic layer was washed with  $\text{H}_2\text{O}$  (4 x 25 mL) dried over  $\text{MgSO}_4$ , and concentrated *in vacuo*. Purification by flash chromatography (hexanes:EtOAc, 1:1) yielded 0.30 g (35%) of alkene **10**. IR ( $\text{CCl}_4$ ) 3640 (w), 3452 (w), 2978 (s), 2978 (m), 2925 (m), 1760 (s), 1715 (m), 1229 (s);  $^1\text{H}$  NMR ( $\text{CDCl}_3$ )  $\delta$  1.94-2.10 (m, 9H), 2.20 (s, 3H), 2.22-2.38 (m, 4H), 3.75 (dq,  $J$  = 2.0, 5.2, 1H), 4.06 (dd,  $J$  = 2.0, 12.4, 1H), 4.30 (dd,  $J$  = 4.8, 12.4, 1H), 4.99-5.33 (m, 5H), 5.54 (dd,  $J$  = 0.8, 9.6, 1H), 5.72-5.81 (m, 1H), 6.09 (d,  $J$  = 9.6, 1H);  $^{13}\text{C}$  NMR (100 MHz,  $\text{CDCl}_3$ )  $\delta$  20.6, 20.8, 20.9, 21.0, 29.0, 35.5, 62.4, 65.3, 70.2, 71.7, 74.2, 76.0, 116.0, 136.7, 169.8, 169.9, 170.4, 170.8, 171.9.



Alkene **10** (0.14 g, 0.33 mmol) and PtO<sub>2</sub> (0.004 g, 0.015 mmol) were weighed into a vial and dissolved in 0.3 mL of freshly distilled THF. Triethoxysilane (0.3 mL, 1.6 mmol) was added to the reaction mixture via syringe in one portion. The vial was flushed with argon and sealed. The reaction mixture stirred at 95 °C for 3 hours, was diluted with 20 mL of EtOH, and filtered through a celite plug. Concentration *in vacuo* yielded a colorless oil. Purification by flash chromatography (hexanes : EtOAc, 1 : 1) gave 0.12 g of an inseparable mixture of siloxane **11** and amide **12**. The mol ratio of **11**:**12** (2.8:1) and percent yields (48% for **11** and 18% for **12**) were determined by integration of the <sup>1</sup>H-NMR signals at 0.61 ppm (corresponding to the protons on the carbon adjacent to the siloxane group in **11**) and 0.88 ppm (corresponding to the protons on the terminal carbon in **12**): IR (CCl<sub>4</sub>) 3448 (w), 2974 (w), 2925 (w), 2880 (w), 1760 (s), 1711 (s), 1221 (s); <sup>1</sup>H NMR (CDCl<sub>3</sub>) δ 0.61 (t, *J* = 8.4, 2H), 0.885 (t, *J* = 7.6, 1H), 1.18-1.42 (m, 12H), 1.45-1.67 (m), 1.96-2.23 (m, 18H), 3.73-3.86 (m, 6H), 4.03-4.12 (m, 1H), 4.27-4.33 (m, 1H), 5.06-5.10 (m, 1H), 5.21 (t, *J* = 10.0, 1H), 5.33-5.34 (m, 1H), 5.53-5.56 (m, 1H), 6.05 (d, *J* = 9.2, 1H). <sup>13</sup>C NMR (100 MHz, CDCl<sub>3</sub>) δ 10.4, 13.3, 18.5, 20.7, 20.9, 20.9, 21.0, 21.1, 22.4, 22.7, 27.3, 28.5, 36.3, 36.4, 58.6, 62.4, 65.3, 70.4, 70.4, 71.8, 74.3, 76.1, 77.4, 169.6, 170.0, 170.5, 170.9, 172.5, 172.6; HRMS (ESI+) calcd. for C<sub>25</sub>H<sub>44</sub>NO<sub>13</sub>Si [M + H]<sup>+</sup> 594.2582, found 594.2613; HRMS (ESI+) calcd. for C<sub>19</sub>H<sub>30</sub>NO<sub>10</sub> [M + H]<sup>+</sup> 432.1870, found 423.1870.

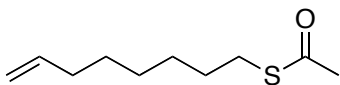


Methyl acrylate (0.1 mL, 1 mmol) was added via syringe to a solution of **2** (0.051 g, 0.12 mmol) dissolved in freshly distilled 1, 2 dichloroethane. Grubb's second-generation metathesis catalyst **A** (0.01 g, 10 mol %) was added to the reaction mixture under argon flow. The reaction mixture stirred at 65 °C for 22 hours. The reaction mixture was concentrated *in vacuo* and purified by flash chromatography (hexanes : EtOAc, 1:1) to give 0.04 g (67%) of ester **13** as a mixture of E/Z isomers. The mixture was a light purple powder: IR (CCl<sub>4</sub>) 3432 (w), 2962 (m), 2925 (m), 2872 (w), 2851 (w), 1744 (s), 1658 (w), 1511 (m), 1433 (m), 1368 (m), 1221 (s), 1045 (s); <sup>1</sup>H NMR (CDCl<sub>3</sub>) δ 1.99-2.05 (m, 12H), 2.27-2.51 (m, 4H), 3.68 (s, 3H), 3.79 (dq, *J* = 2.0, 10.0, 1H), 4.05 (dd, *J* = 2.0, 12.4, 1H), 4.28 (dd, *J* = 4.0, 12.4, 1H), 4.87 (t, *J* = 9.6, 1H), 5.03 (t, *J* = 9.6, 1H), 5.22 (t, *J* = 9.6, 1H), 5.28 (t, *J* = 9.6, 1H), 5.81 (td, *J* = 2.0, 16.0, 1H), 6.28 (d, *J* = 9.2, 1H), 6.88 (dt, *J* = 6.8, 15.6, 1H); <sup>13</sup>C NMR (100 MHz, CDCl<sub>3</sub>) δ 21.0, 21.0 (2 C), 21.1, 27.4, 34.7, 51.9, 62.0, 68.5, 71.0, 73.0, 73.3, 74.0, 78.6, 122.4, 147.0, 167.1, 170.0, 170.3, 171.0, 171.6, 172.0; HRMS (ESI<sup>+</sup>) calcd. for C<sub>21</sub>H<sub>30</sub>NO<sub>12</sub> [M + H]<sup>+</sup> 488.1768, found 488.1738. The E/Z ratio could not be determined using <sup>1</sup>H NMR.



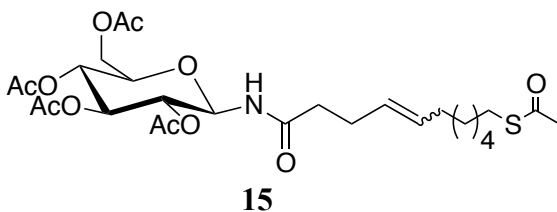
Vinyl triethoxysilane (0.1 mL, 0.5 mmol) was added via syringe to a solution of **2** (0.051 g, 0.12 mmol) dissolved in freshly distilled CH<sub>2</sub>Cl<sub>2</sub>. Grubb's second-generation catalyst **A** (0.01 g, 10 mol %) was added under argon, and the reaction mixture stirred at 40 °C for 20 hours. The reaction mixture was concentrated *in vacuo* and purified by flash chromatography (hexanes : EtOAc, 6:4) to give 0.045 g (63%) of siloxane **14** as a mixture of E/Z isomers (E:Z, 5.5:1). The mixture was a dark, viscous oil: IR (CCl<sub>4</sub>) 3434 (w), 2973 (m), 2932 (m), 2879 (m), 1765(s), 1706 (m), 1549 (s), 1222 (s); <sup>1</sup>H NMR (400 MHz, CDCl<sub>3</sub>) δ 1.19-1.26 (m, 9H), 1.97-2.06 (m, 12H), 2.22-2.57 (m, 4H), 3.76-3.875 (m, 7H), 4.05 (dd, *J* = 1.6, 12.4, 1H), 4.29 (dd, *J* = 4.0, 12.4, 1H), 4.88 (t, *J* = 9.6, 1H), 5.04 (t, *J* = 9.6, 1H), 5.19-5.30 (m, 2H), 5.34-5.45 [2d, 5.36, *J* = 14.4 (Z-isomer), 5.43, *J* = 18.8 (E-isomer), 1H], 6.18 (d, *J* = 9.4, 1H), 6.27 (d, *J* = 9.4, 0.2H), 6.32-6.42 (m, 1H); <sup>13</sup>C NMR (100 MHz, CDCl<sub>3</sub>) δ 18.6, 21.0 (2 C), 21.1, 21.1, 31.7, 35.3, 58.9, 62.0, 68.5, 71.0, 73.0, 73.9, 78.6, 121.0, 151.0, 170.0, 170.3, 171.0, 171.6, 172.7; HRMS (ESI+) calcd. for C<sub>25</sub>H<sub>42</sub>NO<sub>13</sub>Si [M + H]<sup>+</sup> 592.2425, found 592.2390. The E/Z ratio was determined by integration of the <sup>1</sup>H-NMR signals at 6.18 ppm (corresponding to the proton of the amide in the E isomer) and 6.27 ppm (corresponding to the proton of the amide in the Z isomer).





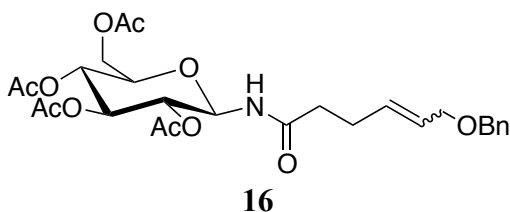
### 1-Octenyl thioacetate

8-Bromo-1-octene (0.57 g, 3.0 mmol) was added via syringe to a solution of potassium thioacetate (1.05 g, 9.0 mmol) dissolved in freshly distilled DMF (8.0 mL). The reaction mixture stirred at RT for 30 hours. The reaction mixture was then diluted in 50 mL of a 1:1 mixture of hexanes and EtOAc and washed with H<sub>2</sub>O (2 x 25 mL). The organic layer was dried over MgSO<sub>4</sub> and concentrated *in vacuo*. Purification by flash chromatography (hexanes : EtOAc, 98:2) yielded 1-octenyl thioacetate (0.60 g, 100%) as a yellow liquid: IR (CCl<sub>4</sub>) 3366 (w), 3076 (w), 2978 (m), 2929 (s), 2855 (s), 1691 (s), 1642 (m), 1352 (m), 1135 (s); <sup>1</sup>H NMR (400 MHz, CDCl<sub>3</sub>) δ 1.24-1.32 (m, 6H), 1.51-1.58 (m, 2H), 1.99-2.043 (m, 2H), 2.30 (s, 3H), 2.84 (t, *J* = 7.2, 2H), 4.90-5.00 (m, 2H), 5.75-5.81 (m, 1H).



1-Octenyl thioacetate (0.070g, 0.4 mmol) was added via syringe to a solution of **2** (0.150 g, 0.4 mmol) dissolved in freshly distilled CH<sub>2</sub>Cl<sub>2</sub>. Grubb's second-generation catalyst **A** (0.03 g, 10 mol %) was added under argon, and the reaction mixture stirred at 40 °C for 20 hours. The reaction mixture was concentrated *in vacuo* and purified by flash chromatography (hexanes : EtOAc, 7:3) to give 0.070 g (35%) of thioester **15** as a mixture of E/Z isomers (E:Z, 3:1). The mixture was a tan, viscous oil: IR (CCl<sub>4</sub>) 3432 (w), 2933 (m), 2851 (m), 1760 (s), 1695 (s), 1511 (m), 1368 (m), 1221 (s); <sup>1</sup>H NMR (400

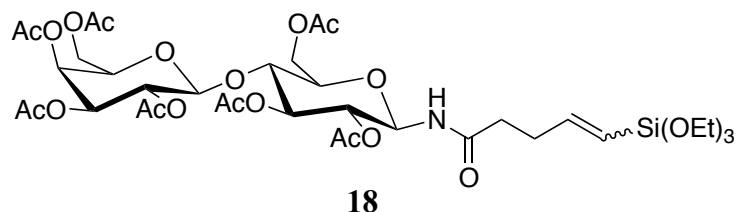
MHz, CDCl<sub>3</sub>)  $\delta$  1.23-1.34 (m, 5H), 1.54-1.62 (m, 4H), 1.91-2.06 (m, 14H), 2.15-2.25 (m, 6H), 2.83 (t,  $J$  = 7.2, 2H), 3.80 (dt,  $J$  = 2.0, 10.0, 1H), 4.05 (dd,  $J$  = 2.0, 12.4, 1H), 4.29 (dd,  $J$  = 4.0, 12.4, 1H), 4.88 (t,  $J$  = 9.6, 1H), 5.04 (t,  $J$  = 9.6, 1H), 5.16-5.46 (m, 4H), 6.20 (d,  $J$  = 9.6, 1H), 6.36 (d,  $J$  = 9.6, 0.3H); <sup>13</sup>C NMR (100 MHz, CDCl<sub>3</sub>)  $\delta$  21.0, 21.0 (2 C), 21.1, 28.3, 28.7, 28.8, 29.4, 29.5, 29.7, 29.8, 31.0, 32.8, 36.9, 62.1, 68.5, 71.0, 73.1, 73.9, 78.5, 128.2, 132.3, 170.0, 170.3, 171.1, 171.4, 173.3, 196.6; HRMS (ESI+) calcd. for C<sub>24</sub>H<sub>36</sub>NO<sub>11</sub>S [M + H]<sup>+</sup> 546.2009, found 546.1997. The E/Z ratio was determined by integration of the <sup>1</sup>H-NMR signals at 6.20 ppm (corresponding to the proton of the amide in the E isomer) and 6.36 ppm (corresponding to the proton of the amide in the Z isomer).



Allyl Benzyl ether (0.10, 0.70 mmol) was added via syringe to a solution of **2** (0.06 g, 0.14 mmol) dissolved in freshly distilled CH<sub>2</sub>Cl<sub>2</sub>. Grubb's second-generation catalyst **A** (0.01 g, 10 mol %) was added under argon, and the reaction mixture stirred at 40 °C for 24 hours. The reaction mixture was concentrated *in vacuo* and purified by flash chromatography (hexanes : EtOAc, 3:7) to give 0.02 g (25%) of ether **16** as a mixture of E/Z isomers (E:Z, could not be determined by <sup>1</sup>H NMR). The mixture was a tan, viscous oil: IR (CCl<sub>4</sub>) 3432 (w), 3027 (w), 2953 (w), 2925 (w), 2885 (w), 1760 (s), 1707 (s), 1548 (m), 1511 (m), 1229 (s), 1045 (s); <sup>1</sup>H NMR (400 MHz, CDCl<sub>3</sub>)  $\delta$  2.00-2.06 (m, 12H), 2.22-2.36 (m, 4H), 3.80 (dq,  $J$  = 2.0, 10.0, 1H), 3.93 (d,  $J$  = 5.2, 1H), 4.05 (dd,  $J$  = 2.0, 12.4, 1H), 4.29 (dd,  $J$  = 4, 12.4, 1H), 4.47 (s, 1H), 4.88 (t,  $J$  = 9.6, 1H), 5.04 (t,  $J$  =

9.6, 1H), 5.20-5.30 (m, 3H), 5.61-5.67 (m, 1H), 6.19 (d,  $J=9.2$ , 1H), 7.24-7.32 (m, 5H).

$^{13}\text{C}$  NMR (100 MHz,  $\text{CDCl}_3$ )  $\delta$  21.0 (2 C), 21.1, 21.2, 27.9, 36.2, 62.0, 68.5, 70.9, 71.0, 72.6, 73.1, 74.0, 78.6, 128.0, 128.2, 128.8, 129.0, 132.2, 138.6, 170.0, 170.3, 171.1, 172.0, 172.9; HRMS (ESI+) calcd. for  $\text{C}_{27}\text{H}_{36}\text{NO}_{11}$   $[\text{M} + \text{H}]^+$  550.2288, found 550.2312.



Vinyl triethoxysilane (0.3 mL, 1.5 mmol) was added via syringe to a solution of alkene **5** (0.13 g, 0.20 mmol) dissolved in freshly distilled  $\text{CH}_2\text{Cl}_2$ . Grubb's second-generation catalyst **A** (0.02 g, 10 mol %) was added under argon, and the reaction mixture stirred at 40 °C for 20 hours. Reaction mixture was concentrated *in vacuo* and purified by flash chromatography (hexanes:EtOAc, 8:2) to give 0.08 g (50%) of siloxane **18** as a mixture of E/Z isomers (E:Z, 3:1). The mixture was a dark, viscous oil: IR ( $\text{CCl}_4$ ) 3427 (w), 2974 (w), 2925 (w), 2884 (w), 1756 (s), 1707 (s), 1552 (m), 1213 (s), 1074 (s);  $^1\text{H}$  NMR (400 MHz,  $\text{CDCl}_3$ )  $\delta$  1.17-1.24 (m, 9H), 1.93-2.415 (m, 25H), 3.70-3.85 (m, 8H), 4.01-4.14 (m, 3H), 4.37-4.45 (2H), 4.76-4.82 (m, 1H), 4.90 (dd,  $J=3.6, 10.4$ , 1H), 5.05-5.43 (m, 5H), 6.10 (d,  $J=9.2$ , 1H), 6.18 (d,  $J=9.2$ , 0.29H), 6.35 (dt,  $J=6.0, 18.8$ , 1H);  $^{13}\text{C}$  NMR (100 MHz,  $\text{CDCl}_3$ )  $\delta$  18.6, 18.6, 20.9, 21.0, 21.1 (2 C), 21.1 (2 C), 21.2, 21.3, 31.7, 35.3, 58.9, 61.3, 62.4, 67.0, 69.4, 71.1, 71.4, 72.7, 74.8, 76.4, 78.5, 101.3, 120.9, 151.1, 169.4, 169.7, 169.8, 170.5, 170.6, 170.7, 170.8, 171.8, 172.5; HRMS (ESI+) calcd. for  $\text{C}_{37}\text{H}_{58}\text{NO}_{21}\text{Si}$   $[\text{M} + \text{H}]^+$  880.3271, found 880.3264. The E/Z ratio was determined by

integration of the  $^1\text{H}$ -NMR signals at 6.10 ppm (corresponding to the proton of the amide in the E isomer) and 6.18 ppm (corresponding to the proton of the amide in the Z isomer).

#### 4.3 *Preparation of Glucose-Functionalized Glass*

A glass cover slip (Fisherbrand Microscope Cover Glass) was immersed in piranha solution (3 : 1 concentrated  $\text{H}_2\text{SO}_4$  : 30%  $\text{H}_2\text{O}_2$ ) for 1 hour, rinsed with Millipore  $\text{H}_2\text{O}$  (50 mL), and then immersed in 7 : 1 buffered oxide etch with surfactant from J. T. Baker for 1 hour. The slide was then rinsed with Millipore  $\text{H}_2\text{O}$  followed by sonication in Millipore  $\text{H}_2\text{O}$  for 10 minutes. The sonication process was repeated with fresh Millipore water. The slide was then rinsed with dichloromethane (50 mL) and dried in an oven at 200 °C for 1.5 hours. After cooling in a desiccator, a solution of glucose-siloxane 1 dissolved in dichloromethane was added drop wise to one side of the glass slide. After sitting undisturbed under nitrogen atmosphere for 30 minutes, the glucose siloxane/dichloromethane solution was reapplied. The glass slide sat undisturbed under nitrogen atmosphere for an additional 30 minutes. The glass slide was rinsed with dichloromethane (20 mL) and was allowed to sit undisturbed under nitrogen atmosphere for 12 hours.

#### 4.4 *XPS Analysis of Bare and Glucose-Functionalized Glass Slides*

The XPS data was collected on a Kratos Axis 165 X-ray photoelectron spectrometer operating in hybrid mode using monochromatic Al  $\text{K}\alpha$  radiation. The instrument maintained a pressure of  $5 \times 10^{-9}$  Torr or better during data collection. The data were collected at a 20° take-off-angle (with respect to the sample plane). Charge

neutralization was required to compensate for sample charging. Survey spectra (not shown here) were collected at a pass energy of 160 eV, while high resolution spectra were collected at a pass energy of 20 eV. All spectra were calibrated to the hydrocarbon peak at 285 eV. The C 1s spectra were fit with a Shirley background and peaks of a 30% Lorentzian 70% Gaussian product function.

#### 4.5 *Preparation of Glucose-Functionalized Bragg Fiber*

A fiber Bragg grating sensor, etched to a diameter of 5  $\mu\text{m}$ , was immersed in a solution of glucose-siloxane conjugate **3** in 95% ethanol for 1 hour at 25 °C. The fiber was then immersed in a 0.2M NaOEt/EtOH solution for 2 hours at 25 °C. The fiber was removed from the sodium ethoxide solution and rinsed with ethanol and then Millipore water.

#### 4.6 *Preparation of APTES-Functionalized Fluorescent Silica Nanoparticles*

Fluorescent silica nanoparticles were prepared as described in chapter 3 of this dissertation. To an evenly dispersed suspension of fluorescent silica nanoparticles (0.01 g) in toluene (5 mL) was added 3-aminopropyltriethoxysilane (APTES) (1mL; 0.95 g; 4.3 mmol). The reaction mixture stirred at room temperature for 2 hours under an argon atmosphere. The particles were then washed with toluene (3 x 5mL) and dried *in vacuo*.

#### 4.7 *Preparation of Lactose-Functionalized Fluorescent Silica Nanoparticles via Reductive Amination*

APTES-functionalized fluorescent silica nanoparticles were evenly suspended in borate buffer (2.5 mL, pH = 8.0). A solution of NaCl (0.15 g) in borate buffer (0.5 mL) was added to make a 1M NaCl solution. Lactose (0.05 g; 0.15 mmol) in borate buffer (0.5 mL) was added to the reaction mixture followed by NaCNBH<sub>3</sub> (0.05 g; 0.80 mmol) in borate buffer (0.5 mL). The reaction mixture stirred at room temperature for 4 days. The particles were then washed with Millipore water (4 x 5 mL) and resuspended in Millipore water (1mL).

#### 4.8 *Phenol/Sulfuric Acid Colorimetric Assay*

A 0.25 mL aliquot of lactose-functionalized fluorescent silica nanoparticles (0.005 g) suspended in Millipore water (1 mL) was placed in a glass test tube. 0.125 mL of a 0.53 M phenol/H<sub>2</sub>O solution was added to the suspension, followed by 0.625 mL of concentrated H<sub>2</sub>SO<sub>4</sub> (the stream of acid was directed toward the surface of the solution rather than against the side of the test tube). After 10 minutes, the samples were gently vortexed. After the solution sat undisturbed for an additional 30 minutes, the absorbance of the solution was measured using an Ocean Optics USB 2000 Spectrometer.

### **Acknowledgements**

The author acknowledges Christopher Stanford, Geunmin Ryu, Mario Dagenais, and Karen Gaskell for the significant contributions they made to the research and discoveries presented throughout this chapter.

## 5 References

- 1) de la Fuente, J. M.; Penades, S. *Biochim. Biophys. Acta. Gen. Subj.* **2006**, 1760, 636-651.
- 2) Ojeda, R.; de Paz, J. L.; Barrientos, A. G.; Martin-Lomas, Manuel; Penades, S. *Carbohydr. Res.* **2007**, 342, 448-459.
- 3) Katz, E.; Willner, I. *Angew. Chem., Int. Ed.* **2004**, 43, 6042-6108.
- 4) Niemeyer, C. M. *Angew. Chem., Int. Ed.* **2001**, 40, 4128-4158.
- 5) Blodgett, K. B. *J. Am. Chem. Soc.* **1935**, 57, 1007-1022.
- 6) Blodgett, K. B.; Langmuir, I. *Phys. Rev.* **1937**, 51, 964-982.
- 7) Bigelow, W. C.; Pickett, D. L.; Zisman, W. A. *J. Colloid Sci.* **1946**, 1, 513.
- 8) Bain, C. D.; Troughton, E. B. *J. Am. Chem. Soc.* **1989**, 111, 321-35.
- 9) Ulman, A. *Chem. Rev.* **1996**, 96, 1533-1554.
- 10) Love, J. C.; Estroff, L. A.; Kriebel, J. K.; Nuzzo, R. G.; Whitesides, G. M. *Chem. Rev.* **2005**, 105, 1103-1169.
- 11) Nuzzo, R. G.; Allara, D. L. *J. Am. Chem. Soc.* **1983**, 105, 4481-4483.
- 12) Nuzzo, R. G.; Zegarski, B. R.; Dubois, L. H. *J. Am. Chem. Soc.* **1987**, 109, 733-740.
- 13) Troughton, E. B.; Bain, C. D.; Whitesides, G. M.; Nuzzo, R. G.; Allara, D. L.; Porter, M. *Langmuir* **1988**, 4, 365-385.
- 14) Lee, L.-H. *SPI (Soc. Plast. Ind.) Reinf. Plast./Compos. Div., Annu. Tech. Conf., Proc., 23rd* **1968**, 9D-1-9D-14.
- 15) Lee, L.-H. *J. Colloid Interf. Sci.* **1968**, 27, 751-60.
- 16) Zisman, W. A. *Ind. Eng. Chem., Prod. Res. Develop.* **1969**, 8, 98-111.

- 17) Sagiv, J. *J. Am. Chem. Soc.* **1980**, 102, 92-98.
- 18) Kahn, F. J.; Taylor, G. N.; Schonhorn, H. *Proc. IEEE.* **1973**, 61, 823-8.
- 19) Silverman, B. M.; Wieghaus, K. A.; Schwartz, J. *Langmuir* **2005**, 21, 225-228.
- 20) Cattani-Scholz, A.; Pedone, D.; Dubey, M.; Neppl, S.; Nickel, B.; Feulner, P.; Schwartz, J.; Abstreiter, G.; Tornow, M. *ACS Nano* **2008**, 2, 1653-1660.
- 21) Tsoi, S.; Fok, E.; Sit, J. C.; Veinot, J. G. C. *Chem. Mater.* **2006**, 18, 5260-5266.
- 22) Wu, W.; He, Q.; Jiang, C. *Nanoscale Res. Lett.* **2008**, 3, 397-415.
- 23) Allara, D. L.; Nuzzo, R. G. *Langmuir* **1985**, 1, 45-52.
- 24) Ogawa, H.; Chihera, T.; Taya, K. *J. Am. Chem. Soc.* **1985**, 107, 1365-1369.
- 25) Schlotter, N. E.; Porter, M.D. *Chem. Phys. Lett.* **1986**, 132, 93.
- 26) Tao, Y. T. *J. Am. Chem. Soc.* **1993**, 115, 4350-4358.
- 27) Howarter, J. A.; Youngblood, J. P. *Langmuir* **2006**, 22, 11142-11147.
- 28) Chinwangso, P.; Jamison, A. C.; Lee, T. R. *Acc. Chem. Res.* **2011**, 44, 511-519.
- 29) Wu, W.; He, Q.; Jiang, C. *Nanoscale Res. Lett.* **2008**, 3, 397-415.
- 30) Caruso, F. *Adv. Mater.* **2001**, 13, 11-22.
- 31) Willner, I.; Katz, E. *Angew. Chem., Int. Ed.* **2000**, 39, 1181-1218.
- 32) Nobs, L.; Buchegger, F.; Gurny, R.; Allemann, E. *J. Pharm. Sci.* **2004**, 93, 1980-1992.
- 33) Houseman, B. T.; Gawalt, E. S.; Mrksich, M. *Langmuir* **2003**, 19, 1522-1531.
- 34) Zhang, Q.; Huang, R. F.; Guo, L.-H. *Chin. Sci. Bull.* **2009**, 54, 2620-2626.
- 35) Wu, Y.; Chen, C.; Liu, S. *Anal. Chem.* **2009**, 81, 1600-1607.
- 36) Tang, D.; Su, B.; Tang, J.; Ren, J.; Chen, G. *Anal. Chem.* **2010**, 82, 1527-1534.
- 37) Lahiri, J.; Isaacs, L.; Tien, J.; Whitesides, G. M. *Anal. Chem.* **1999**, 71, 777-90.



- 38) Azioune, A.; Ben Slimane, A.; Hamou, L. A.; Pleuvy, A.; Chehimi, M. M.; Perruchot, C.; Armes, S. P. *Langmuir* **2004**, 20, 3350-3356.
- 39) Kim, M. I.; Ham, H. O.; Oh, S.-D.; Park, H. G.; Chang, H. N.; Choi, S.-H. *J. Mol. Catal. B: Enzym.* **2006**, 39, 62-68.
- 40) Wang, Z.; Miu, T.; Xu, H.; Duan, N.; Ding, X.; Li, S. *J. Microbiol. Methods.* **2010**, 83, 179-184.
- 41) Zhang, X.; Song, C.; Chen, L.; Zhang, K.; Fu, A.; Jin, B.; Zhang, Z.; Yang, K. *Biosens. Bioelectron.* **2011**, 26, 3958-3961.
- 42) Wei, H.; Zhou, L.; Li, J.; Liu, J.; Wang, E. *J. Colloid Interf. Sci.* **2008**, 321, 310-314.
- 43) Betancor, L.; Lopez-Gallego, F.; Hidalgo, A.; Alonso-Morales, N.; Cesar Mateo, G. D.-O.; Fernandez-Lafuente, R.; Guisan, J. M. *Enzyme Microb. Technol.* **2006**, 39, 877-882.
- 44) Xu, H.; Zhang, Z. *Biosens. Bioelectron.* **2007**, 22, 2743-2748.
- 45) Angeloni, S.; Ridet, J. L.; Kusy, N.; Gao, H.; Crevoisier, F.; Guinchard, S.; Kochhar, S.; Sigrist, H.; Sprenger, N. *Glycobiology* **2004**, 15, 31-41.
- 46) Sigrist, H.; Collioud, A.; Clemence, J.-F.; Gao, H.; Luginbuehl, R.; Saenger, M.; Sundarababu, G. *Opt. Eng.* **1995**, 34, 2339-48.
- 47) Maltzahn, G.; Ren, Y.; Park, D.; Kotamraju, V. R.; Jayakumar, J.; Fogal, M.; Ruoslahti, E.; Bhatia, S. *Bioconjugate Chem.* **2008**, 19, 1570-1578.
- 48) Houseman, B. T.; Huh, J. H.; Kron, S. J.; Mrksich, M. *Nat. Biotechnol.* **2002**, 20, 270-274.
- 49) Godula, K.; Bertozzi, C. R. *J. Am. Chem. Soc.* **2010**, 132, 9963-9965.

- 50) Zhi, Z.-L.; Powell, A. K.; Turnbull, J. E. *Anal. Chem.* **2006**, 78, 4786-4793.
- 51) de Boer, A. R.; Hokke, C. H.; Deelder, A. M.; Wuhrer, M. *Anal. Chem.* **2007**, 79, 8107-8113.
- 52) Park, S.; Lee, M.-R.; Shin, I. *Bioconjugate Chem.* **2009**, 20, 155-162.
- 53) Zhou, X.; Turchi, C.; Wang, D. *J. Proteome Res.* **2009**, 8, 5031-5040.
- 54) Clo, E.; Blixt, O.; Jensen, K. J. *Eur. J. Org. Chem.* **2010**, 540-554.
- 55) Toshima, K.; Tatsuta, K. *Chem. Rev.* **1993**, 93, 1503-1531.
- 56) Yoshimura, Y.; Shimizu, H.; Hinou, H.; Nishimura, S. *Tetrahedron Lett.* **2005**, 46, 4701-4705.
- 57) Barrientos, A.; de la Fuente, J.; Rojas, T.; Fernandez, A.; Penades, S. *Chem. Eur. J.* **2003**, 9, 1909-1921.
- 58) Shimizu, H.; Sakamoto, M.; Nagahori, N.; Nishimura, S. *Tetrahedron* **2007**, 63, 2418-2425.
- 59) Lin, C.; Yeh, Y.; Yang, C'; Chen, C.; Chen, G.; Chen, C.; Wu, Y. *J. Am. Chem. Soc.* **2002**, 124, 3508-3509.
- 60) Halkes, M. K.; de Souza, A. C.; Maljaars, E.; Gerwig, G.; Kamerling, J. *Eur. J. Org. Chem.* **2005**, 3650-3659.
- 61) Zhang, Y.; Luo, S.; Tang, Y.; Hou, K.; Cheng, J.; Zeng, X.; Wang, P. G. *Anal. Chem.* **2006**, 78, 2001-2008.
- 62) Boubbou, K.; Gruden, C.; Huang, X. *J. Am. Chem. Soc.* **2007**, 129, 13392-13393.
- 63) Earhart, C.; Jana, N.; Erathodiyil, N.; Ying, J. *Langmuir* **2008**, 24, 6215-6219.
- 64) Damkaci, F.; DeShong, P. *J. Am. Chem. Soc.* **2003**, 125, 4408-4409.

- 65) Kadalbajoo, M.; Park, J.; Opdahl, A.; Suda, H.; Kitchens, C.; Garno, J.; Batteas, J.; Tarlov, M.; DeShong, P.; *Langmuir* **2007**, 23, 700-707.
- 66) De, M.; Ghosh, P. S.; Rotello, V. M. *Adv. Mater.* **2008**, 20, 4225-4241.
- 67) Stanford, C. J.; Ryu, G.; Dagenais, M.; Hurley, M. T.; Gaskell, K. J.; De Shong, P. *J. Sens.* **2009**, Article ID 982658.
- 68) Ryu, G.; Dagenais, M.; Hurley, M. T.; De Shong, P. *IEEE J. Sel. Top. Quantum Electron.* **2010**, 16, 647-653.
- 69) Buskas, T.; Soderberg, E.; Konradsson, P.; Fraser-Reid, B. *J. Org. Chem.* **2000**, 65, 958-963.
- 70) Chatterjee, A. K.; Morgan, J. P.; Scholl, M.; Grubbs, R. H. *J. Am. Chem. Soc.* **2000**, 122, 3783-3784.
- 71) Grubbs, R. H. *Tetrahedron* **2004**, 60, 7117-7140.
- 72) Chatterjee, A.; Grubbs, R. H. *Angew. Chem., Int. Ed.* **2002**, 41, 3171-3174.
- 73) O'Leary, D. J.; Blackwell, H. E.; Washenfelder, R. A.; Grubbs, R. H. *Tetrahedron Lett.* **1998**, 39, 7427-7430.
- 74) Chatterjee, A. K.; Grubbs, R. H. *Org. Lett.* **1999**, 1, 1751-1753.
- 75) Blackwell, H. E.; O'Leary, D. J.; Chatterjee, A. K.; Washenfelder, R. A.; Bussmann, D. A.; Grubbs, R. H. *J. Am. Chem. Soc.* **2000**, 122, 58-71.
- 76) Choi, T.-L.; Chatterjee, A. K.; Grubbs, R. H. *Angew. Chem., Int. Ed.* **2001**, 40, 1277-1279.
- 77) Chatterjee, A. K.; Sanders, D. P.; Grubbs, R. H. *Org. Lett.* **2002**, 4, 1939-1942.
- 78) Chatterjee, A. K.; Choi, T.-L.; Sanders, D. P.; Grubbs, R. H. *J. Am. Chem. Soc.* **2003**, 125, 11360-11370.

- 79) O'Leary, D. J.; Blackwell, H. E.; Washenfelder, R. A.; Grubbs, R. H.  
*Tetrahedron Lett.* **1998**, 39, 7427.
- 80) Roy, R.; Das, S. K. *Chem. Commun.* **2000**, 519-529.
- 81) Leeuwenburgh Michiel, A.; van der Marel Gijsbert, A.; Overkleeft Herman, S.  
*Curr. Opin. Chem. Biol.* **2003**, 7, 757-765.
- 82) Jorgensen, M.; Hadwiger, P.; Madsen, R.; Stutz, A. E.; Wrodnigg, T. M. *Curr. Org. Chem.* **2000**, 4, 565-588.
- 83) Hu, Y.-J.; Roy, R. *Tetrahedron Lett.* **1999**, 40, 3305-3308.
- 84) Vernall Andrea, J.; Abell Andrew, D. *Org. Biomol. Chem.* **2004**, 2, 2555-2557.
- 85) Hadwiger, P.; Stutz, A. E. *Synlett.* **1999**, 1787-1789.
- 86) Plettenburb, O.; Mui, C.; Bodmer-Narkevitch, V.; Wong, C. *Adv. Synth. Catal.* **2002**, 344, 622-626.
- 87) Bruchner, P.; Koch, D.; Voigtmann, Ulrike, Blechert, S. *Synth. Commun.* **2007**, 37, 2757-2769.
- 88) Timmer, M.; Chumillas, M. V.; Donker-Koopman, W.; Aerts, J. M. F. G.; van der Marel, G.; Overkleeft, H. *J. Carbohydr. Chem.* **2005**, 24, 335-351.
- 89) Wan, Q.; Cho, Y. S.; Lambert, T.; Danishefsky, S. *J. Carbohydr. Chem.* **2005**, 24, 425-440.
- 90) Otsuka, H.; Akiyama, Y.; Nagasaki, Y. Kataoka, K. *J. Am. Chem. Soc.* **2001**, 123, 8226-8230.
- 91) Houseman, B. T.; Mrksich, M. *Chem. Biol.* **2002**, 9, 443-454.
- 92) Vollhardt, D. *J. Phys. Chem. C.* **2007**, 111, 6805-6812.
- 93) Borch, R. F.; Bernstein, M. D.; Durst, H. D. *J. Amer. Chem. Soc.* **1971**, 93,

2897-904.

- 94) Dubois, M.; Gilles, K. A.; Hamilton, J. K.; Rebers, P. A.; Smith, F. *Anal. Chem.* **1956**, 28, 350-356.
- 95) Gildersleeve, J. C.; Oyelaran, O.; Simpson, J. T.; Allred, B. *Bioconjugate Chem.* **2008**, 19, 1485-1490.
- 96) Damkaci, F. *Ph.D. Thesis, University of Maryland, College Park.* **2004**.
- 97) Park, J. *Ph.D. Thesis, University of Maryland, College Park.* **2008**.

## **Chapter 2: Mesoporous Silica as Controlled Release Devices: Synthesis, Characterization, and pH-Sensitive Release**

### **1 Introduction**

Since the Mobil Corporation first introduced Mobil Crystalline Material (MCM)-41<sup>1</sup>, a large body of research has been devoted to developing novel mesoporous silica materials with controlled pore size and uniform pore structure, such as Santa Barbara amorphous silica (SBA)-n,<sup>2</sup> Michigan State University silica (MSU)-n,<sup>3</sup> folded sheet-derived mesoporous silica (FSM)-16,<sup>4</sup> and Korean Institute of Technology silica (KIT)-1.<sup>5-7</sup> These porous silica materials are generally ten to hundreds of microns in dimension, contain regular, periodic pores in the mesoscale range (2-50 nm), and are used as catalysts and absorption/purification materials.<sup>1, 7</sup> However, integrating mesopore formation strategies into standard silica nanoparticle synthesis lead to a new class of mesoporous materials that are now known as mesoporous silica nanoparticles (MSN). Researchers are able to create monodisperse MSN with high surface areas, large cavity volumes, and are able to easily functionalized the silica surface with a range of organic and biologically relevant molecules—making these porous materials ideal for controlled release systems and vehicles for the delivery of chemotherapeutics.<sup>6-52</sup> This chapter reviews the methods that are used to synthesize mesoporous silica materials, and then focuses on the work that has been done by DeShong and coworkers to create MSN-based controlled release and drug delivery systems.

### 1.1 Preparation of Mesoporous Silica

Mesoporous silica materials are synthesized by the templated polymerization of a silica precursor around amphiphilic surfactant or nonionic block copolymer self-assembled mesophase structures.<sup>1-3</sup> The surfactant scaffold is then removed via calcination or chemical extraction (Figure 17). Electrostatic, hydrogen bonding, and van der Waals interactions between the surfactant and a silica species drive templation.<sup>53-54</sup> For example, under alkaline conditions, formation of MCM-41 and MCM-48 occurs through the association of silicate anions with cationic surfactant molecules, represented as  $S^+I^-$ , where  $S^+$  is the cationic surfactant and  $I^-$  is the silicate anion.<sup>53-54</sup> Other MSN types, including SBA-1 and SBA-3, are formed in acidic media where the acid counter-anion is used to mediate the coordination between cationic surfactants and positively charged silica precursors. Such templated pathways are represented as  $S^+X^-I^+$ , where  $X^-$  is  $Cl^-$  or  $Br^-$  and  $I^+$  is a positively charged silica species.<sup>53-54</sup>

In aqueous solutions, above critical micelle concentrations, surfactants form micelles, vesicles, and/or microemulsions. However, at higher concentrations (30% by wt. or greater), surfactant micelles and polar lipids self-assemble into a range of lyotropic liquid-crystalline mesophases with different 3-dimensional structures.<sup>55</sup> Mesophases are thermodynamically distinct phases between a low-temperature solid phase and a high-temperature isotropic liquid phase and are formed as a result of either repulsive or attractive inter-micelle interactions.<sup>55-56</sup> Mesophases that result from repulsive inter-micelle interactions are typically single liquid crystalline phases that fill an entire sample volume, while mesophases that result from attractive inter-micelle interactions phase separate and are found within two-phase systems.<sup>56</sup> An example of a mesophase is the

hexagonal array of rod-like micelles observed with concentrated aqueous solutions of cetyltrimethylammonium bromide (CTAB). The self-assembly of the micelles in the CTAB/H<sub>2</sub>O mesophase is governed by long-range repulsive interactions between individual micelles. The micelles arrange in a manner in which inter-micelle spacing is maximized, thereby creating a single liquid crystalline mesophase throughout the sample volume and minimizing the Gibbs free energy of the system.<sup>56</sup>

Though a wide variety of mesophase structures have been reported, the most common are lamellar, hexagonal, and cubic.<sup>55, 57</sup> The structure of the mesophase is dependent upon the physical properties of the surfactant and can be defined by the local effective surfactant packing parameter,  $g$ , where  $g = V/a_0l$ , and  $V$  is the total volume of the surfactant chains including any cosolvent molecules incorporated between the chains,  $a_0$  is the effective head group area at the micelle surface, and  $l$  is the kinetic surfactant tail length or the curvature elastic energy.<sup>55-57</sup> Mesophase morphology is also highly dependent on the concentration of the surfactant, pressure, temperature, and co-solvents or additives.<sup>55</sup>

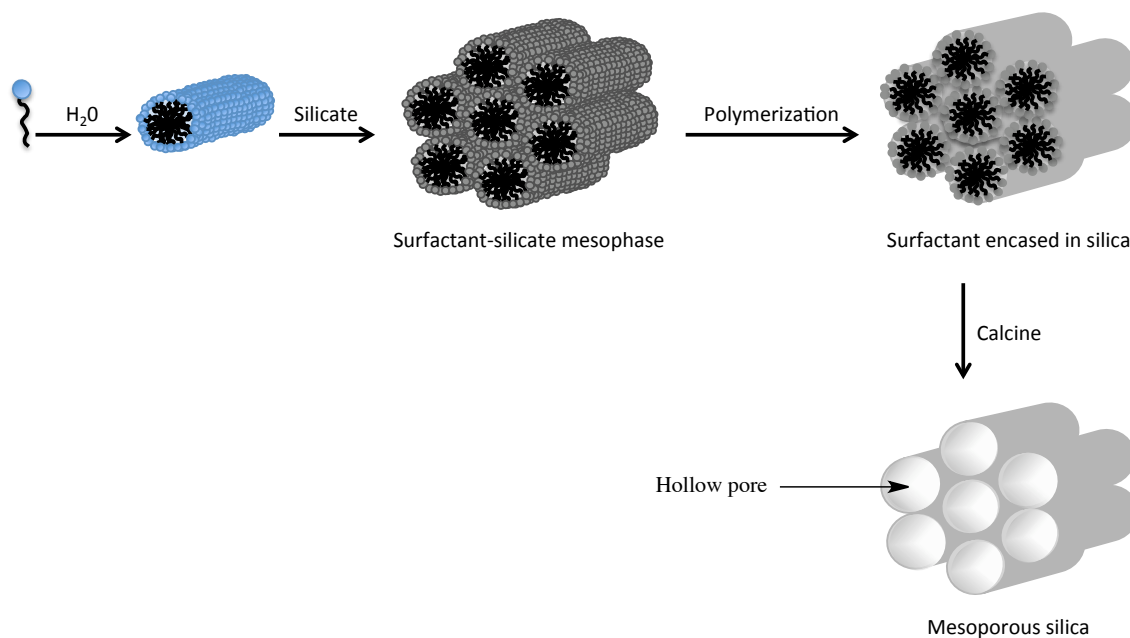
Stuckey and coworkers have shown that the addition of a silica precursor to a micellar cationic surfactant solution under aqueous alkaline conditions results in the formation of surfactant-silicate mesophases. Stucky et. al. hypothesize that the formation of mesophase assemblies at surfactant concentrations lower than typically observed is due to the presence of anionic silicate species formed from the hydrolysis of the silica precursor under the basic reaction conditions.<sup>56</sup> The multivalent, anionic silicate species associate with the cationic head groups of the surfactant on the surface of preformed micelles and mediate the assembly of the micelles into liquid crystalline mesophases by



increasing attractive inter-micelle interactions.<sup>56</sup> Stucky states that the increased attractive interactions between micelles results in micellar aggregation and phase separation, “whereby one or more concentrated silicate-surfactant-rich phases adopt morphologies that minimize the total Gibbs free energy...”<sup>56</sup>

As an example of surfactant-silicate mesophase formation followed by templated silicate polymerization, consider the mechanism of MCM-41 silica formation, which is outlined in Figure 17. MCM-41 is prepared using cetyltrimethylammonium bromide (CTAB) as the surfactant and a silica precursor, such as tetraethyl orthosilicate (TEOS), under aqueous alkaline conditions. The sequence of events leading to the formation of MCM-41 silica material is as follows: (1) CTAB molecules self-assemble into rod-like micelles. (2) Under basic conditions, the silica precursor is hydrolyzed, forming silicate anions. (3) Silicate anions displace the bromide ions associated with the positively charge ammonium ions on the surface of the CTAB micelles and facilitate the formation of hexagonal surfactant-silicate mesophases. (4) Silicate polymerization occurs on the surface and between the hexagonally arrayed micelles resulting in surfactant mesophases encased in a silica matrix. (5) Removal of the surfactant via calcination or chemical extraction leads to the formation of hollow pores within the polymerized silica matrix.<sup>1, 56</sup>

**Figure 17:** Templated MCM-41 synthesis.<sup>1, 56</sup>



Due to the fact that silicate polymerization is template by the surfactant-silicate mesophase, the structure of the mesophase dictates the pore morphology of the resulting mesoporous silica. Stucky and coworkers have demonstrated how the choice of surfactant and reaction conditions (specifically temperature, reaction time, and pH) determine the pore architecture of mesoporous silica materials.<sup>57</sup> Table 4 lists common mesoporous silica systems with their mesophase structure and the surfactant used to prepare the material. Refer to the cited reference for reactions conditions.

**Table 4:** Mesoporous silica materials

Silica Type	Surfactant	Solvent / Base or Acid	Mesophase Structure	Reference
MCM-41	$C_{16}H_{33}(CH_3)_3 N^+$	H <sub>2</sub> O / NaOH	2D hexagonal $p6m$	1
	$C_{16-6-16}^a$	H <sub>2</sub> O / NaOH		57
MCM-48	$C_{16}H_{33}(CH_3)_3 N^+$	H <sub>2</sub> O, EtOH / NH <sub>4</sub> OH	Cubic $Ia3d$	58
	$C_{22-12-22}^a$	H <sub>2</sub> O / NaOH		57
SBA-1	$C_{16}H_{33}(CH_2CH_3)_3 N^+$	H <sub>2</sub> O / HCl	Cubic $Pm3n$	57
SBA-2	$C_{16-2-1}^b$	H <sub>2</sub> O / NaOH	3D hexagonal $P6_3/mmc$	57
SBA-15	EO <sub>20</sub> PO <sub>70</sub> EO <sub>20</sub> <sup>c</sup>	H <sub>2</sub> O / HCl	2D hexagonal $p6mm$	54
SBA-16	EO <sub>106</sub> PO <sub>70</sub> EO <sub>106</sub> <sup>d</sup>	H <sub>2</sub> O / HCl	Cubic $Im3m$	54

a: A “Gemini surfactant”. A synthetic amphiphile with the general formula  $C_{m-s-m}$  that contains, in sequence, a hydrophobic chain of length, m, an ionic group, a spacer group of length, s, an ionic group, and a hydrophobic chain of length, m. b: A “divalent surfactant”. A synthetic amphiphile with the general formula  $C_{n-s-l}$  that contains a hydrophilic chain of length, n, an ionic group, a spacer of length, s, and a terminal ionic group. c: Commercial name: Pluronic F123. d: Commercial name: Pluronic F12

## 1.2 Mesoporous Silica Nanoparticles

In their seminal 1968 publication, Stöber and colleagues describe the preparation of solid silica spheres of uniform size using alkyl-siloxanes and ammonium hydroxide in alcohol/water mixtures.<sup>59</sup> Particle sizes can be controlled by the choice of alcohol and range from 50 nm to 2  $\mu$ m. This method for creating monodispersed, sub-micron sized silica particles is now widely known as the “Stöber method”.

Materials now known as mesoporous silica nanoparticles (MSN) were first reported by Unger.<sup>60</sup> Unger et al. incorporated silica mesopore formation principles into the Stöber method. Introducing cetyltrimethylammonium bromide (CTAB) into Stöber’s general synthetic procedure yielded spherical silica particles having diameters ranging from 400 nm to 1  $\mu$ m and containing pore structures similar to that of MCM-41.<sup>60</sup> Since that time, researchers have modified and refined this strategy to create MSN systems with controlled particle size and monodispersity.<sup>61-63</sup> However, both Cui and Lin have demonstrated that mesoporous silica nanoparticles can be prepared from classic MCM-41 formation methods using dilute reaction conditions and by controlling the rate of silica

precursor addition.<sup>20, 39-40, 64</sup> In addition, Imai and coworkers<sup>65</sup> have prepared nano-sized, mesoporous silica particles using a binary surfactant system, while Brinker<sup>66-67</sup> and Zachariah<sup>68</sup> have employed aerosol techniques to prepare MSN.

### *1.3 MSN as Controlled Release, Drug Delivery Systems*

Site-specific, controlled-release drug delivery systems are highly sought after due to their potential to increase the efficiency and reduce the side effects of systemic chemotherapy. Conceptually, the goal of a site-specific, controlled-release drug delivery system is to carry a payload of chemotherapeutics directly to a pre-selected type of cancerous tissue. Once the loaded, drug delivery system has reached the tumor, release of the chemotherapeutic payload from the device is triggered. Thus, drug delivery systems would increase the amount of drug that reaches the tumor and reduce the collateral damage of the drug to healthy tissue and cells. Mesoporous silica nanoparticles (MSN) have emerged as material well suited for site-specific, controlled-release drug delivery systems due to their high surface area and large payload capacity, ease of surface modification/functionalization, and biocompatibility.<sup>69</sup>

Vallet-Regi and coworkers were the first to study MCM-41 material as drug delivery systems and proved that MCM-41 could be used to absorb and then later release ibuprofen.<sup>8</sup> Since their initial work, they and others have demonstrated that surface-functionalization<sup>9-13, 24</sup>, pore size<sup>14-16</sup>, pore structure<sup>15-17</sup>, loading conditions<sup>18</sup>, as well as the chemical characteristics of the loaded analyte<sup>18-19</sup> affect both the absorption and release of the analyte into and out of porous silica material. Importantly, these studies show that attractive<sup>9</sup> and repulsive<sup>13</sup> electrostatic interactions as well as hydrophobic

effects<sup>24</sup> between the entrapped molecules and the silica surface affect the rate of release from these porous materials. Recently, Ng et al. used confocal laser scanning microscopy to show that cationic molecules have a different release profile than anionic molecules from mesoporous silica spheres due to the affinity between the cationic molecules and the negatively charged silica surface.<sup>19</sup>

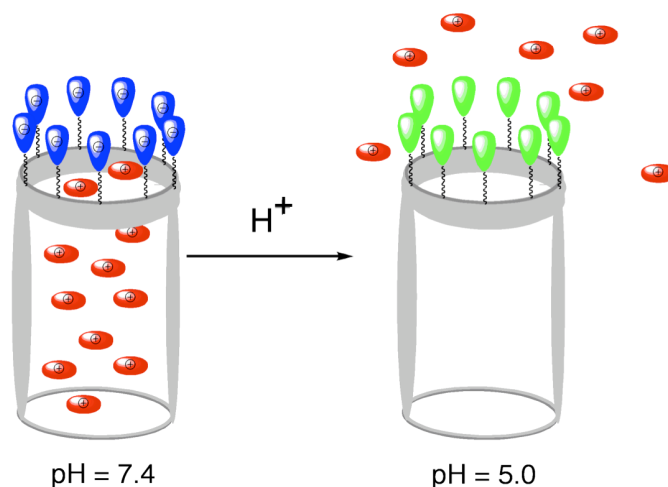
While the above systems utilize pore size and electrostatic interactions for controlled release, others have developed more complex systems in which stimuli responsive capping agents, supramolecular assemblies, or polymers are employed to control the release of guest molecules. Fujiwara demonstrated the potential of stimuli responsive controlled release devices by controlling the uptake and release of guest molecules into and out of coumarin-functionalized MCM-41 using UV radiation.<sup>26</sup> Lin and coworkers have designed several systems in which CdS or gold nanoparticles are used to “cap” loaded MSN. The nanoparticles can be removed from the surface of the MSN upon the addition of a reducing agent or by irradiating the system with 365 nm light.<sup>6-7, 20-22</sup> More recently, Zhu and Guo have developed a pH-sensitive drug delivery systems by using acid sensitive zinc oxide quantum dots to seal the pores of drug-loaded MSN.<sup>44</sup> Zink and Stoddart have made controlled release systems from mesoporous silica films and particles using supramolecular nanovalves that are governed by redox chemistry<sup>27-29</sup>, pH<sup>30-33</sup>, or light<sup>34</sup>. Kim has also reported a gated-release system utilizing a pH responsive supramolecular motif on the MSN surface.<sup>35</sup> Additionally, both You<sup>25</sup> and Bhatia<sup>43</sup> have reported temperature-controlled release devices utilizing a surface bound temperature-responsive polymer, while Hong<sup>36</sup> and Hu<sup>45</sup> have created systems in which release is governed by a pH responsive polymer. Similarly, Lin et al. designed insulin

loaded MSN that are sealed with glucose responsive proteins.<sup>23</sup> And, very recently, Wang<sup>37</sup> coated the surface of MSN with polyelectrolyte multilayers to obtain a controlled release system that is responsive toward reducing agents, while Liu and coworkers<sup>46</sup> used a pH-sensitive polyelectrolyte multilayer regime to control the release of cisplatin from MSN.

## **2 Results and Discussion**

It is established that MSN can be taken into a cell through endocytosis.<sup>7, 69</sup> The pH inside an endosome is lower than cytosolic environment in a cell.<sup>70</sup> Thus, one can anticipate that a release strategy that employs pH as a trigger for release would be particularly attractive.<sup>32, 44-51</sup> Ultimately, our goal is to create a MSN drug delivery system that shows no release at physiological pH (7.4) and fast release at pH 5, the typical pH within an endosome (Figure 18). This type of delivery system would ensure that the entrapped drug would be released from the nanoparticle only after the nanoparticle has been endocytosed into the target tissue. Herein, we report on our initial steps toward such a system and the work that has been done to maximize the loading efficiency of mesoporous silica nanoparticles and to better understand how surface coverage and pH affect the release of the cationic dye, rhodamine 6G, from MSN.

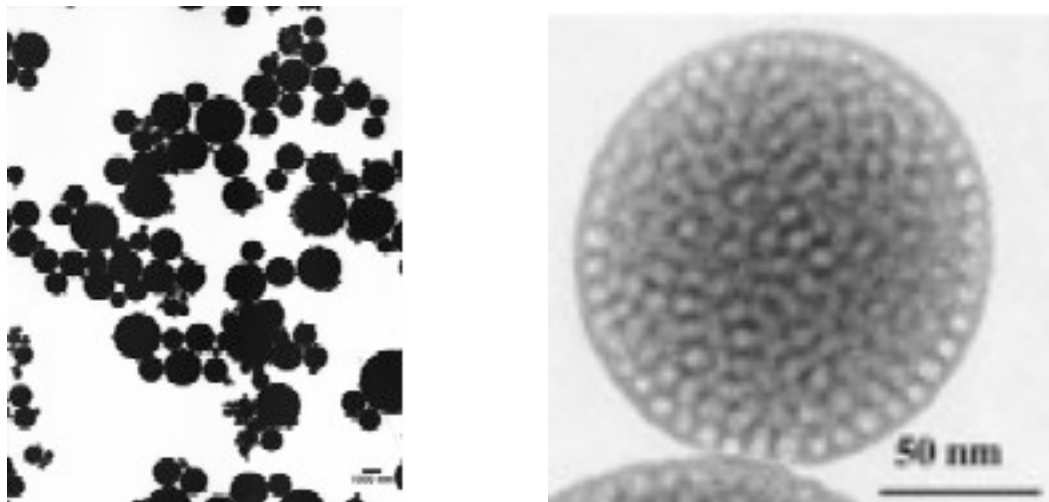
**Figure 18:** Schematic representation of a pH driven controlled release device



### 2.1 Characterization of MSN

To ensure the presence of colloidal material would not interfere with measuring the UV-Vis absorbance of the supernatant during the kinetic release studies, a gravity filtration technique (described above) was employed to obtain MSN of appropriate size. The larger particles comprising the retentate after the final filtration cycle were used in the kinetic release studies because they can be quickly and easily separated from the supernatant via centrifugation. Dynamic light scattering showed that the MSN used in the kinetic release studies had an average diameter of 1.6  $\mu\text{m}$ . Though the particles are micron-sized, we propose that they are an appropriate model for nano-scale systems since the pore morphologies of nano- and micron-sized particles are identical. Figure 19 depicts TEM images of the MSN.

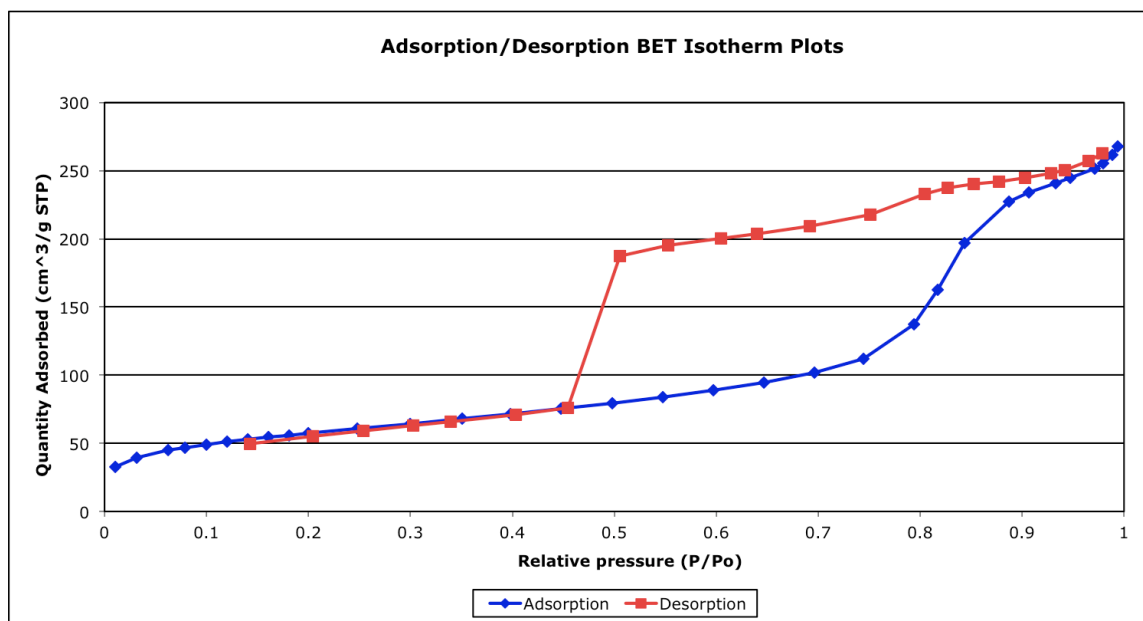
**Figure 19:** TEM images of MSN used in release studies. The figure on the right shows the porous character of the particles.



To quantify the porous nature of the particles, BET gas sorptometry was conducted. The surface area of the particles was measured to be  $206.88 \text{ m}^2/\text{g}$ . Though the BET surface area of our MSN is less than other MSN materials<sup>1-3, 8, 20</sup>, the adsorption/desorption isotherms (Figure 20) are indicative of typical mesoporous systems, having type IV physisorption isotherms with H2 hysteresis. The H2 hysteresis and the forced closure of the hysteresis loop indicate random pore distribution and an interconnected pore system.<sup>71</sup> The cumulative volume of the pores was calculated to be  $0.42 \text{ cm}^3/\text{g}$ , and the average pore width was calculated as  $86.12 \text{ \AA}$ . The cumulative pore volume and average pore width were calculated using the BJH model from the adsorption isotherm branch.



**Figure 20:** Nitrogen adsorption/desorption BET isotherms of MSN.



The zeta potentials of non-coated (bare) and APTES-coated MSN were measured at pH 7.4 and 5.0 in buffer solution having an ionic strength (I) of 0.16 M to quantify the surface charge of the particles under the release conditions. The zeta potential measurement results are shown in Table 5. As expected, the amine-functionalized MSN have positive potentials, while the bare MSN have negative potentials. In addition, the APTES-coated particles have a greater positive potential, and the bare MSN have a smaller negative potential at pH 5.0 than at pH 7.4, which was anticipated due to the increased acidity of the solution. It should be noted that the zeta potential measurements for the bare MSN at pH 5.0 were not reproducible (12 trials were required to obtain three measurements that were of good quality) which can be attributed to the fact that the particles were near their point of zero-charge.

**Table 5:** Zeta potential measurements of APTES-coated and bare MSN at pH 7.4 and 5.0.

MSN Type	pH	Zeta Potential (STD), mV
Bare	7.4	-25.5 (1.2)
Bare	5.0	-3.4 (0.5)
APTES-coated	7.4	+12.2 (2.2)
APTES-coated	5.0	+41.1 (1.0)

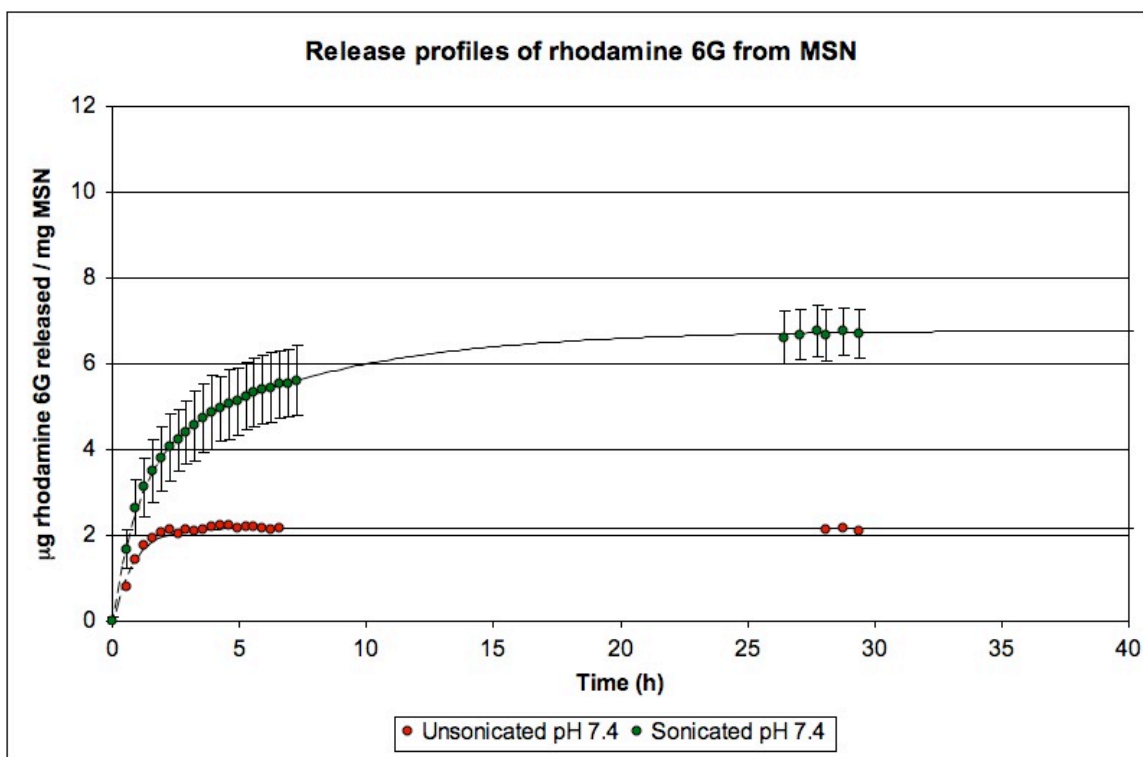
## 2.2 Loading and Release Studies

In the course of our studies, we discovered that the MSN must be sonicated in dye solution to maximize loading. Figure 21 shows the difference in release profiles of rhodamine 6G (R6G) from MSN that were sonicated in dye solution versus MSN that were only allowed to soak in dye solution and were not sonicated. (All loading conditions were identical except for sonication, and the releases were conducted in PBS buffer at 25 °C). The results clearly indicate that sonication increases the amount of dye that is loaded into the MSN; simply letting the particles soak in dye solution does not optimize their loading capacity. MSN that were sonicated in dye solution released ~4.5 µg of R6G per mg of MSN more than MSN that were not sonicated.

Analysis of the release profiles from sonicated and unsonicated MSN revealed an interesting phenomenon. The release of R6G from unsonicated bare MSN at pH 7.4 was best modeled by single exponential function (Eq. 3). The release from sonicated bare MSN, however, was best fit by the double exponential function (Eq. 1). The parameters for each function are given in Table 6. The double exponential release seen from

sonicated MSN is attributed to two different diffusion processes which are discussed in more detail below.<sup>19</sup> We propose that the sonication process enables R6G to penetrate completely into the center of the MSN (Figure 21) which results in a biphasic release pattern. Conversely, we believe that unsonicated MSN have R6G bound only to the exterior surface (Figure 22) and thus show a single diffusion process that fits a single exponential function.

**Figure 21:** Release profiles of rhodamine 6G from MSN with and without sonication.



The data points for release of R6G from MSN with sonication are an average of three trials with standard deviation shown. The data points for release of R6G from MSN without sonication are from a single trial. The release profiles were fit to an exponential function (black line).

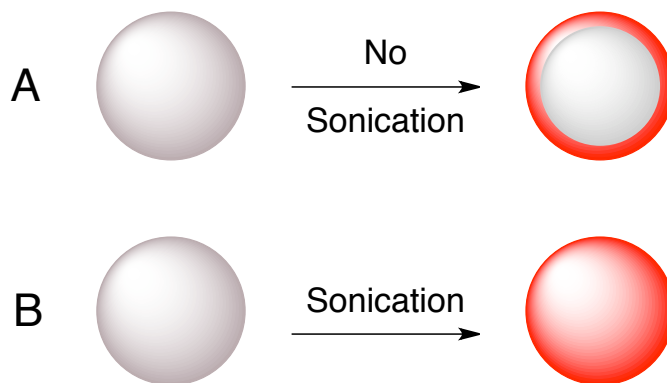
**Table 6:** Fit parameters for release of rhodamine 6G from sonicated and unsonicated MSN at pH 7.4.

Sonication	Total Release, P, $\mu\text{g}/\text{mg}$ MSN <sup>a</sup>	Percent Phase 2, F <sub>2</sub> , % <sup>a</sup>	$k_1$ , 1/h <sup>a</sup>	$k_2$ , 1/h <sup>a</sup>	Half-Life of S <sub>1</sub> , h <sup>b</sup>	Half-Life of S <sub>2</sub> , h <sup>b</sup>	Phase 1 Release, S <sub>1</sub> , $\mu\text{g}/\text{mg}$ MSN <sup>b</sup>	Phase 2 Release, S <sub>2</sub> , $\mu\text{g}/\text{mg}$ MSN <sup>b</sup>
Yes	6.78(12)	48(15)	1.0(4)	0.14(6)	0.69(17)	4.9(15)	3.5(10)	3.3(10)
No	2.16(2)	---	1.21(8)	---	0.58(3)	---	---	---

<sup>a</sup>In parentheses is the estimated standard error of the fit on the last significant digit(s).

<sup>b</sup>In parentheses is the standard error calculated from the error of the fit on the last significant digit(s).

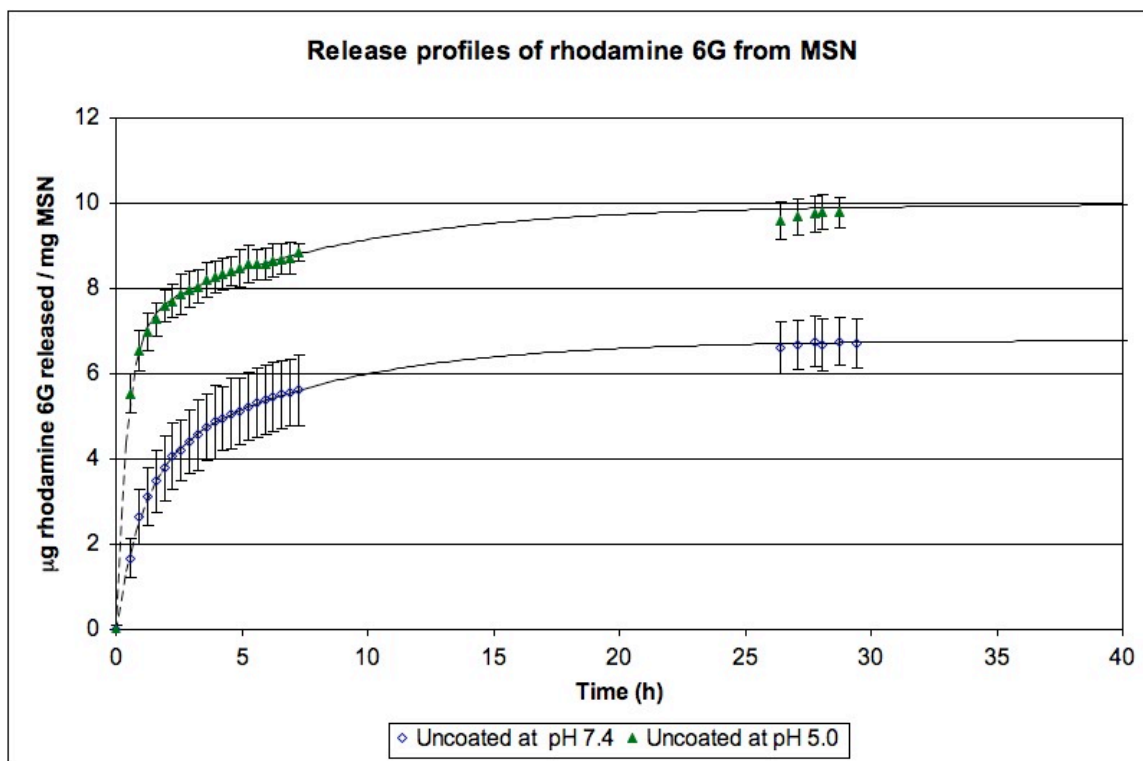
**Figure 22:** Schematic representation of the effect of sonication on MSN loading. A: Loading without sonication. B: Loading with sonication.



After determining how to maximize the MSN's loading capabilities, we studied the effect of pH on release kinetics. Figure 23 compares the release of rhodamine 6G from unmodified MSN at pH 5.0 and pH 7.4. At both pH values, there is an initial burst of release within the first 3 hours followed by a slower release period that levels off after about 40 hours. This result is similar to release from other reported MSN systems.<sup>8-14, 19</sup> The rate and amount of release at pH 5.0 is much greater than at pH 7.4 for uncoated

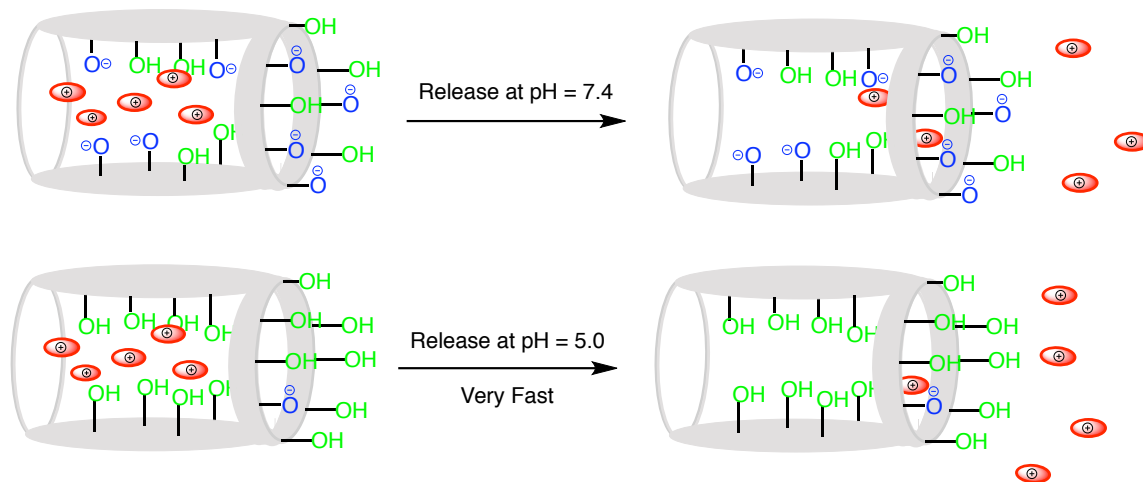
MSN. At pH 5.0, the uncoated particles released 3  $\mu\text{g}$  of rhodamine 6G more per mg of MSN than at pH 7.4 ( $\sim 10.0$   $\mu\text{g}$  of rhodamine 6G per mg of MSN at pH 5.0 versus  $\sim 7.0$   $\mu\text{g}$  of rhodamine 6G per mg of MSN at pH 7.4). These results are consistent with the findings of Tang et al., where the release rate of famotidine from carboxylic acid modified MSU increased in acidic gastric medium.<sup>12</sup> The increase in rate and amount released can be attributed to decreased electrostatic interactions between the positively charged rhodamine 6G molecules and the silica surface at pH 5.0 (Figure 24). At pH 7.4, the surface of MSN has a greater negative charge than at pH 5.0, as indicated by the zeta potentials of the particles. At pH 7.4, the particles have a zeta potential of -25.5 mV, while at pH 5.0, the MSN have a zeta potential of -3.40 mV (Table 5). The difference in zeta potential is attributed to the protonation of negatively charged silanol groups on the silica surface under more acidic conditions.

**Figure 23:** Release profiles of rhodamine 6G from bare MSN at pH 7.4 and 5.0.



The data points are an average of three trials with standard deviation shown. The release profiles were fit to an exponential function (black line).

**Figure 24:** Schematic representation of release of rhodamine 6G from bare MSN at pH 7.4 and 5.0.



Both of the release profiles from the bare MSN, at pH 5.0 and pH 7.4, were better modeled by a two-phase (double) exponential function (see experimental; eq. 1). The fit parameters for release from bare MSN at pH 7.4 and pH 5.0 are shown in Table 7. From the fit parameters, the half-life and span of each phase were calculated (Table 7).

**Table 7:** Two-phase fit parameters for release of rhodamine 6G from bare MSN.

pH	Total Release, P, $\mu\text{g}/\text{mg}$ MSN <sup>a</sup>	Percent Phase 2, F <sub>2</sub> , % <sup>a</sup>	$k_1$ , 1/h <sup>a</sup>	$k_2$ , 1/h <sup>a</sup>	Half-Life of S <sub>1</sub> , h <sup>b</sup>	Half-Life of S <sub>2</sub> , h <sup>b</sup>	Phase 1 Release, S <sub>1</sub> , $\mu\text{g}/\text{mg}$ MSN <sup>b</sup>	Phase 2 Release, S <sub>2</sub> , $\mu\text{g}/\text{mg}$ MSN <sup>b</sup>
5.0	9.97(7)	29(2)	2.3(2)	0.12(2)	0.30(2)	5.6(6)	7.1(2)	2.9(2)
7.4	6.78(12)	48(15)	1.0(4)	0.14(6)	0.69(17)	4.9(15)	3.5(10)	3.3(10)

<sup>a</sup>In parentheses is the estimated standard error of the fit on the last significant digit(s).

<sup>b</sup>In parentheses is the standard error calculated from the error of the fit on the last significant digit(s).

These results are consistent with the findings of Ng et al.<sup>19</sup> Using confocal laser scanning microscopy (CLSM), Ng et al. monitored the release of rhodamine 6G from

mesoporous silica microspheres. It was found that the release of rhodamine 6G from bare mesoporous silica microspheres was biphasic and could not be described as a simple diffusion process.<sup>19</sup> The authors reported an initial fast release period, which was followed by a second slow release period. The initial rapid release phase is attributed to the release of dye molecules located near the exterior of the mesoporous spheres, while the slower release period is attributed to the release of dye molecules that were initially located near the center of the particles. Using CLSM, it was observed that a layer of surface adsorbed R6G molecules formed near the exterior of the mesoporous particles. It is hypothesized that this layer of adsorbed R6G reduced the effective pore size of the particles and inhibited the escape of R6G molecules initially located near the center of the particles, thus reducing the rate at which these dye molecules diffused from the particles.<sup>19</sup>

Having demonstrated the effect of pH on release from MSN with anionic surfaces, we were interested in seeing how pH affects release from MSN with cationic surfaces. Therefore, we modified the surface of MSN with (3-aminopropyl)triethoxysilane (APTES). Figure 25 depicts the release profile of rhodamine 6G from APTES-coated MSN at pH 7.4 and pH 5.0. Though the release profile at pH 7.4 from the amine-coated MSN appears to be similar to the release profile of uncoated MSN at the same pH, there is an initial lag period seen during the first 90 minutes. Clearly, release from APTES-coated MSN at pH 5.0 is much different than the other release profiles: there is initially a slow release period seen during the first four hours, which is followed by a faster release phase that begins to level off after about 20 hours (Figure 25). Casasus et al. have reported similar release profiles of a ruthenium

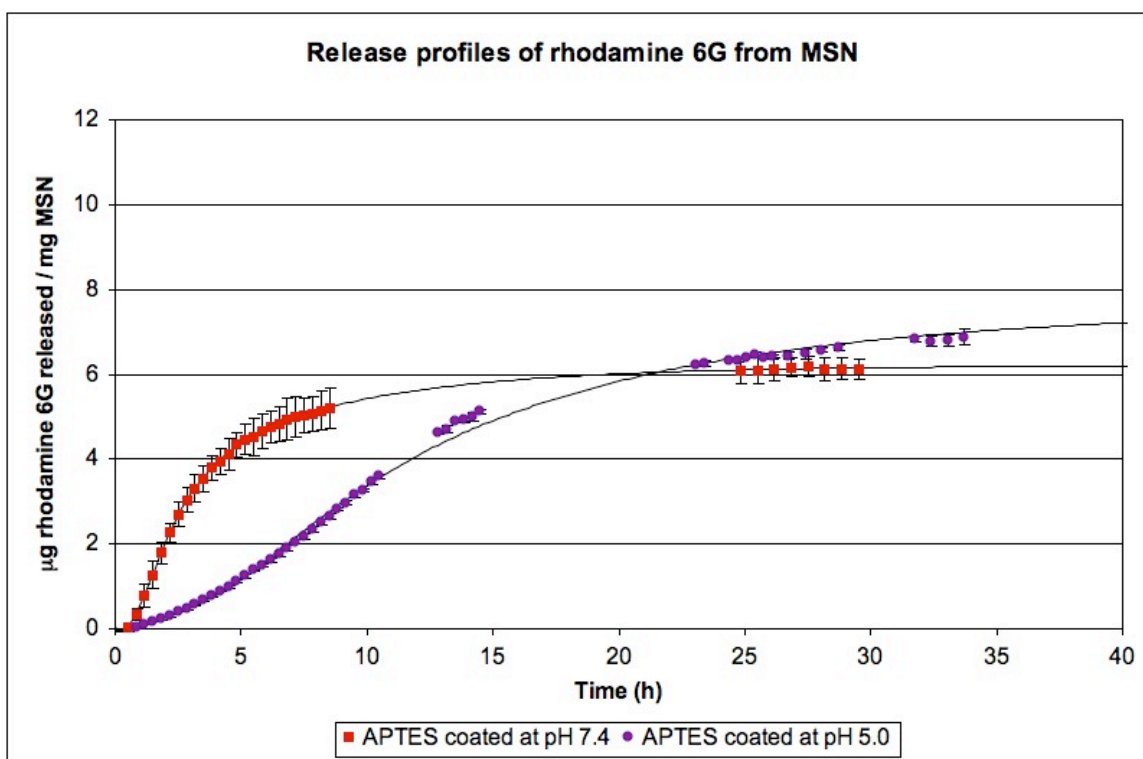


dye from polyamine coated MCM-41 at pH 4.0.<sup>13</sup> However, their analogues 3-aminopropyl functionalized system did not exhibit the same delayed release profile.<sup>13</sup> This difference may be associated with the method used to functionalize the surface of the MSN with APTES. Casasus functionalized MSN with APTES under anhydrous conditions, while we silanized our MSN in PBS solution. It is documented that water promotes multilayer formation and better surface coverage during the silanization of silica.<sup>72-74</sup> As with the uncoated particles, more total release is seen at pH 5.0 than at 7.4 for the amine coated-MSN. Approximately 7.5  $\mu\text{g}$  of R6G was released per mg of MSN at pH 5.0, while about 6.0  $\mu\text{g}$  of R6G was released per mg of MSN at pH 7.4 (Figure 25). The initial lag period seen at pH 7.4 and the unique release profile at pH 5.0 seen for the amine-coated MSN can be rationalized by considering the surface coverage and charge of these particles. We hypothesize that the repulsive interaction between the positively charged amine groups and cationic rhodamine 6G molecules inhibit the escape of entrapped R6G molecules within the MSN matrix (Figure 26). At pH 7.4, protonated amine groups and negatively charged silanol groups create a zwitterionic surface on amine-functionalized MSN. Based upon the positive zeta potential (+12.2 mV) we assume that there are more protonated amine groups than negatively charged silanol moieties. However, at pH 5.0, the surfaces of the MSN have a greater positive charge (+41.1 mV) due to the neutralization of the silanol groups. The increased positive surface charge of the amine-coated MSN can account for the more significant lag period observed at pH 5.0. It should be noted that the basic rhodamine 6G molecules are expected to be protonated and positively charged under both pH conditions. Molecular modeling reported by Casasus et al. suggest that amine monolayers will expand under

acidic conditions due to coulombic repulsion between adjacent protonated amine groups.

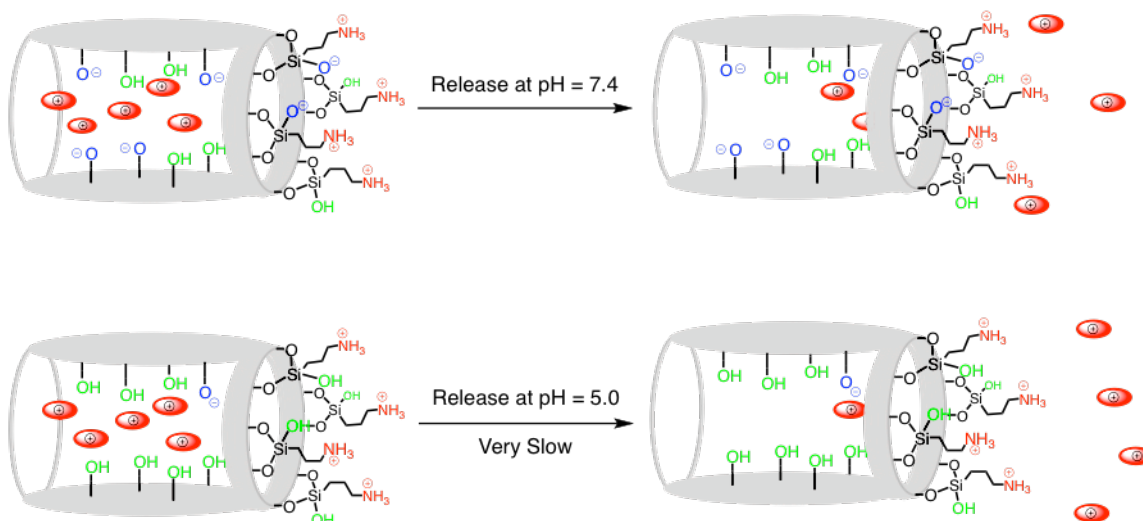
<sup>13</sup> This expanded monolayer will decrease the effective diameter of the pore openings of the MSN and thereby hinder the ability of rhodamine 6G molecules to escape from the MSN matrix. Thus, the decreased dimensions of the pore openings and repulsive interaction between rhodamine 6G and the protonated amine groups located on the surface of the MSN could be the cause of the lag seen at pH 7.4 and the diminished release rate seen at pH 5.0 for these amine-coated MSN.

**Figure 25:** Release profiles of rhodamine 6G from amine-coated MSN at pH 7.4 and 5.0.



The data points are an average of three trials with standard deviation shown. The release profiles were fit to an exponential function (black line).

**Figure 26:** Schematic representation of release of rhodamine 6G from APTES-coated MSN at pH 7.4 and 5.0.



Interestingly, both of the release profiles from the APTES-functionalized MSN, at pH 5.0 and pH 7.4, were better modeled by the single-phase exponential (see experimental; eq. 3). The fit parameters and calculated half-life are shown in Table 8.

**Table 8:** One-phase fit parameters and half-life for release of rhodamine 6G from APTES-coated MSN.

pH	Total Release, P, $\mu\text{g}/\text{mg MSN}^{\text{a}}$	$k$ , $1/\text{h}^{\text{a}}$	Half-Life, $\text{h}^{\text{b}}$
5.0	8.46(15)	0.050(2)	13.9(4)
7.4	6.19(5)	0.23(1)	3.06(6)

<sup>a</sup>In parentheses is the estimated standard error of the fit on the last significant digit(s).

<sup>b</sup>In parentheses is the standard error estimated from the error of the fit on the last significant digit(s).

The single-phase release kinetics from APTES-functionalized MSN can be explained by considering the effect of the amine coating on the release of rhodamine 6G molecules from the MSN. As stated above, Ng hypothesizes that the slow second release phase observed from bare mesoporous silica particles was due to a layer of adsorbed rhodamine 6G molecules near the exterior of the particles, which inhibited the escape of rhodamine 6G molecules initially located near the center of the particle.<sup>19</sup> We reason that the APTES coating on the surface of the MSN also acted as a barrier to dye molecules escaping from within the MSN. However, we hypothesize that the APTES coating was a more significant barrier to release and reduced the rate of release to a greater extent than the proposed layer of adsorbed rhodamine 6G molecules near the exterior of the MSN. In addition, unlike the adsorbed R6G layer, the amine coating also inhibited the release of R6G molecules initially located near the exterior of the particles. Therefore, the rate of release from APTES-functionalized MSN was dependent on the ability of R6G molecules to diffuse through the amine coating. We theorize that release from APTES-functionalized MSN was defined as a single diffusion process due to the fact that all escaping molecules had to navigate through the APTES coating, regardless if the molecules were initially located near the exterior or the center of the MSN.

### **3 Conclusions**

The loading and release of rhodamine 6G from unmodified and amine-coated MSN has been studied and the features of this release have been measured. It was found that sonication of MSN in dye solution was necessary to maximize the loading capacity of the particles. It was also determined that both surface modification and pH affect the

rate and amount of release from MSN, which is governed by coulombic interactions. Release from bare MSN at both pH 7.4 and pH 5.0 followed the same general pattern—an initial burst of release followed by a slower, delayed release period. The increased release from the uncoated MSN at pH 5.0 is attributed to decreased electrostatic interactions between the silica surface and entrapped rhodamine 6G molecules. The initial lag period seen for the amine-coated MSN at pH 7.4 and the unique release profile seen for the same particles at pH 5.0 can be explained by repulsive interactions between protonated amine groups on the exterior surface of the MSN and rhodamine 6G molecules. Release profiles from APTES-coated MSN better fit a single exponential function while release profiles from bare MSN better fit a double exponential function—indicating that the release of R6G from bare MSN is a two-phase process.

## **4 Experimental**

### *4.1 General*

All materials were used as received from the supplier. Rhodamine 6G (R6G) was obtained from Sigma Aldrich (BioChemika, for fluorescence: 83697). (3-Aminopropyl)triethoxysilane (APTES) was obtained from Sigma Aldrich (Fluka: 09324). Tetraethyl orthosilicate was obtained from Sigma Aldrich. Pluronic® F-127 was obtain from BASF. All aqueous solutions were made using water filtered through a Millipore water filtration system unless otherwise indicated. Phosphate buffered saline (PBS) solutions were prepared from phosphate buffered saline tablets obtained from Sigma Aldrich (Sigma, tablets: P4417) as directed. The PBS solutions prepared had a measured pH of 7.4 and an ionic strength of 0.16 M. Acetic acid (0.78 mL, 13.63 mmol)

and sodium acetate (2.88 g, 35.11 mmol) used to prepare the acetate buffer (400 mL, pH = 5.0) were obtained from J.T. Baker. An Ocean Optics USB 2000 Spectrometer was used to measure the absorbance (A) of the supernatant during release studies. A Branson 321 desk sonicator was used to sonicate MSN samples. Zeta potentials were measured using a Zetasizer Nano ZS90 from Malvern Instruments Ltd. BET and BJH measurements were obtained using a Micromeritics Tristar II 3020 Surface Area Analyzer. The surface area of standard silica-alumina pellets received from Micromeritics was measured to verify the instrument was in proper working condition.

#### 4.2 *Fabrication of MSN*

MSN were prepared in the Zachariah lab in the Department of Chemistry at the University of Maryland, College Park. MSN were fabricated by a template-assisted sol-gel process that was implemented via aerosol technique. Aerosol droplets were created from a stainless steel pressure atomizer containing the precursor mixing solution consisting of tetraethyl orthosilicate (2.6 g, 13 mmol) and Pluronic® F-127 (0.55 g, 0.04 mmol) dissolved in absolute ethanol (17.3 mL) and deionized water (9.0 mL) adjusted to pH = 1.2 with HCl. Droplets being carried through a stainless steel tube by dried air passed through a diffusion-dryer to remove most of the solvent and then through a tube furnace at 400 °C. Normal residence time was 1 second under the gas flow rate of 3.5 L/min used in the experiments. Particles were collected on a 0.2 µm pore Millipore HTPP membrane filter housed in a stainless steel holder (covered by heating tape to prevent re-condensation of solvent vapor). After being removed from the membrane, particles were calcined at 500 °C for 4 h to remove the surfactant and yield MSN.

#### 4.3 *Gravity Filtration*

A 2.0 mg/mL stock suspension of MSN in Millipore water was made, vortexed, and then sonicated using a Bransonic 321 desk sonicator for 30 minutes. The suspension was then allowed to settle for 24 hours. The upper 45 mL of supernatant was removed by pipette and the remaining retentate was diluted back to 50 mL using fresh Millipore water. The suspension was vortexed and then sonicated for 30 minutes. This procedure was repeated three (3) times. The particles remaining after the fourth cycle were dried in vacuo and were used in the release studies.

#### 4.4 *Rhodamine 6G Loading*

The MSN comprising the retentate (dried) remaining after the gravity filtration process were added to a 0.15 mg/mL solution of rhodamine 6G in PBS buffer to make a 2 mg/mL suspension of MSN in rhodamine 6G solution. The suspension was vortexed and then sat undisturbed for 48 hours. The particles were sonicated in the 0.15 mg/mL rhodamine 6G solution where indicated.

#### 4.5 *MSN Functionalization*

An aliquot of the MSN / rhodamine 6G suspension was removed from the stock solution and sonicated for 30 minutes. 3-Aminopropyl triethoxy silane (APTES) was added to the aliquot to yield a 0.1 mL APTES / mg MSN solution. The reaction mixture stirred at room temperature for 10 minutes and was then centrifuged. The supernatant was removed. The functionalized MSN were immediately used in a release experiment.

#### 4.6 Rhodamine 6G Release Quantification using UV-Vis Spectroscopy

An aliquot of the MSN / rhodamine 6G suspension (5.0 mL) was removed from the stock solution and sonicated for 30 minutes. The sample suspension was then centrifuged and the supernatant was removed by pipette. The particles were washed with PBS buffer (5.0 mL) and centrifuged for 5 minutes. The supernatant was removed via pipette. The washing process was repeated twice more. After the final washing process, the MSN were resuspended in buffer solution at the desired pH and 25 °C. PBS buffer was used for release at pH 7.4, while acetate buffer was used for release at pH 5.0. A 2.0 mL aliquot was removed from the suspension and centrifuged. The absorbance of the supernatant was measured using an Ocean Optics USB 2000 Spectrometer. The analyzed supernatant and the 2.0 mL aliquot were then returned to the sample suspension. This process was repeated every twenty minutes until no further release was observed.

#### 4.7 Mathematical Modeling of Release from MSN

For each release profile, GraphPad Prism was used to perform nonlinear least squares fitting to both a double exponential and a single exponential function, and the best fit model was chosen using the Extra Sum-of-Squares F test.

The double exponential function, which describes two processes that have rates proportional to the diffusivity and the local concentration of the dye is defined as

$$M = S_1(1 - e^{-k_1 t}) + S_2(1 - e^{-k_2 t}) \quad (1)$$

where  $S_1$  is the amount released during the first phase and  $S_2$  is the amount released during the second phase,  $k_1$  is the rate constant of the first phase,  $k_2$  is the rate constant of the second phase, and  $S_1$  and  $S_2$  are related by



$$S_1 = P(100 - F_2)(0.01) \quad (2a)$$

$$S_2 = P(F_2)(0.01) \quad (2b)$$

where  $P$  is the total amount released and  $F_2$  is the percent of release that occurs in the second phase.

The single-phase exponential function is defined as:

$$M = P(1 - e^{-kt}) \quad (3)$$

where  $P$  is the total amount released and  $k$  is the rate constant.

### Acknowledgements

The author acknowledges Peter DeMuth, Stephanie Galanie, Chunwei Wu, and Michael Zachariah for the significant contributions they made to the research and discoveries presented throughout this chapter.

### References

- 1) Kresge, C. T.; Leonowicz, M. E.; Roth, W. J.; Vartuli, J. C.; Beck, J. S. *Nature* **1992**, 359, 710-712.
- 2) Zhao, D.; Feng, J.; Huo, Q.; Melosh, N.; Fredrickson, G.; Chmelka, B.; Stucky, G. *Science* **1998**, 279, 548-552.
- 3) Bagshaw, S. A.; Prouzet, E.; Pinnavaia, T. J. *Science* **1995**, 269, 1242-1244.
- 4) Inagaki, S.; Fukushima, Y.; Kuroda, K. *J. Chem. Soc., Chem. Commun.* **1993**, 680-682.
- 5) Ryoo, R.; Kim, J. M.; Ko, C. H.; Shin, C. H. *J. Phys. Chem.* **1996**, 100, 17718-

17721.

- 6) Giri, S.; Trewn, B.; Lin, V. *Nanomedicine* **2007**, 2, 99-111.
- 7) Trewn, B.; Slowing, I.; Giri, S.; Chen, H.; Lin, V. *Acc. Chem. Res.* **2007**, 40, 846-853.
- 8) Vallet-Regi, M.; Ramila, A.; del Real, R. P.; Perez-Pariente, J. *Chem. Mater.* **2001**, 13, 308–311.
- 9) Munoz, B.; Ramila, A.; Perez-Pariente, J.; Diaz, I.; Vallet-Regi, M. *Chem. Mater.* **2003**, 15, 500-503.
- 10) Song, S.-W.; Hidajat, K.; Kawi, S. *Langmuir* **2005**, 21, 9568-9575.
- 11) Xu, W.; Gao, Q.; Xu, Yao.; Wu, D.; Sun, Y.; Shen, W.; Deng, F. *J. Solid State Chem.* **2008**, 181, 2837-2844.
- 12) Tang, Q.; Xu, Y.; Wu, D.; Sun, Y. *J. Solid State Chem.* **2006**, 179, 1513-1520.
- 13) Casasus, R.; Climent, E.; Marcos, M. D.; Martinez-Manez, R.; Sancenon, F.; Soto, J.; Amoros, P.; Cano, J.; Ruiz, E. *J. Am. Chem. Soc.* **2008**, 130, 1903-1917.
- 14) Horcajada, P.; Ramila, A.; Perez-Pariente, J.; Vallet-Regi, M. *Micropor. Mesopor. Mater.* **2004**, 68, 105-109.
- 15) Andersson, J.; Rosenholm, J.; Areva, S.; Linden, M. *Chem. Mater.* **2004**, 16, 4160-4167.
- 16) Qu, F.; Zhu, G.; Huang, S.; Shougui, L.; Sun, J.; Zhang, D.; Qiu, S. *Micropor.*

*Mesopor. Mater.* **2006**, 92, 1-9.

- 17) Stromme, M.; Brohede, U.; Atluri, R.; Garcia-Bennet, A. E. *Nanomedicine and Nanobiotechnology* **2009**, 1, 140-148.
- 18) Salonen, J.; Laitinen, L.; Kaukonen, A. M.; Tuura, J.; Björkqvist, M.; Heikkilä, T. Vähä-Heikkilä, K.; Hirvonen, J.; Lehto, V.-P. *J. Controlled Release* **2005**, 108, 362-374.
- 19) Ng, J. B. S.; Kamali-Zare, P.; Brismar, H.; Bergstrom, L. *Langmuir* **2008**, 24, 11096-11102.
- 20) Lai, C.-Y.; Trewyn, B. G.; Jeftinija, D. M.; Jeftinija, K.; Xu, S.; Jeftinija, S.; Lin, V. S.-Y. *J. Am. Chem. Soc.* **2003**, 125, 4451-4459.
- 21) Slowing, I. I.; Vivero-Escoto, J. L.; Wu, C-W.; Lin, V. S.-Y. *Adv. Drug Delivery Reviews* **2008**, 60, 1278-1288.
- 22) Vivero-Escoto, J. L.; Slowing, I. I.; Wu, C-W.; Lin, V. S.-Y. *J. Am. Chem. Soc.* **2009**, 131, 3462-3463.
- 23) Zhao, Y.; Trewyn, B. G.; Slowing, I. I.; Lin, V. S.-Y. *J. Am. Chem. Soc.* **2009**, 131, 8398-8400.
- 24) Lu, J.; Liong, M.; Zink, J.; Tamanoi, F. *Small* **2007**, 3, 1341-1346
- 25) You, Y.-Z.; Kalebaila, K.; Brock, S.; Oupichy, D. *Chem. Mater.* **2008**, 20, 3354-3359.
- 26) Mal, N. K.; Fujiwara, M.; Tanaka, Y.; Taguchi, T.; Matsukata, M. *Chem. Mater.*

**2003**, 15, 3385-3394.

- 27) Hernandez, R.; Tseng, H.-R.; Wong, J. W.; Stoddart, J. F.; Zink, J. I. *J. Am. Chem. Soc.* **2004**, 126, 3370-3371.
- 28) Nguyen, T.; Tseng, H.-R.; Celestre, P.; Flood, A.; Liu, Y.; Stoddart, J. F.; Zink, J. *PNAS* **2005**, 102, 10029-10034.
- 29) Nguyen, T.; Liu, Y.; Saha, S.; Leung, K.; Stoddart, J. F.; Zink, J. *J. Am. Chem. Soc.* **2007**, 129, 626-634.
- 30) Angelos, S.; Yang, Y.-W.; Petal, K.; Stoddart, J. F.; Zink, J. I. *Angew. Chem. Int. Ed.* **2008**, 47, 2222-2226.
- 31) Khashab, N. M.; Trabolsi, A.; Lau, Y. A.; Ambrogio, M. W.; Friedman, D. C.; Khatib, H. A.; Zink, J. I.; Stoddart, J. F. *Eur. J. Org. Chem.* **2009**, 1669-1673.
- 32) Du, L.; Liao, S.; Khatib, H. A.; Stoddart, J. F.; Zink, J. I. *J. Am. Chem. Soc.* **2009**, 131, 15136-15142.
- 33) Angelos, S.; Khashab, N. M.; Yang, Y.-W.; Trabolsi, A.; Khatib, H. A.; Stoddart, J. F.; Zink, J. I. *J. Am. Chem. Soc.* **2009**, 131, 12912-12914.
- 34) Ferris, D. P.; Zhao, Y.-L.; Khashab, N. M.; Khatib, H. A.; Stoddart, J. F.; Zink, J. I. *J. Am. Chem. Soc.* **2009**, 131, 1686-1688.
- 35) Park, C.; Oh, K.; Lee, S. C.; Kim, C. *Angew. Chem. Int. Ed.* **2007**, 46, 1455-1457.
- 36) Hong, C.-Y.; Li, X.; Pan, C.-Y. *J. Mater. Chem.* **2009**, 19, 5155-5160.

- 37) Zhu, C.-L.; Song, X.-Y.; Zhou, W.-H.; Yang, H. H.; Wen, Y.-H.; Wang, X.-R. *J. Mater. Chem.* **2009**, 19, 7765-7770.
- 38) Beck, J. C.; Vartuli, J. C.; Roth, W. J.; Leonowicz, M. E.; Kresge, C. T.; Schmitt, K. D.; Chu, C. T.-W.; Olsen D. H.; Sheppard, E. W.; McCullen, S. B.; Higgins, J. B.; Schlenker, J. L. *J. Am. Chem. Soc.* **1992**, 114, 10834-10843.
- 39) Slowing, I. I.; Vivero-Escoto, J. L.; Trewyn, B. G.; Lin, V. S. Y. *J. Mater. Chem.* **2010**, 20, 7924-7937.
- 40) Wu, S.-H.; Hung, Y.; Mou, C.-Y. *Chem. Commun.* **2011**, 47, 9972-9985.
- 41) He, Q.; Shi, J. *J. Mater. Chem.* **2011**, 21, 5845-5855.
- 42) Popat, A.; Hartono, S. B.; Stahr, F.; Liu, J.; Qiao, S. Z.; Lu, G. Q. *Nanoscale* **2011**, 3, 2801-2818.
- 43) Singh, N.; Karambelkar, A.; Gu, L.; Lin, K.; Miller, J. S.; Chen, C. S.; Sailor, M. J.; Bhatia, S. N. *J. Am. Chem. Soc.* **2011**, ACS ASAP.
- 44) Muhammad, F.; Guo, M.; Qi, W.; Sun, F.; Wang, A.; Guo, Y.; Zhu, G. *J. Am. Chem. Soc.* **2011**, 133, 8778-8781.
- 45) Yuan, L.; Tang, Q.; Yang, D.; Zhang, J. Z.; Zhang, F.; Hu, J. *J. Phys. Chem. C* **2011**, 115, 9926-9932.
- 46) Wan, X.; Zhang, G.; Liu, S. *Macromol. Rapid Commun.* **2011**, 32, 1082-1089.
- 47) Knezevic, N. Z.; Trewyn, B. G.; Lin, V. S. Y. *Chem. Eur. J.* **2011**, 17, 3338-3342, S3338/1-S3338/6.

- 48) Chen, C.; Pu, F.; Huang, Z.; Liu, Z.; Ren, J.; Qu, X. *Nucleic Acids Res.* **2011**, 39, 1638-1644.
- 49) Cheng, S.-H.; Liao, W.-N.; Chen, L.-M.; Lee, C.-H. *J. Mater. Chem.* **2011**, 21, 7130-7137.
- 50) Ma, Y.; Zhou, L.; Zheng, H.; Xing, L.; Li, C.; Cui, J.; Che, S. *J. Mater. Chem.* **2011**, 21, 9483-9486.
- 51) Shen, S.-C.; Ng, W. K.; Shi, Z.; Chia, L.; Neoh, K. G.; Tan, R. B. H. *J. Mater. Sci.: Mater. Med.* **2011**, 22, 2283-2292.
- 52) Shen, J.; He, Q.; Gao, Y.; Shi, J.; Li, Y. *Nanoscale* **2011**, 3, 4314-4322.
- 53) Huo, Q.; Margolese, D. I.; Ciesla, U.; Feng, P.; Gier, T. E.; Sieger, P.; Leon, R.; Petroff, P. M.; Schueth, F.; Stucky, G. D. *Nature* **1994**, 368, 317-21.
- 54) Zhao, D.; Huo, Q.; Feng, J.; Chmelka, B. F.; Stucky, G. D. *J. Am. Chem. Soc.* **1998**, 120, 6024-6036.
- 55) Gruner, S. M. *J. Phys. Chem.* **1989**, 93, 7562-70.
- 56) Firouzi, A.; Atef, F.; Oertli, A. G.; Stucky, G. D.; Chmelka, B. F. *J. Am. Chem. Soc.* **1997**, 119, 3596-3610.
- 57) Huo, Q.; Margolese, D. I.; Stucky, G. D. *Chem. Mater.* **1996**, 8, 1147-60.
- 58) Schumacher, K.; Ravikovitch, P. I.; Du Chesne, A.; Neimark, A. V.; Unger, K. K. *Langmuir* **2000**, 16, 4648-4654.
- 59) Stöber, W.; Fink, A.; Bohn, E. *J. Colloid Interf. Sci.* **1968**, 26, 62-9.

- 60) Grün, M.; Lauer, I.; Unger, K. K. *Adv. Mater.* **1997**, 9, 254-257.
- 61) Nooney, R. I.; Thirunavukkarasu, D.; Chen, Y.; Josephs, R.; Ostafin, A. E. *Chem. Mater.* **2002**, 14, 4721-4728.
- 62) Lu, F.; Wu, S.-H.; Hung, Y.; Mou, C.-Y. *Small* **2009**, 5, 1408-1413.
- 63) Kim, T.-W.; Chung, P.-W.; Lin, V. S. Y. *Chem. Mater.* **2010**, 22, 5093-5104.
- 64) Cai, Q.; Luo, Z.-S.; Pang, W.-Q.; Fan, Y.-W.; Chen, X.-H.; Cui, F.-Z. *Chem. Mater.* **2001**, 13, 258-263.
- 65) Ikari, K.; Suzuki, K.; Imai, H. *Langmuir* **2006**, 22, 802-806.
- 66) Lu, Y.; Fan, H.; Stump, A.; Ward, T. L.; Rieker, T.; Brinker, C. J. *Nature* **1999**, 398, 223-226.
- 67) Brinker, C. J.; Lu, Y.; Sellinger, A.; Fan, H. *Adv. Mater.* **1999**, 11, 579-585.
- 68) Prakash, A.; McCormick, A. V.; Zachariah, M. R. *Chem. Mater.* **2004**, 16, 1466-1471.
- 69) Lu, J.; Liong, M.; Li, Z.; Zink, J. I.; Tamanoi, F. *Small* **2010**, 6, 1794-1805.
- 70) Apostolovic, B.; Klok, H.-A. *Biomacromolecules* **2008**, 9, 3173-3180.
- 71) Groen, J. C.; Peffer, L. A. A.; Perez-Ramirez, J. *Micropor. Mesopor. Mat.* **2003**, 60, 1-17.
- 72) Howarter, J. A.; Youngblood, J. P. *Langmuir* **2006**, 22, 11142-11147.
- 73) Yoshida, W.; Castro, R. P.; Jou, J.-D.; Cohen, Y. *Langmuir* **2001**, 17, 5882-5888.

- 74) Kallury, K. M. R.; Macdonald, P. M.; Thompson, M. *Langmuir* **1994**, 10, 492-499.



## **Chapter 3: MSN-Based Fluorescent Silica Nanoparticles for Application in Diagnostics**

### **1 Introduction**

Fluorescent silica nanoparticles (FSN) have recently gained attention for their potential in diagnostic applications. For example, FSN have been used to image tumors<sup>1</sup>, probe ligand-receptor interactions<sup>2-3</sup>, and detect pathogens<sup>3-6</sup>. Fluorescent silica nanoparticles are particularly attractive for these applications because they can be prepared in a wide variety of colors, have strong, stable fluorescence, and are biocompatible.<sup>7-12</sup> Importantly, these characteristics give FSN distinct advantages over quantum dot systems, which are often used for similar applications, but are hindered by cytotoxicity and unstable fluorescence.<sup>13-15</sup>

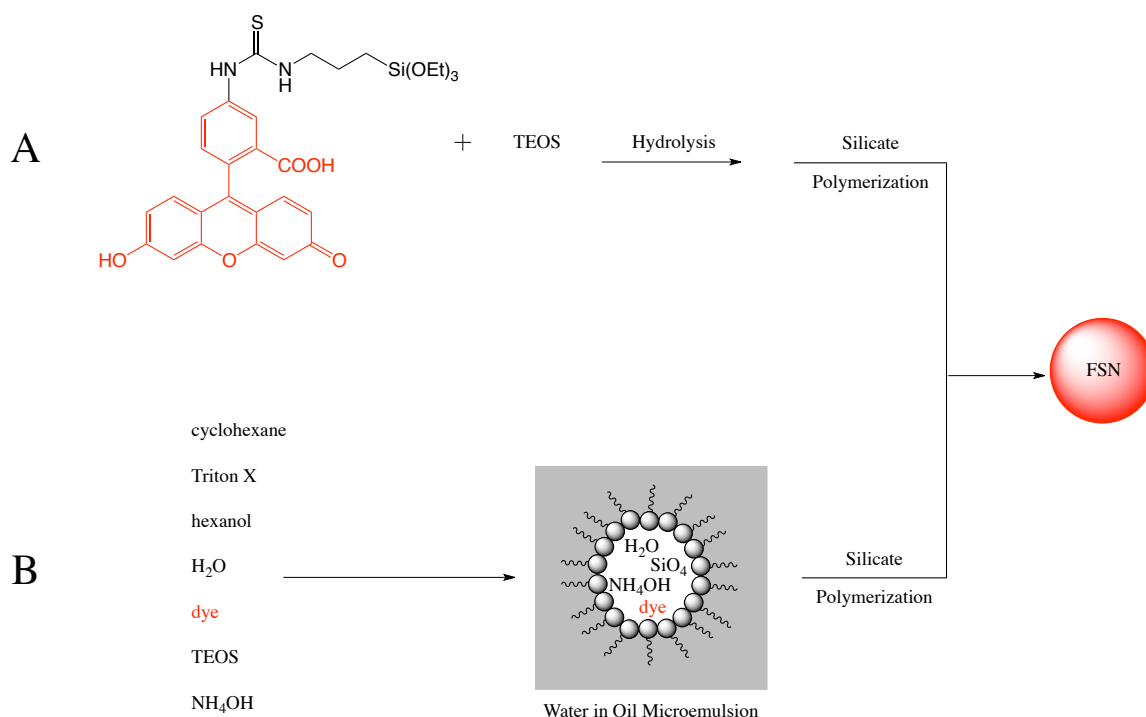
Preparing fluorescent silica nanoparticles suitable for use in diagnostics poses several challenges. Unlike metallic quantum dots, which have intrinsic fluorescent properties, the fluorescent character of fluorescent silica nanoparticles is derived from dye molecules incorporated into the silica matrix. Therefore, measures need to be taken to ensure that the dye molecules remain within the silica matrix and do not leach from the particles. In addition, to obtain particles that reproducibly exhibit the same function from batch to batch, the method used to prepare the FSN must yield particles that are uniform and monodisperse. For use in diagnostic applications, FSN are functionalized with biomolecules, such as protein and carbohydrates, which serve as recognition or receptor moieties. However, biomolecules that are nonspecifically (passively) bound to surfaces through electrostatic or hydrophobic interactions often lose their biological function.

Thus, a strategy to selectively, controllably, and covalently attach a biomolecule to the surface is needed. This chapter presents the work accomplished within the DeShong lab to overcome these challenges and prepare fluorescent silica nanoparticles for application in flow cytometry and solid-phase immunoassays.

### *1.1 Fluorescent Silica Nanoparticle Synthesis*

Fluorescent silica nanoparticles are typically prepared in one of two ways: (1) incorporation of siloxane-functionalized dyes into typical sol gel silica nanoparticle synthesis<sup>4, 6, 11, 13, 16-27</sup> (Figure 27, A), or (2) entrapment of dyes into silica nanoparticles prepared via microemulsion techniques<sup>5, 7-10, 12, 28-37</sup> (Figure 27, B). In the first method, the siloxane-functionalized dye is hydrolyzed to a silicate derivative, undergoes polymerization with other silicate anions in solution, and becomes covalently incorporated into the silica framework of the nanoparticles. Others have expanded this methodology to create analogous fluorescent mesoporous silica nanoparticles.<sup>38-41</sup> The second method is illustrated in Figure 29, B.<sup>42</sup> The components of the reaction mixture generate a water in oil microemulsion. Silicate anions (from the hydrolysis of TEOS) and hydrophilic dye molecules reside within the aqueous phase of the microemulsion. As silicate polymerization occurs within the aqueous phase, the dye molecules become entrapped within the Si-O-Si matrix, yielding fluorescent silica nanoparticles.

**Figure 27:** Common strategies used to prepare fluorescent silica nanoparticles: (A) Incorporation of siloxane-functionalized dye molecules into the sol-gel preparation of solid SiNPs. (B) Incorporation of dyes into water in oil micro-emulsion techniques.



## 2 Results and Discussion

### 2.1 MSN-Based FSN Synthesis

While studying the release of rhodamine 6G from mesoporous silica nanoparticles (discussed in chapter 2 of this dissertation), it was observed that dye-loaded MSN, prepared via wet-impregnation, were exceptionally bright, but released dye over time. Having the ability to contain the dye within the particles would result in strongly fluorescent materials with potential diagnostic applications. Notably, Rocha et al. report preparing non-leachable fluorescent silica nanoparticles by loading MSN with dye via

impregnation and then entrapping the dye with a silica coating.<sup>43</sup> However, through the understanding of mesoporous silica nanoparticle formation, we rationalized that incorporating hydrophobically modified dye into mesoporous silica nanoparticle synthesis would be a facile, one-step method to produce highly fluorescent silica nanoparticles that would not leach dye.

As discussed in chapter 2 of this dissertation, mesoporous silica nanoparticles (MSN) are synthesized by the templated polymerization of silicate around a surfactant mesophase.<sup>44-45</sup> The surfactant within the as-synthesized MSN is then removed via calcination or chemical extraction, yielding mesoporous silica nanoparticles. Figure 28 illustrates MCM-41 type MSN synthesis.<sup>44-45</sup> We hypothesized that a hydrophobically modified dye would become incorporated into the surfactant-silicate mesophase and then become entrapped within the silica matrix of the as-synthesized MSN, resulting in fluorescent silica nanoparticles (Figure 29). The fluorescent, as-synthesized MSN would not be calcined and hydrophobic interactions between the hydrophobically modified dye and the interior of the surfactant mesophase would secure the dye within the particle. Thus, we introduced fatty acid modified rhodamine B, **1** (Figure 30), into the MSN synthesis protocol described by Okuyama.<sup>46</sup> The particles produced from this methodology are fluorescent, spherical and approximately 100 nm in diameter. Figure 31 depicts TEM images of the prepared FSN. It should be noted that Imai et al. report making FSN by incorporating dye molecules into their binary surfactant MSN synthetic methodology.<sup>47</sup> The authors theorize that dye is incorporated into the hydrophobic core of the surfactant micelles and becomes entrapped in the as-synthesized MSN.<sup>47</sup>

**Figure 28:** Schematic illustration of MCM-41 type mesoporous silica nanoparticle synthesis.<sup>44-45</sup>

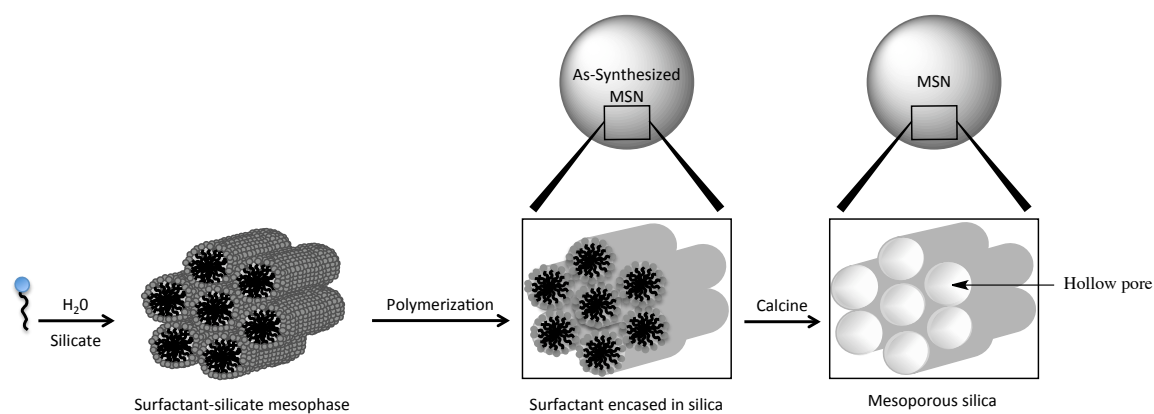


**Figure 29:** Schematic illustration of MSN-based fluorescent silica nanoparticle synthesis.

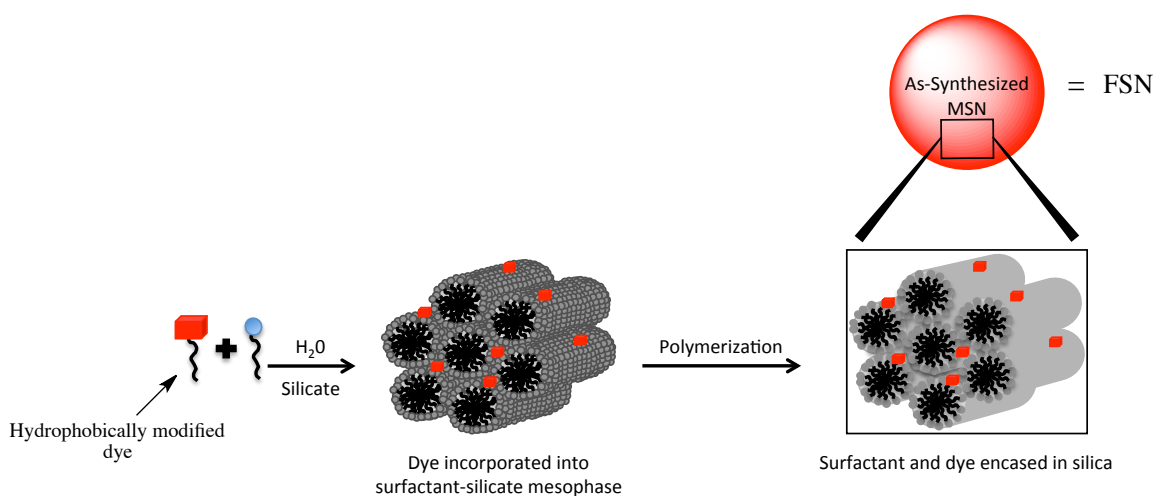


**Figure 30:** Structure of the hydrophobically modified rhodamine B derivative used to prepare FSN.

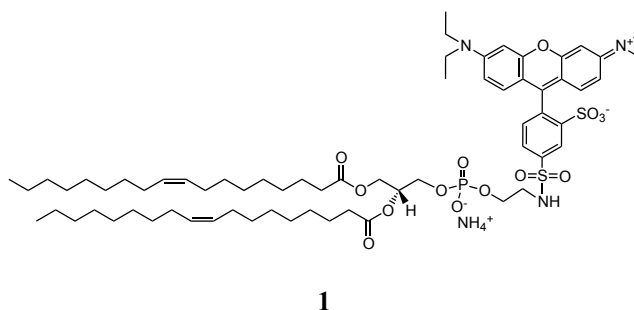
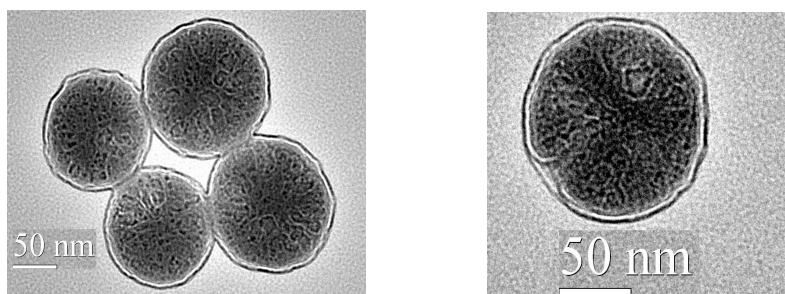


**Figure 31:** TEM images of prepared MSN-based FSN.



With fluorescent silica nanoparticles in hand, studies were conducted to examine the feasibility of using these materials in diagnostic applications. The goals of the following experiments were to (1) analyze the fluorescent character of the particles and determine how the hydrophobically modified dye is incorporated into the particles, (2) evaluate if any dye is leached from the particles under simulated physiological conditions, and (3) develop a strategy to selectively and covalently attach protein antibodies to the FSN surface, which would help ensure that the protein would retain its biological function after it is bound to the surface.

## 2.2 Fluorescence Microscopy Analysis of FSN

The fluorescent properties of the prepared fluorescent silica nanoparticles were analyzed using confocal microscopy. Z-scan confocal imaging of the fluorescent silica nanoparticles indicates that the hydrophobically modified dye is incorporated and evenly distributed throughout the particles (Figure 32). If the dye were only absorbed to the surface of the MSN, the Z-scan confocal images would appear as fluorescent rings, not as solid circles. Figure 33 compares fluorescent intensity of the FSN with CdSe quantum dots. Importantly, the fluorescent silica nanoparticles show strong, stable fluorescence that is approximately 5 times more intense than the fluorescence from CdSe quantum dots. The breaks seen in the fluorescent image of the CdSe quantum dots are due to “blinking” phenomena typical of quantum dots.

**Figure 32:** Fluorescent, z-scan confocal images of MSN-based FSN. The focus of the microscope was moved forward 1 micron in succession from a-h.

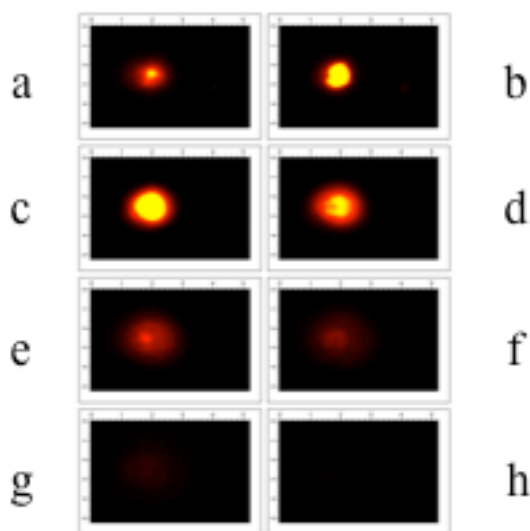
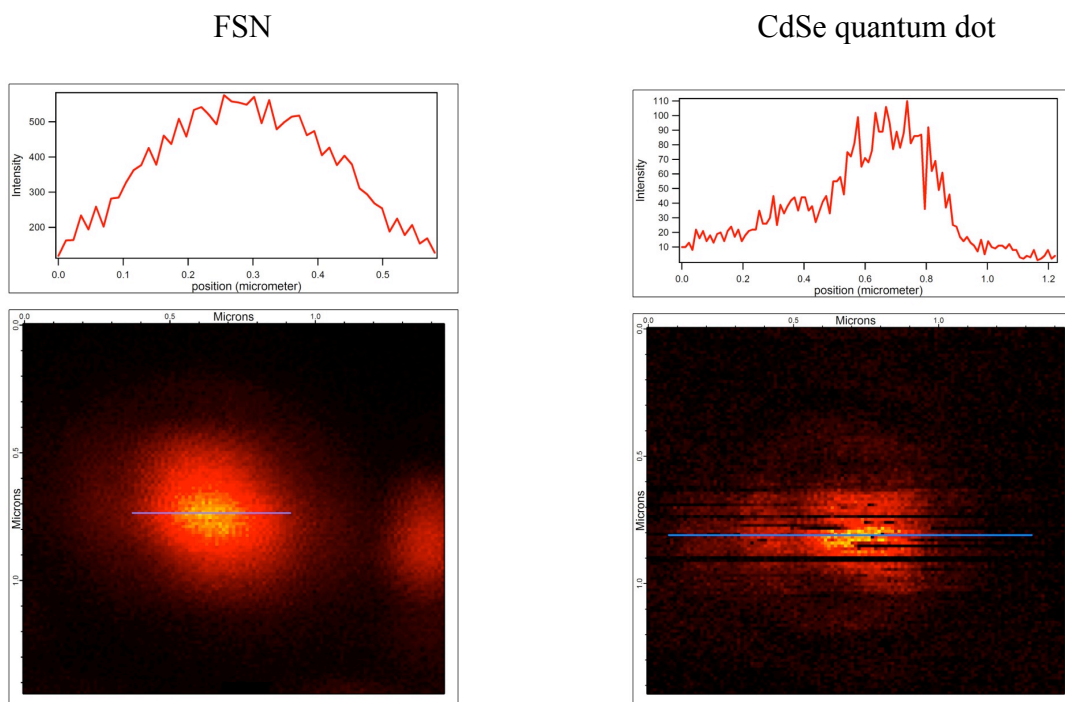


**Figure 33:** Comparison of fluorescence intensity of MSN-based FSN and CdSe quantum dots.



### 2.3 Dye Release Experiments

As mentioned above, Imai and coworkers prepared fluorescent silica particles by incorporating unmodified dyes into their MSN synthesis strategy.<sup>47</sup> Though Imai et al. report that the resulting fluorescent particles retain their color and stay suspended in solution for a prolonged period of time, they do not state if any dye is leached from the particles. For FSN to be suitable for *in vitro* and *in vivo* diagnostic applications, FSN cannot leach dye. Prepared FSN were suspended in PBS buffer and the supernatant was analyzed using UV-vis spectroscopy. It was found that no dye is released from the

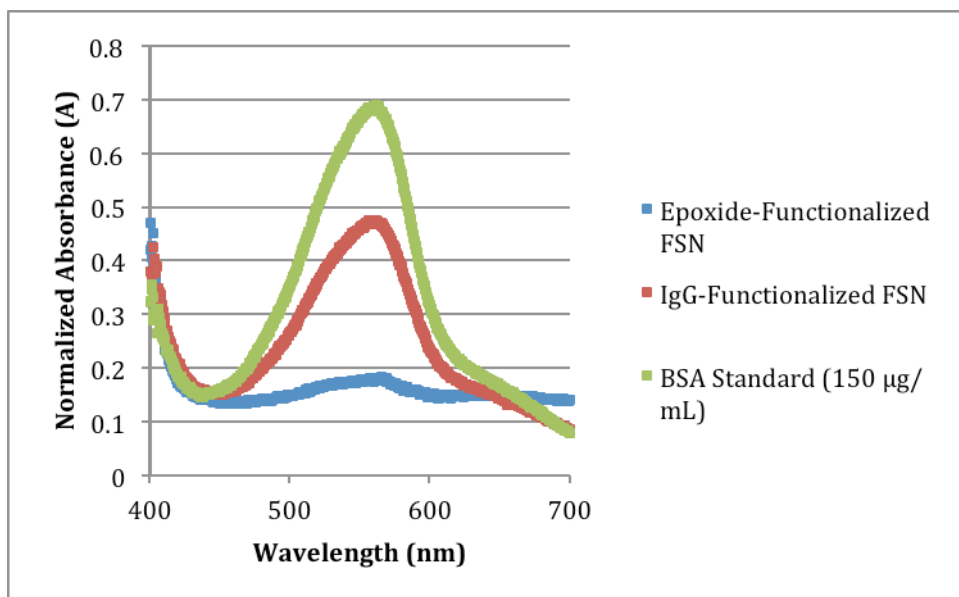


fluorescent silica nanoparticles at 25 °C after 7 days, indicating that the FSN are stable enough to be used in diagnostic applications.

#### 2.4 *Protein Functionalization of MSN-Based FSN*

For diagnostic applications, such as flow cytometry and solid phase-immunoassays, the FSN were functionalized with protein antibodies. As outlined in chapter 1 of this dissertation, there are a variety of methods commonly used to covalently attach proteins to surfaces.<sup>48-49</sup> Initially, the method described by Guo<sup>50</sup> was followed to functionalize FSN with mouse anti-goat IgG. Briefly, FSN were functionalized with GPTES to yield particles bearing surface epoxide moieties. The epoxide functionalized FSN were then treated with mouse anti-goat IgG under high salt concentrations. Binding of protein to FSN was verified using a standard bicinchoninic acid (BCA) colorimetric assay.<sup>51-52</sup> An absorbance at 562 nm in the BCA assay indicates the presence of protein within the sample. Figure 34 shows the absorbance spectra from the BCA assay of mouse anti-goat IgG functionalized FSN prepared using Guo's method. Epoxide-coated FSN were used as a control and a BSA solution (150 µg/mL) was used as an internal standard. The results from the assay indicate that protein was successfully bound to the sample.

**Figure 34:** Absorbance spectra from the BCA assay of mouse anti-goat IgG functionalized FSN prepared using Guo's method.<sup>50</sup>

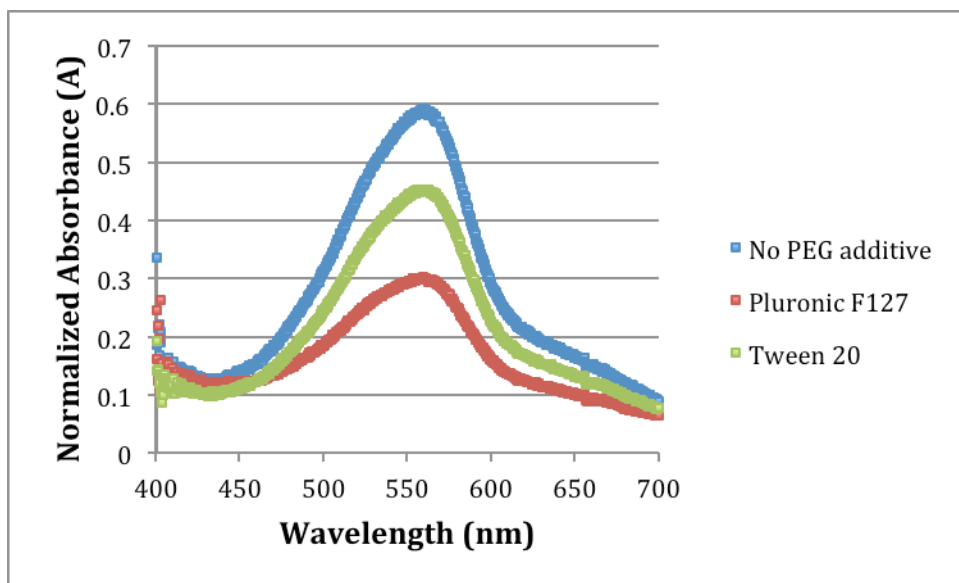


The absorbance spectra shown are from a BCA assay of one trial. Only one trial was performed.

Having demonstrated that protein was bound to the FSN, the functionalized particles were tested for application in a solid-support immunoassay used to detect *Neisseria gonorrhoea*. Unfortunately, these efforts were unsuccessful. Further studies revealed that, under the same reaction conditions, protein nonspecifically binds to bare (non-epoxide functionalized) FSN. Due to the fact that nonspecifically bound proteins are known to lose their biological activity, we postulated that the failure of the IgG functionalized particles in the immunoassay was due to the protein nonspecifically binding and denaturing on the surface of the FSN. Therefore, we set out to develop a strategy to selectively and controllably functionalize FSN with antibodies. The development of this strategy required (1) the prevention of nonspecific binding, and (2) an easy and reliable way to covalently attach antibody proteins to the FSN surface.

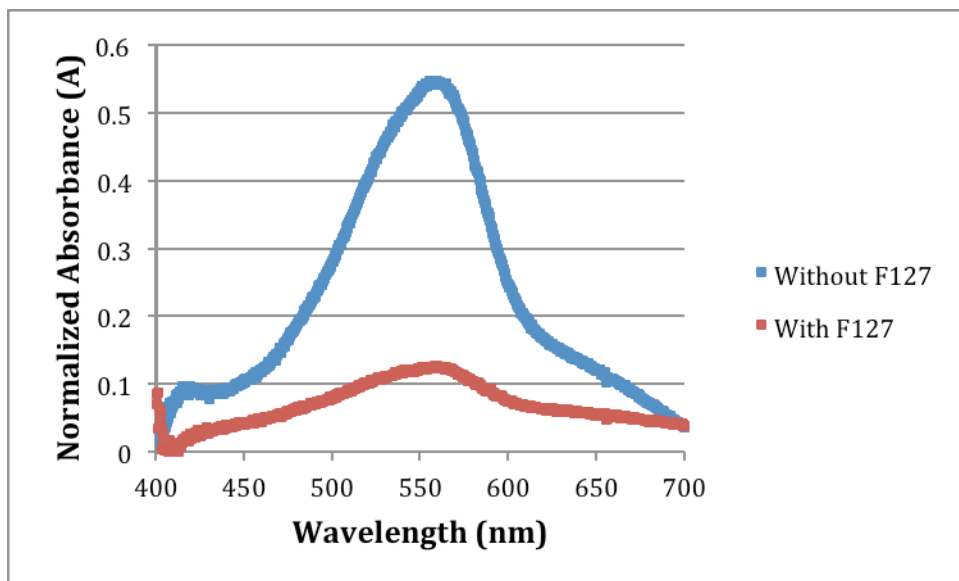
To control the binding of antibodies to the FSN and help ensure that the antibodies retain their biological activity, nonspecific binding of antibodies to the FSN surface through hydrophobic and electrostatic interactions must be prevented. It is well established that polyethylene glycol (PEG) derivatives can be used to prevent nonspecific binding of proteins to surfaces.<sup>53-54</sup> Therefore, nonspecific binding of proteins was studied using PEGylated FSN, which were prepared by reacting bare FSN with PEGTMS. Surprisingly, a significant amount of protein nonspecifically bound to PEGylated FSN. However, it was found that the addition of PEG derivatives to the reaction mixture reduced nonspecific binding. Figure 35 depicts the absorbance spectra from the BCA assay of PEGylated FSN treated with BSA with no PEG additive, with Tween 20, and with the triblock copolymer Pluronic F127 (EO<sub>106</sub>PO<sub>70</sub>EO<sub>106</sub>). The results from the assay show that BSA nonspecifically bound to PEGylated FSN when no PEG additive was used, and that Tween 20, a PEG polymer commonly used to prevent nonspecific binding, was not as effective as Pluronic F127 in preventing the nonspecific binding of BSA to PEGylated FSN (Figure 35). Pluronic F127 also proved to be very effective in preventing the nonspecific binding of goat anti-listeria IgG, rabbit anti-goat IgG, and goat anti-gonococcus IgG antibodies to PEGylated FSN. Figure 36 shows the results from the BCA assay of goat anti-listeria IgG antibody treated PEGylated FSN with and without Pluronic F127. Similar results were seen with PEGylated FSN that have been treated with rabbit anti-goat IgG antibody, and PEGylated FSN that have been treated with goat anti-gonococcus IgG antibody in the presence of Pluronic F127.

**Figure 35:** Absorbance spectra from the BCA assay of BSA treated PEGylated FSN with no additional PEG additive (blue), Tween 20 (green), and Pluronic F127 (red).



The absorbance spectra shown are from a BCA assay of one trial. Only one trial was performed.

**Figure 36:** Absorbance spectra from the BCA assay of goat anti-listeria IgG antibody treated PEGylated FSN with (red) and without (blue) Pluronic F127.



The absorbance spectra shown are from a BCA assay of one trial. Only one trial was performed.

In developing a strategy to covalently attach protein to the FSN, we hypothesized that using a mixed multilayer system consisting of PEG and a reactive moiety would be more effective in selectively conjugating protein to the surface and preventing protein denaturation. Zhang<sup>55</sup> and Yi<sup>56</sup> have successfully used such strategies to bind antibodies to silica surfaces. Though several coupling methodologies were studied, it was found that immobilizing proteins to FSN functionalized with a mixed PEG/epoxide coating in the presence of Pluronic F127 was most efficient. Figure 37 depicts the functionalization strategy schematically. It is hypothesized that PEGTMS and GPTES form a mixed-multilayer on the silica surface as shown in figure 38. PEG/epoxide functionalized particles that were exposed to goat anti-gonococcus IgG antibody, and then thoroughly washed with PBS buffer, tested positive for protein in the BCA assay—indicating that the antibody was successfully conjugated to the particles. The absorbance spectrum from the BCA assay of these particles (referred to as IgG-functionalized particles) is shown in Figure 39 (green absorbance spectra). PEG/epoxide functionalized FSN that were not exposed to antibody were used as a control in the BCA assay (Figure 39, red absorbance spectra). As an additional control, PEG/epoxide functionalized particles were first pretreated with ethanolamine to deactivate the epoxide moieties, and then were exposed to goat anti-gonococcus IgG antibody. BCA analysis indicates that less protein bound to the ethanolamine-pretreated PEG/epoxide particles than to PEG/epoxide particles that were not pretreated with ethanolamine (Figure 39, blue and green spectra, respectively). This result indicates that the protein was primarily immobilized onto the surface of the IgG-functionalized particles (non ethanolamine-pretreated particles) via covalent linkages. From a standard curve generated from goat anti-gonococcus IgG antibody, it

was calculated that the protein concentration within the FSN sample was approximately 8  $\mu\text{g}$  of antibody per mg of FSN.

**Figure 37:** Strategy used to prepare IgG-functionalized FSN.

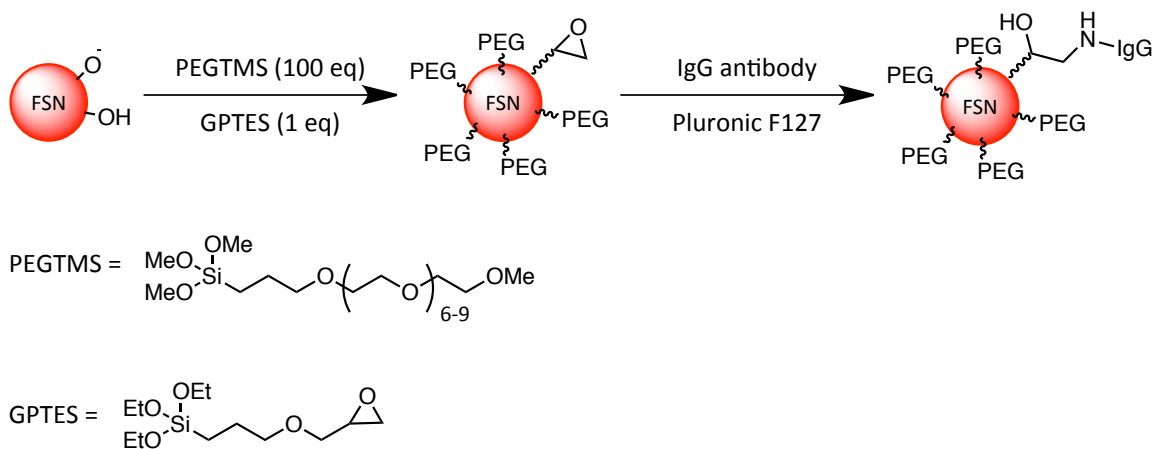


**Figure 38:** Proposed mixed-multilayer formed on PEGTMS/GPTES functionalized FSN.

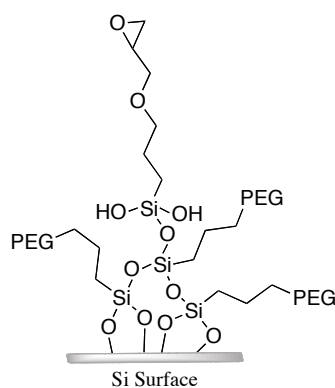
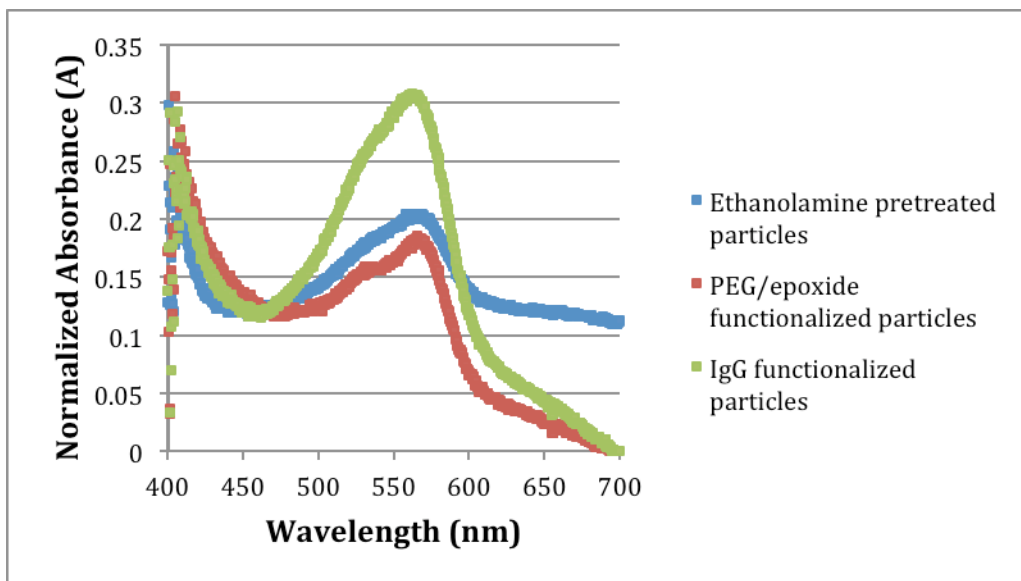


**Figure 39:** Absorbance spectra from the BCA assay of goat anti-gonococcus IgG antibody functionalized FSN (green), PEG/epoxide functionalized FSN (red; control), and ethanolamine pretreated PEG/epoxide FSN (blue; control).



The absorbance spectra shown are from a BCA assay of one trial. The results are representative of the results from three individual trials. In each case, a stronger absorbance at 560 nm was observed for PEG/epoxide FSN that were not pretreated with ethanolamine and exposed to IgG antibody (referred to as IgG functionalized particles, green absorbance spectra) than for PEG/epoxide FSN that were pretreated with ethanolamine and then exposed to IgG antibody (referred to as ethanolamine pretreated particles, blue absorbance spectra).

### 3 Conclusions

Fluorescent silica nanoparticles were prepared by incorporating a hydrophobically modified dye into a mesoporous silica nanoparticle synthesis procedure. The FSN do not leach dye and have strong, stable fluorescence that is 5 times more intense than that of quantum dots. For diagnostic applications, a method to selectively and covalently bind antibodies to the surface of the FSN was devised. It was found that the triblock copolymer, Pluronic F127, is effective in preventing nonspecific binding of proteins to FSN. Antibodies were selectively and covalently attached to FSN that were functionalized with a mixed PEG/epoxide coating in the presence of F127. The antibody-

functionalized particles are now being tested for application in flow cytometry experiments by Stein and coworkers in the Department of Cell Biology and Molecular Genetics at the University of Maryland, College Park.

## **4 Experimental**

### *4.1 General*

All chemicals were used as received from the supplier. 2-[Methoxy(polyethyleneoxy)propyl]trimethoxysilane (PEGTMS) and (3-Glycidoxypropyl)trimethoxysilane (GPTES) were obtained from Gelest, Inc. Tetraethyl orthosilicate (TEOS) was obtained from Sigma Aldrich. Pluronic® F-127 was obtained from BASF. All aqueous solutions were made using water filtered through a Millipore water filtration system unless otherwise indicated. Phosphate buffered saline (PBS) solutions were prepared from phosphate buffered saline tablets obtained from Sigma Aldrich (Sigma, tablets: P4417) as directed. The PBS solutions prepared had a measured pH of 7.4. The fatty acid modified rhodamine B dye, **1**, [1,2-dioleoyl-*sn*-glycero-3-phosphoethanolamine-N-(lissamine rhodamine B sulfonyl) (ammonium salt)] was purchased from Advanti Polar Lipids, Inc. An Ocean Optics USB 2000 Spectrometer was used to obtain absorbance spectra. Room temperature is defined as 20 °C.

### *4.2 MSN-Based Fluorescent Silica Nanoparticle Preparation*

Rhodamine dye, **1**, [1,2-dioleoyl-*sn*-glycero-3-phosphoethanolamine-N-(lissamine rhodamine B sulfonyl) (ammonium salt)] (0.001 g) was transferred to a three-necked



round bottom flask in chloroform (1 mL) and dried *in vacuo*. Water (15 mL) and cetyltrimethylammonium bromide (CTAB) (0.050 g) were added to the reaction vessel followed by 3 mL of an aqueous solution containing lysine HCl (0.017 g) and NaHCO<sub>3</sub> (0.012 g). The mixture was heated to 60 °C. To the vigorously stirring, heated reaction mixture was added a mixture of TEOS (0.532 mL) in heptane (5.00 mL). The TEOS/heptane mixture was added drop-wise in ten 0.5 mL aliquots. The reaction mixture stirred at 60°C for 2h, giving rise to a red/pink precipitate. The reaction mixture was cooled and transferred to a centrifuge tube. The precipitate (FSN) was spun down and washed with PBS solution (10 mL) via centrifugation/resuspension three times and then dried *in vacuo*.

#### 4.3 Fluorescence Imaging

Dilute solutions of FSN in water were spin-coated onto glass slides. The particles were excited with 488 nm wavelength light. The images were acquired using 0.24  $\mu$ W laser power with 5 ms dwell time per pixel. Integrated intensities,  $I_{ave}$ , were calculated using the equation:

$$I_{ave} = \frac{1}{N} \sum_i (I_i - B)$$

#### 4.4 PEG Functionalized FSN

FSN (0.010 g) were suspended in toluene (5.00 mL) and sonicated until evenly dispersed. The solution was placed under an argon atmosphere. PEGTMS (0.610 mL, 1.3 mmol) was added to the rapidly stirring solution in one aliquot. The mixture stirred under argon atmosphere at room temperature for 2 hours. The reaction mixture was

transferred to a centrifuge tube. The functionalized particles were spun down and washed with toluene (5 mL) via centrifugation/resuspension three times and then dried *in vacuo*.

#### 4.5 *PEG/Epoxide Functionalized FSN*

FSN (0.010 g) were suspended in toluene (5.00 mL) and sonicated until evenly dispersed. The solution was placed under an argon atmosphere. PEGTMS (0.610 mL, 1.3 mmol) was added to the rapidly stirring solution in one aliquot. The mixture stirred under argon atmosphere at room temperature for 30 minutes. An aliquot (0.100 mL) of a solution of GPTES (0.030 mL) in toluene (0.970 mL) (0.01 mmol of GPTES added) was then added to the reaction mixture. The mixture continued to stir under argon atmosphere at room temperature for 1.5 hours. The reaction mixture was transferred to a centrifuge tube. The functionalized particles were spun down and washed with toluene (5 mL) via centrifugation/resuspension three times and then dried *in vacuo*.

#### 4.6 *Conjugation of Goat Anti-Gonococcus IgG Antibody to PEG/Epoxide Functionalized FSN*

PEG/Epoxide functionalized FSN (0.005 g) were suspended in PBS solution (1.50 mL). An aliquot (0.150 mL) of a solution of Pluronic F127 in water (2 mg/mL) was added followed by 0.075 mL of a solution of goat anti-gonococcus IgG antibody in PBS (2 mg/mL). The reaction mixture was sonicated until particles were evenly distributed, and then stirred at room temperature for 18 hours. The particles were spun down and washed with PBS (5 mL) via centrifugation/resuspension three times and then resuspended in PBS (1 mL).

As a control, PEG/Epoxide functionalized FSN were pretreated with ethanolamine to inactivate the epoxide moieties. PEG/Epoxide functionalized FSN (0.005 g) were suspended in PBS solution (2.00 mL). Ethanolamine (0.050 mL) was added and the reaction mixture was sonicated, and then stirred at room temperature for 3 hours. Afterward, the reaction mixture was incubated at 40 °C for 1 hour. The particles were then spun down and washed with PBS (5 mL) via centrifugation/resuspension three times. The pretreated particles were then exposed to goat anti-gonococcus IgG antibody in the same manner described above for the non-pretreated PEG/Epoxide functionalized particles.

#### *4.7 BCA Assay Protocol*

BCA assays were conducted using reagents from a Pierce BCA Protein Assay Kit purchased from Thermo Scientific. The “Enhanced Test Tube Protocol” found in the instructions manual accompanying the BCA assay kit was employed. Briefly, 0.100 mL of a 5 mg/mL suspension of particles in PBS solution was transferred to a 1 dram vial. 2.00 mL of freshly prepared BCA “working reagent” was added to the vial. The vial was capped and placed in a water bath set at 60 °C for 30 minutes. Afterward, the vial was removed from the water bath and placed in a freezer for 10 minutes. The vial was removed from the freezer, allowed to warm to room temperature, and then the absorbance of the solution was measured using an Ocean Optics USB 2000 Spectrometer.

## Acknowledgements

The author acknowledges Edda Liu, Zifan Wang, Amanda Mahle, Daniel Rabin, Stephanie Galanie, Michael Zachariah, Douglas English, and Daniel Stein for the significant contributions they made to the research and discoveries presented throughout this chapter.

## 5 References

- 1) Wan, J.; Meng, X.; Liu, E.; Chen, K. *Nanotechnology* **2010**, 21, 235104.
- 2) Yang, L.-Z.; Chen, Z.-L. *Anal. Lett.* **2011**, 44, 687-697.
- 3) Wang, X.; Ramstroem, O.; Yan, M. *Chem. Commun.* **2011**, 47, 4261-4263.
- 4) Qin, D.; He, X.; Wang, K.; Tan, W. *Biosens. Bioelectron.* **2008**, 24, 626-631.
- 5) Wang, Z.; Miu, T.; Xu, H.; Duan, N.; Ding, X.; Li, S. *J. Microbiol. Methods.* **2010**, 83, 179-184.
- 6) Zhang, X.; Song, C.; Chen, L.; Zhang, K.; Fu, A.; Jin, B.; Zhang, Z.; Yang, K. *Biosens. Bioelectron.* **2011**, 26, 3958-3961.
- 7) Fent, K.; Weisbrod, C. J.; Wirth-Heller, A.; Pieves, U. *Aquat. Toxicol.* **2010**, 100, 218-228.
- 8) Ow, H.; Larson, D. R.; Srivastava, M.; Baird, B. A.; Webb, W. W.; Wiesner, U. *Nano Lett.* **2005**, 5, 113-117.
- 9) Sokolov, I.; Naik, S. *Small* **2008**, 4, 934-939.
- 10) Ha, S.-W.; Camalier, C. E.; Beck, G. R., Jr.; Lee, J.-K. *Chem. Commun.* **2009**, 2881-2883.
- 11) Herz, E.; Marchincin, T.; Connelly, L.; Bonner, D.; Burns, A.; Switalski, S.;

- Wiesner, U. *J. Fluoresc.* **2010**, 20, 67-72.
- 12) Roy, S.; Woolley, R.; MacCraith, B. D.; McDonagh, C. *Langmuir* **2010**, 26, 13741-13746.
- 13) Penn, S. G.; He, L.; Natan, M. J. *Curr. Opin. Chem. Biol.* **2003**, 7, 609-615.
- 14) Katz, E.; Willner, I. *Angew. Chem., Int. Ed.* **2004**, 43, 6042-6108.
- 15) Zhong, Wenwan. *Anal. Bioanal. Chem.* **2009**, 394, 47-59.
- 16) Langhals, H.; Esterbauer, A. J. *Chem. Eur. J.* **2009**, 15, 4793-4796.
- 17) Faisal, M.; Hong, Y.; Liu, J.; Yu, Y.; Lam, J. W. Y.; Qin, A.; Lu, P.; Tang, B. Z. *Chem. Eur. J.* **2010**, 16, 4266-4272.
- 18) Xie, C.; Yin, D.; Li, J.; Zhang, L.; Liu, B.; Wu, M. *Nano Biomed. Eng.* **2009**, 1, 39-47.
- 19) Burns, A.; Sengupta, P.; Zedayko, T.; Baird, B.; Wiesner, U. *Small* **2006**, 2, 723-726.
- 20) Verhaegh, N. A. M.; Blaaderen, A. V. *Langmuir* **1994**, 10, 1427-1438.
- 21) Montalti, M.; Prodi, L.; Zaccheroni, N.; Zattoni, A.; Reschiglian, P.; Falini, G. *Langmuir* **2004**, 20, 2989-2991.
- 22) Chen, X.-L.; Zou, J.-L.; Zhao, T.-T.; Li, Z.-B. *J. Fluoresc.* **2007**, 17, 235-241.
- 23) Folling, J.; Polyakova, S.; Belov, V.; van Blaaderen, A.; Bossi Mariano, L.; Hell Stefan, W. *Small* **2008**, 4, 134-142.
- 24) Moro, A. J.; Schmidt, J.; Doussineau, T.; Lapresta-Fernandez, A.; Wegener, J.; Mohr, G. *J. Chem. Commun.* **2011**, 47, 6066-6068.
- 25) Cho, Y.-S.; Yoon, T.-J.; Jang, E.-S.; Soo Hong, K.; Young Lee, S.; Ran Kim, O.; Park, C.; Kim, Y.-J.; Yi, G.-C.; Chang, K. *Cancer Lett.* **2010**, 299, 63-71.

- 26) Wang, Y.; Gildersleeve, J. C.; Basu, A.; Zimmt, M. B. *J. Phys. Chem. B* **2010**, 114, 14487-14494.
- 27) Langhals, H.; Esterbauer, A. J. *Chem. Eur. J.* **2009**, 15, 4793-4796.
- 28) Gao, X.; He, J.; Deng, L.; Cao, H. *Opt. Mater.* **2009**, 31, 1715-1719.
- 29) Yang, H.-H.; Qu, H.-Y.; Lin, P.; Li, S.-H.; Ding, M.-T.; Xu, J.-G. *Analyst* **2003**, 128, 462-466.
- 30) Santra, S.; Zhang, P.; Wang, K.; Tapeç, R.; Tan, W. *Anal. Chem.* **2001**, 73, 4988-4993.
- 31) Lebret, V.; Raehm, L.; Durand, J.-O.; Smaïhi, M.; Gerardin, C.; Nerambourg, N.; Werts, M. H. V.; Blanchard-Desce, M. *Chem. Mater.* **2008**, 20, 2174-2183.
- 32) Sokolov, I.; Kievsky, Y. Y.; Kaszpurenko, J. M. *Small* **2007**, 3, 419-423.
- 33) Godoy-Navajas, J.; Aguilar-Caballos, M.-P.; Gomez-Hens, A. *J. Fluoresc.* **2010**, 20, 171-180.
- 34) Yao, K. S.; Li, S. J.; Tzeng, K. C.; Cheng, T. C.; Chang, C. Y.; Chiu, C. Y.; Liao, C. Y.; Hsu, J. J.; Lin, Z. P. *Adv. Mater. Res.* **2009**, 513-516.
- 35) Cao, A.; Ye, Z.; Cai, Z.; Dong, E.; Yang, X.; Liu, G.; Deng, X.; Wang, Y.; Yang, S.-T.; Wang, H.; Wu, M.; Liu, Y. *Angew. Chem., Int. Ed.* **2010**, 49, 3022-3025.
- 36) Lee, K. G.; Kim, J. C.; Wi, R.; Min, J. S.; Ahn, J. K.; Kim, D. H. *J. Nanosci. Nanotechnol.* **2011**, 11, 686-690.
- 37) Lee, K. G.; Wi, R.; Park, T. J.; Yoon, S. H.; Lee, J.; Lee, S. J.; Kim, D. H. *Chem. Commun.* **2010**, 46, 6374-6376.
- 38) Fowler, C. E.; Mann, S.; Lebeau, B. *Chem. Commun.* **1998**, 1825-1826.
- 39) Lebeau, B.; Fowler, C. E.; Mann, S.; Farcet, C.; Charleux, B.; Sanchez, C. *J.*

- Mater. Chem.* **2000**, 10, 2105-2108.
- 40) Lin, Y.-S.; Tsai, C.-P.; Huang, H.-Y.; Kuo, C.-T.; Hung, Y.; Huang, D.-M.; Chen, Y.-C.; Mou, C.-Y. *Chem. Mater.* **2005**, 17, 4570-4573.
  - 41) Slowing, I.; Trewyn, B. G.; Lin, V. S. Y. *J. Am. Chem. Soc.* **2006**, 128, 14792-14793.
  - 42) Chhabra, V.; Pillai, V.; Mishra, B. K.; Morrone, A.; Shah, D. O. *Langmuir* **1995**, 11, 3307-3311.
  - 43) Rocha, L. A.; Caiut, J. M. A.; Messaddeq, Y.; Ribeiro, S. J. L.; Martines, M. A. U.; Freiria, J. d. C.; Dexpert-Ghys, J.; Verelst, M. *Nanotechnology* **2010**, 21, 155603.
  - 44) Kresge, C. T.; Leonowicz, M. E.; Roth, W. J.; Vartuli, J. C.; Beck, J. S. *Nature* **1992**, 359, 710-712.
  - 45) Firouzi, A.; Atef, F.; Oertli, A. G.; Stucky, G. D.; Chmelka, B. F. *J. Am. Chem. Soc.* **1997**, 119, 3596-3610.
  - 46) Nandiyanto, A. B. D.; Kim, S. G.; Iskandar, F.; Okuyama, K. *Micropor. and Mesopor. Mat.* **2009**, 120, 447-453.
  - 47) Muto, S.; Oaki, Y.; Imai, H. *Chem. Lett.* **2006**, 35, 880-881.
  - 48) Willner, I.; Katz, E. *Angew. Chem., Int. Ed.* **2000**, 39, 1181-1218.
  - 49) Katz, E.; Willner, I. *Angew. Chem. Int. Ed.* **2004**, 43, 6042-6108.
  - 50) Zhang, Q.; Huang, R. F.; Guo, L.-H. *Chin. Sci. Bull.* **2009**, 54, 2620-2626.
  - 51) Smith, P. K.; Krohn, R. I.; Hermanson, G. T.; Mallia, A. K.; Gartner, F. H.; Provenzano, M. D.; Fujimoto, E. K.; Goeke, N. M.; Olson, B. J.; Klenk, D. C. *Anal. Biochem.* **1985**, 150, 76-85.

- 52) Wiechelman, K. J.; Braun, R. D.; Fitzpatrick, J. D. *Anal. Biochem.* **1988**, 175, 231-7.
- 53) Silin, V.; Weetall, H.; Vanderah, D. J. *J. Colloid Interface Sci.* **1997**, 185, 94-103.
- 54) Houseman, B. T.; Mrksich, M. *Chemistry and Biology.* **2002**, 9, 443-454.
- 55) Wolcott, A.; Gerion, D.; Visconte, M.; Sun, J.; Schwartzberg, A.; Chen, S.; Zhang, J. Z. *J. Phys. Chem. B* **2006**, 110, 5779-5789.
- 56) Cho, Y.-S.; Yoon, T.-J.; Jang, E.-S.; Soo Hong, K.; Young Lee, S.; Ran Kim, O.; Park, C.; Kim, Y.-J.; Yi, G.-C.; Chang, K. *Cancer Lett.* **2010**, 299, 63-71.



## List of References by Chapter

### Chapter 1

- 1) de la Fuente, J. M.; Penades, S. *Biochim. Biophys. Acta. Gen. Subj.* **2006**, 1760, 636-651.
- 2) Ojeda, R.; de Paz, J. L.; Barrientos, A. G.; Martin-Lomas, Manuel; Penades, S. *Carbohydr. Res.* **2007**, 342, 448-459.
- 3) Katz, E.; Willner, I. *Angew. Chem., Int. Ed.* **2004**, 43, 6042-6108.
- 4) Niemeyer, C. M. *Angew. Chem., Int. Ed.* **2001**, 40, 4128-4158.
- 5) Blodgett, K. B. *J. Am. Chem. Soc.* **1935**, 57, 1007-1022.
- 6) Blodgett, K. B.; Langmuir, I. *Phys. Rev.* **1937**, 51, 964-982.
- 7) Bigelow, W. C.; Pickett, D. L.; Zisman, W. A. *J. Colloid Sci.* **1946**, 1, 513.
- 8) Bain, C. D.; Troughton, E. B. *J. Am. Chem. Soc.* **1989**, 111, 321-35.
- 9) Ulman, A. *Chem. Rev.* **1996**, 96, 1533-1554.
- 10) Love, J. C.; Estroff, L. A.; Kriebel, J. K.; Nuzzo, R. G.; Whitesides, G. M. *Chem. Rev.* **2005**, 105, 1103-1169.
- 11) Nuzzo, R. G.; Allara, D. L. *J. Am. Chem. Soc.* **1983**, 105, 4481-4483.
- 12) Nuzzo, R. G.; Zegarski, B. R.; Dubois, L. H. *J. Am. Chem. Soc.* **1987**, 109, 733-740.
- 13) Troughton, E. B.; Bain, C. D.; Whitesides, G. M.; Nuzzo, R. G.; Allara, D. L.; Porter, M. *Langmuir* **1988**, 4, 365-385.
- 14) Lee, L.-H. *SPI (Soc. Plast. Ind.) Reinf. Plast./Compos. Div., Annu. Tech. Conf., Proc., 23rd* **1968**, 9D-1-9D-14.
- 15) Lee, L.-H. *J. Colloid Interf. Sci.* **1968**, 27, 751-60.

- 16) Zisman, W. A. *Ind. Eng. Chem., Prod. Res. Develop.* **1969**, 8, 98-111.
- 17) Sagiv, J. *J. Am. Chem. Soc.* **1980**, 102, 92-98.
- 18) Kahn, F. J.; Taylor, G. N.; Schonhorn, H. *Proc. IEEE.* **1973**, 61, 823-8.
- 19) Silverman, B. M.; Wieghaus, K. A.; Schwartz, J. *Langmuir* **2005**, 21, 225-228.
- 20) Cattani-Scholz, A.; Pedone, D.; Dubey, M.; Neppl, S.; Nickel, B.; Feulner, P.; Schwartz, J.; Abstreiter, G.; Tornow, M. *ACS Nano* **2008**, 2, 1653-1660.
- 21) Tsoi, S.; Fok, E.; Sit, J. C.; Veinot, J. G. C. *Chem. Mater.* **2006**, 18, 5260-5266.
- 22) Wu, W.; He, Q.; Jiang, C. *Nanoscale Res. Lett.* **2008**, 3, 397-415.
- 23) Allara, D. L.; Nuzzo, R. G. *Langmuir* **1985**, 1, 45-52.
- 24) Ogawa, H.; Chihera, T.; Taya, K. *J. Am. Chem. Soc.* **1985**, 107, 1365-1369.
- 25) Schlotter, N. E.; Porter, M.D. *Chem. Phys. Lett.* **1986**, 132, 93.
- 26) Tao, Y. T. *J. Am. Chem. Soc.* **1993**, 115, 4350-4358.
- 27) Howarter, J. A.; Youngblood, J. P. *Langmuir* **2006**, 22, 11142-11147.
- 28) Chinwangso, P.; Jamison, A. C.; Lee, T. R. *Acc. Chem. Res.* **2011**, 44, 511-519.
- 29) Wu, W.; He, Q.; Jiang, C. *Nanoscale Res. Lett.* **2008**, 3, 397-415.
- 30) Caruso, F. *Adv. Mater.* **2001**, 13, 11-22.
- 31) Willner, I.; Katz, E. *Angew. Chem., Int. Ed.* **2000**, 39, 1181-1218.
- 32) Nobs, L.; Buchegger, F.; Gurny, R.; Allemann, E. *J. Pharm. Sci.* **2004**, 93, 1980-1992.
- 33) Houseman, B. T.; Gawalt, E. S.; Mrksich, M. *Langmuir* **2003**, 19, 1522-1531.
- 34) Zhang, Q.; Huang, R. F.; Guo, L.-H. *Chin. Sci. Bull.* **2009**, 54, 2620-2626.
- 35) Wu, Y.; Chen, C.; Liu, S. *Anal. Chem.* **2009**, 81, 1600-1607.
- 36) Tang, D.; Su, B.; Tang, J.; Ren, J.; Chen, G. *Anal. Chem.* **2010**, 82, 1527-1534.

- 37) Lahiri, J.; Isaacs, L.; Tien, J.; Whitesides, G. M. *Anal. Chem.* **1999**, 71, 777-90.
- 38) Azioune, A.; Ben Slimane, A.; Hamou, L. A.; Pleuvy, A.; Chehimi, M. M.; Perruchot, C.; Armes, S. P. *Langmuir* **2004**, 20, 3350-3356.
- 39) Kim, M. I.; Ham, H. O.; Oh, S.-D.; Park, H. G.; Chang, H. N.; Choi, S.-H. *J. Mol. Catal. B: Enzym.* **2006**, 39, 62-68.
- 40) Wang, Z.; Miu, T.; Xu, H.; Duan, N.; Ding, X.; Li, S. *J. Microbiol. Methods.* **2010**, 83, 179-184.
- 41) Zhang, X.; Song, C.; Chen, L.; Zhang, K.; Fu, A.; Jin, B.; Zhang, Z.; Yang, K. *Biosens. Bioelectron.* **2011**, 26, 3958-3961.
- 42) Wei, H.; Zhou, L.; Li, J.; Liu, J.; Wang, E. *J. Colloid Interf. Sci.* **2008**, 321, 310-314.
- 43) Betancor, L.; Lopez-Gallego, F.; Hidalgo, A.; Alonso-Morales, N.; Cesar Mateo, G. D.-O.; Fernandez-Lafuente, R.; Guisan, J. M. *Enzyme Microb. Technol.* **2006**, 39, 877-882.
- 44) Xu, H.; Zhang, Z. *Biosens. Bioelectron.* **2007**, 22, 2743-2748.
- 45) Angeloni, S.; Ridet, J. L.; Kusy, N.; Gao, H.; Crevoisier, F.; Guinchard, S.; Kochhar, S.; Sigrist, H.; Sprenger, N. *Glycobiology* **2004**, 15, 31-41.
- 46) Sigrist, H.; Collioud, A.; Clemence, J.-F.; Gao, H.; Luginbuehl, R.; Saenger, M.; Sundarababu, G. *Opt. Eng.* **1995**, 34, 2339-48.
- 47) Maltzahn, G.; Ren, Y.; Park, D.; Kotamraju, V. R.; Jayakumar, J.; Fogal, M.; Ruoslahti, E.; Bhatia, S. *Bioconjugate Chem.* **2008**, 19, 1570-1578.
- 48) Houseman, B. T.; Huh, J. H.; Kron, S. J.; Mrksich, M. *Nat. Biotechnol.* **2002**, 20, 270-274.

- 49) Godula, K.; Bertozzi, C. R. *J. Am. Chem. Soc.* **2010**, 132, 9963-9965.
- 50) Zhi, Z.-L.; Powell, A. K.; Turnbull, J. E. *Anal. Chem.* **2006**, 78, 4786-4793.
- 51) de Boer, A. R.; Hokke, C. H.; Deelder, A. M.; Wührer, M. *Anal. Chem.* **2007**, 79, 8107-8113.
- 52) Park, S.; Lee, M.-R.; Shin, I. *Bioconjugate Chem.* **2009**, 20, 155-162.
- 53) Zhou, X.; Turchi, C.; Wang, D. *J. Proteome Res.* **2009**, 8, 5031-5040.
- 54) Clo, E.; Blixt, O.; Jensen, K. J. *Eur. J. Org. Chem.* **2010**, 540-554.
- 55) Toshima, K.; Tatsuta, K. *Chem. Rev.* **1993**, 93, 1503-1531.
- 56) Yoshimura, Y.; Shimizu, H.; Hinou, H.; Nishimura, S. *Tetrahedron Lett.* **2005**, 46, 4701-4705.
- 57) Barrientos, A.; de la Fuente, J.; Rojas, T.; Fernandez, A.; Penades, S. *Chem. Eur. J.* **2003**, 9, 1909-1921.
- 58) Shimizu, H.; Sakamoto, M.; Nagahori, N.; Nishimura, S. *Tetrahedron* **2007**, 63, 2418-2425.
- 59) Lin, C.; Yeh, Y.; Yang, C'; Chen, C.; Chen, G.; Chen, C.; Wu, Y. *J. Am. Chem. Soc.* **2002**, 124, 3508-3509.
- 60) Halkes, M. K.; de Souza, A. C.; Maljaars, E.; Gerwig, G.; Kamerling, J. *Eur. J. Org. Chem.* **2005**, 3650-3659.
- 61) Zhang, Y.; Luo, S.; Tang, Y.; Hou, K.; Cheng, J.; Zeng, X.; Wang, P. G. *Anal. Chem.* **2006**, 78, 2001-2008.
- 62) Boubbou, K.; Gruden, C.; Huang, X. *J. Am. Chem. Soc.* **2007**, 129, 13392-13393.
- 63) Earhart, C.; Jana, N.; Erathodiyil, N.; Ying, J. *Langmuir* **2008**, 24, 6215-6219.

- 64) Damkaci, F.; DeShong, P. *J. Am. Chem. Soc.* **2003**, 125, 4408-4409.
- 65) Kadalbajoo, M.; Park, J.; Opdahl, A.; Suda, H.; Kitchens, C.; Garino, J.; Batteas, J.; Tarlov, M.; DeShong, P.; *Langmuir* **2007**, 23, 700-707.
- 66) De, M.; Ghosh, P. S.; Rotello, V. M. *Adv. Mater.* **2008**, 20, 4225-4241.
- 67) Stanford, C. J.; Ryu, G.; Dagenais, M.; Hurley, M. T.; Gaskell, K. J.; De Shong, P. *J. Sens.* **2009**, Article ID 982658.
- 68) Ryu, G.; Dagenais, M.; Hurley, M. T.; De Shong, P. *IEEE J. Sel. Top. Quantum Electron.* **2010**, 16, 647-653.
- 69) Buskas, T.; Soderberg, E.; Konradsson, P.; Fraser-Reid, B. *J. Org. Chem.* **2000**, 65, 958-963.
- 70) Chatterjee, A. K.; Morgan, J. P.; Scholl, M.; Grubbs, R. H. *J. Am. Chem. Soc.* **2000**, 122, 3783-3784.
- 71) Grubbs, R. H. *Tetrahedron* **2004**, 60, 7117-7140.
- 72) Chatterjee, A.; Grubbs, R. H. *Angew. Chem., Int. Ed.* **2002**, 41, 3171-3174.
- 73) O'Leary, D. J.; Blackwell, H. E.; Washenfelder, R. A.; Grubbs, R. H. *Tetrahedron Lett.* **1998**, 39, 7427-7430.
- 74) Chatterjee, A. K.; Grubbs, R. H. *Org. Lett.* **1999**, 1, 1751-1753.
- 75) Blackwell, H. E.; O'Leary, D. J.; Chatterjee, A. K.; Washenfelder, R. A.; Busmann, D. A.; Grubbs, R. H. *J. Am. Chem. Soc.* **2000**, 122, 58-71.
- 76) Choi, T.-L.; Chatterjee, A. K.; Grubbs, R. H. *Angew. Chem., Int. Ed.* **2001**, 40, 1277-1279.
- 77) Chatterjee, A. K.; Sanders, D. P.; Grubbs, R. H. *Org. Lett.* **2002**, 4, 1939-1942.
- 78) Chatterjee, A. K.; Choi, T.-L.; Sanders, D. P.; Grubbs, R. H. *J. Am. Chem. Soc.*

- 2003**, 125, 11360-11370.
- 79) O'Leary, D. J.; Blackwell, H. E.; Washenfelder, R. A.; Grubbs, R. H.  
*Tetrahedron Lett.* **1998**, 39, 7427.
- 80) Roy, R.; Das, S. K. *Chem. Commun.* **2000**, 519-529.
- 81) Leeuwenburgh Michiel, A.; van der Marel Gijsbert, A.; Overkleeft Herman, S.  
*Curr. Opin. Chem. Biol.* **2003**, 7, 757-765.
- 82) Jorgensen, M.; Hadwiger, P.; Madsen, R.; Stutz, A. E.; Wrodnigg, T. M. *Curr. Org. Chem.* **2000**, 4, 565-588.
- 83) Hu, Y.-J.; Roy, R. *Tetrahedron Lett.* **1999**, 40, 3305-3308.
- 84) Vernall Andrea, J.; Abell Andrew, D. *Org. Biomol. Chem.* **2004**, 2, 2555-2557.
- 85) Hadwiger, P.; Stutz, A. E. *Synlett.* **1999**, 1787-1789.
- 86) Plettenburb, O.; Mui, C.; Bodmer-Narkevitch, V.; Wong, C. *Adv. Synth. Catal.* **2002**, 344, 622-626.
- 87) Bruchner, P.; Koch, D.; Voigtmann, Ulrike, Blechert, S. *Synth. Commun.* **2007**, 37, 2757-2769.
- 88) Timmer, M.; Chumillas, M. V.; Donker-Koopman, W.; Aerts, J. M. F. G.; van der Marel, G.; Overkleeft, H. *J. Carbohydr. Chem.* **2005**, 24, 335-351.
- 89) Wan, Q.; Cho, Y. S.; Lambert, T.; Danishefsky, S. *J. Carbohydr. Chem.* **2005**, 24, 425-440.
- 90) Otsuka, H.; Akiyama, Y.; Nagasaki, Y. Kataoka, K. *J. Am. Chem. Soc.* **2001**, 123, 8226-8230.
- 91) Houseman, B. T.; Mrksich, M. *Chem. Biol.* **2002**, 9, 443-454.
- 92) Vollhardt, D. *J. Phys. Chem. C.* **2007**, 111, 6805-6812.

- 93) Borch, R. F.; Bernstein, M. D.; Durst, H. D. *J. Amer. Chem. Soc.* **1971**, 93, 2897-904.
- 94) Dubois, M.; Gilles, K. A.; Hamilton, J. K.; Rebers, P. A.; Smith, F. *Anal. Chem.* **1956**, 28, 350-356.
- 95) Gildersleeve, J. C.; Oyelaran, O.; Simpson, J. T.; Allred, B. *Bioconjugate Chem.* **2008**, 19, 1485-1490.
- 96) Damkaci, F. *Ph.D. Thesis, University of Maryland, College Park.* **2004**.
- 97) Park, J. *Ph.D. Thesis, University of Maryland, College Park.* **2008**.

## Chapter 2

- 1) Kresge, C. T.; Leonowicz, M. E.; Roth, W. J.; Vartuli, J. C.; Beck, J. S. *Nature* **1992**, 359, 710-712.
- 2) Zhao, D.; Feng, J.; Huo, Q.; Melosh, N.; Fredrickson, G.; Chmelka, B.; Stucky, G. *Science* **1998**, 279, 548-552.
- 3) Bagshaw, S. A.; Prouzet, E.; Pinnavaia, T. J. *Science* **1995**, 269, 1242–1244.
- 4) Inagaki, S.; Fukushima, Y.; Kuroda, K. *J. Chem. Soc., Chem. Commun.* **1993**, 680–682.
- 5) Ryoo, R.; Kim, J. M.; Ko, C. H.; Shin, C. H. *J. Phys. Chem.* **1996**, 100, 17718-17721.
- 6) Giri, S.; Trewn, B.; Lin, V. *Nanomedicine* **2007**, 2, 99-111.
- 7) Trewn, B.; Slowing, I.; Giri, S.; Chen, H.; Lin, V. *Acc. Chem. Res.* **2007**, 40, 846-853.

- 8) Vallet-Regi, M.; Ramila, A.; del Real, R. P.; Perez-Pariente, J. *Chem. Mater.* **2001**, 13, 308–311.
- 9) Munoz, B.; Ramila, A.; Perez-Pariente, J.; Diaz, I.; Vallet-Regi, M. *Chem. Mater.* **2003**, 15, 500-503.
- 10) Song, S.-W.; Hidajat, K.; Kawi, S. *Langmuir* **2005**, 21, 9568-9575.
- 11) Xu, W.; Gao, Q.; Xu, Yao.; Wu, D.; Sun, Y.; Shen, W.; Deng, F. *J. Solid State Chem.* **2008**, 181, 2837-2844.
- 12) Tang, Q.; Xu, Y.; Wu, D.; Sun, Y. *J. Solid State Chem.* **2006**, 179, 1513-1520.
- 13) Casasus, R.; Climent, E.; Marcos, M. D.; Martinez-Manez, R.; Sancenon, F.; Soto, J.; Amoros, P.; Cano, J.; Ruiz, E. *J. Am. Chem. Soc.* **2008**, 130, 1903-1917.
- 14) Horcajada, P.; Ramila, A.; Perez-Pariente, J.; Vallet-Regi, M. *Micropor. Mesopor. Mater.* **2004**, 68, 105-109.
- 15) Andersson, J.; Rosenholm, J.; Areva, S.; Linden, M. *Chem. Mater.* **2004**, 16, 4160-4167.
- 16) Qu, F.; Zhu, G.; Huang, S.; Shougui, L.; Sun, J.; Zhang, D.; Qiu, S. *Micropor. Mesopor. Mater.* **2006**, 92, 1-9.
- 17) Stromme, M.; Brohede, U.; Atluri, R.; Garcia-Bennet, A. E. *Nanomedicine and Nanobiotechnology* **2009**, 1, 140-148.
- 18) Salonen, J.; Laitinen, L.; Kaukonen, A. M.; Tuura, J.; Björkqvist, M.; Heikkilä, T. Vähä-Heikkilä, K.; Hirvonen, J.; Lehto, V.-P. *J. Controlled Release* **2005**, 108,



362-374.

- 19) Ng, J. B. S.; Kamali-Zare, P.; Brismar, H.; Bergstrom, L. *Langmuir* **2008**, 24, 11096-11102.
- 20) Lai, C.-Y.; Trewyn, B. G.; Jeftinija, D. M.; Jeftinija, K.; Xu, S.; Jeftinija, S.; Lin, V. S.-Y. *J. Am. Chem. Soc.* **2003**, 125, 4451-4459.
- 21) Slowing, I. I.; Vivero-Escoto, J. L.; Wu, C-W.; Lin, V. S.-Y. *Adv. Drug Delivery Reviews* **2008**, 60, 1278-1288.
- 22) Vivero-Escoto, J. L.; Slowing, I. I.; Wu, C-W.; Lin, V. S.-Y. *J. Am. Chem. Soc.* **2009**, 131, 3462-3463.
- 23) Zhao, Y.; Trewyn, B. G.; Slowing, I. I.; Lin, V. S.-Y. *J. Am. Chem. Soc.* **2009**, 131, 8398-8400.
- 24) Lu, J.; Liong, M.; Zink, J.; Tamanoi, F. *Small* **2007**, 3, 1341-1346
- 25) You, Y.-Z.; Kalebaila, K.; Brock, S.; Oupichy, D. *Chem. Mater.* **2008**, 20, 3354-3359.
- 26) Mal, N. K.; Fujiwara, M.; Tanaka, Y.; Taguchi, T.; Matsukata, M. *Chem. Mater.* **2003**, 15, 3385-3394.
- 27) Hernandez, R.; Tseng, H.-R.; Wong, J. W.; Stoddart, J. F.; Zink, J. I. *J. Am. Chem. Soc.* **2004**, 126, 3370-3371.
- 28) Nguyen, T.; Tseng, H.-R.; Celestre, P.; Flood, A.; Liu, Y.; Stoddart, J. F.; Zink, J. *PNAS* **2005**, 102, 10029-10034.

- 29) Nguyen, T.; Liu, Y.; Saha, S.; Leung, K.; Stoddart, J. F.; Zink, J. *J. Am. Chem. Soc.* **2007**, 129, 626-634.
- 30) Angelos, S.; Yang, Y.-W.; Petal, K.; Stoddart, J. F.; Zink, J. I. *Angew. Chem. Int. Ed.* **2008**, 47, 2222-2226.
- 31) Khashab, N. M.; Trabolsi, A.; Lau, Y. A.; Ambrogio, M. W.; Friedman, D. C.; Khatib, H. A.; Zink, J. I.; Stoddart, J. F. *Eur. J. Org. Chem.* **2009**, 1669-1673.
- 32) Du, L.; Liao, S.; Khatib, H. A.; Stoddart, J. F.; Zink, J. I. *J. Am. Chem. Soc.* **2009**, 131, 15136-15142.
- 33) Angelos, S.; Khashab, N. M.; Yang, Y.-W.; Trabolsi, A.; Khatib, H. A.; Stoddart, J. F.; Zink, J. I. *J. Am. Chem. Soc.* **2009**, 131, 12912-12914.
- 34) Ferris, D. P.; Zhao, Y.-L.; Khashab, N. M.; Khatib, H. A.; Stoddart, J. F.; Zink, J. I. *J. Am. Chem. Soc.* **2009**, 131, 1686-1688.
- 35) Park, C.; Oh, K.; Lee, S. C.; Kim, C. *Angew. Chem. Int. Ed.* **2007**, 46, 1455-1457.
- 36) Hong, C.-Y.; Li, X.; Pan, C.-Y. *J. Mater. Chem.* **2009**, 19, 5155-5160.
- 37) Zhu, C.-L.; Song, X.-Y.; Zhou, W.-H.; Yang, H. H.; Wen, Y.-H.; Wang, X.-R. *J. Mater. Chem.* **2009**, 19, 7765-7770.
- 38) Beck, J. C.; Vartuli, J. C.; Roth, W. J.; Leonowicz, M. E.; Kresge, C. T.; Schmitt, K. D.; Chu, C. T.-W.; Olsen, D. H.; Sheppard, E. W.; McCullen, S. B.; Higgins, J. B.; Schlenker, J. L. *J. Am. Chem. Soc.* **1992**, 114, 10834-10843.

- 39) Slowing, I. I.; Vivero-Escoto, J. L.; Trewyn, B. G.; Lin, V. S. Y. *J. Mater. Chem.* **2010**, 20, 7924-7937.
- 40) Wu, S.-H.; Hung, Y.; Mou, C.-Y. *Chem. Commun.* **2011**, 47, 9972-9985.
- 41) He, Q.; Shi, J. *J. Mater. Chem.* **2011**, 21, 5845-5855.
- 42) Popat, A.; Hartono, S. B.; Stahr, F.; Liu, J.; Qiao, S. Z.; Lu, G. Q. *Nanoscale* **2011**, 3, 2801-2818.
- 43) Singh, N.; Karambelkar, A.; Gu, L.; Lin, K.; Miller, J. S.; Chen, C. S.; Sailor, M. J.; Bhatia, S. N. *J. Am. Chem. Soc.* **2011**, ACS ASAP.
- 44) Muhammad, F.; Guo, M.; Qi, W.; Sun, F.; Wang, A.; Guo, Y.; Zhu, G. *J. Am. Chem. Soc.* **2011**, 133, 8778-8781.
- 45) Yuan, L.; Tang, Q.; Yang, D.; Zhang, J. Z.; Zhang, F.; Hu, J. *J. Phys. Chem. C* **2011**, 115, 9926-9932.
- 46) Wan, X.; Zhang, G.; Liu, S. *Macromol. Rapid Commun.* **2011**, 32, 1082-1089.
- 47) Knezevic, N. Z.; Trewyn, B. G.; Lin, V. S. Y. *Chem. Eur. J.* **2011**, 17, 3338-3342, S3338/1-S3338/6.
- 48) Chen, C.; Pu, F.; Huang, Z.; Liu, Z.; Ren, J.; Qu, X. *Nucleic Acids Res.* **2011**, 39, 1638-1644.
- 49) Cheng, S.-H.; Liao, W.-N.; Chen, L.-M.; Lee, C.-H. *J. Mater. Chem.* **2011**, 21, 7130-7137.
- 50) Ma, Y.; Zhou, L.; Zheng, H.; Xing, L.; Li, C.; Cui, J.; Che, S. *J. Mater. Chem.*

- 2011**, 21, 9483-9486.
- 51) Shen, S.-C.; Ng, W. K.; Shi, Z.; Chia, L.; Neoh, K. G.; Tan, R. B. H. *J. Mater. Sci.: Mater. Med.* **2011**, 22, 2283-2292.
  - 52) Shen, J.; He, Q.; Gao, Y.; Shi, J.; Li, Y. *Nanoscale* **2011**, 3, 4314-4322.
  - 53) Huo, Q.; Margolese, D. I.; Ciesla, U.; Feng, P.; Gier, T. E.; Sieger, P.; Leon, R.; Petroff, P. M.; Schueth, F.; Stucky, G. D. *Nature* **1994**, 368, 317-21.
  - 54) Zhao, D.; Huo, Q.; Feng, J.; Chmelka, B. F.; Stucky, G. D. *J. Am. Chem. Soc.* **1998**, 120, 6024-6036.
  - 55) Gruner, S. M. *J. Phys. Chem.* **1989**, 93, 7562-70.
  - 56) Firouzi, A.; Atef, F.; Oertli, A. G.; Stucky, G. D.; Chmelka, B. F. *J. Am. Chem. Soc.* **1997**, 119, 3596-3610.
  - 57) Huo, Q.; Margolese, D. I.; Stucky, G. D. *Chem. Mater.* **1996**, 8, 1147-60.
  - 58) Schumacher, K.; Ravikovitch, P. I.; Du Chesne, A.; Neimark, A. V.; Unger, K. K. *Langmuir* **2000**, 16, 4648-4654.
  - 59) Stöber, W.; Fink, A.; Bohn, E. *J. Colloid Interf. Sci.* **1968**, 26, 62-9.
  - 60) Grün, M.; Lauer, I.; Unger, K. K. *Adv. Mater.* **1997**, 9, 254-257.
  - 61) Nooney, R. I.; Thirunavukkarasu, D.; Chen, Y.; Josephs, R.; Ostafin, A. E. *Chem. Mater.* **2002**, 14, 4721-4728.
  - 62) Lu, F.; Wu, S.-H.; Hung, Y.; Mou, C.-Y. *Small* **2009**, 5, 1408-1413.

- 63) Kim, T.-W.; Chung, P.-W.; Lin, V. S. Y. *Chem. Mater.* **2010**, 22, 5093-5104.
- 64) Cai, Q.; Luo, Z.-S.; Pang, W.-Q.; Fan, Y.-W.; Chen, X.-H.; Cui, F.-Z. *Chem. Mater.* **2001**, 13, 258-263.
- 65) Ikari, K.; Suzuki, K.; Imai, H. *Langmuir* **2006**, 22, 802-806.
- 66) Lu, Y.; Fan, H.; Stump, A.; Ward, T. L.; Rieker, T.; Brinker, C. J. *Nature* **1999**, 398, 223-226.
- 67) Brinker, C. J.; Lu, Y.; Sellinger, A.; Fan, H. *Adv. Mater.* **1999**, 11, 579-585.
- 68) Prakash, A.; McCormick, A. V.; Zachariah, M. R. *Chem. Mater.* **2004**, 16, 1466-1471.
- 69) Lu, J.; Liong, M.; Li, Z.; Zink, J. I.; Tamanoi, F. *Small* **2010**, 6, 1794-1805.
- 70) Apostolovic, B.; Klok, H.-A. *Biomacromolecules* **2008**, 9, 3173-3180.
- 71) Groen, J. C.; Peffer, L. A. A.; Perez-Ramirez, J. *Micropor. Mesopor. Mat.* **2003**, 60, 1-17.
- 72) Howarter, J. A.; Youngblood, J. P. *Langmuir* **2006**, 22, 11142-11147.
- 73) Yoshida, W.; Castro, R. P.; Jou, J.-D.; Cohen, Y. *Langmuir* **2001**, 17, 5882-5888.
- 74) Kallury, K. M. R.; Macdonald, P. M.; Thompson, M. *Langmuir* **1994**, 10, 492-499.

### Chapter 3

- 1) Wan, J.; Meng, X.; Liu, E.; Chen, K. *Nanotechnology* **2010**, 21, 235104.
- 2) Yang, L.-Z.; Chen, Z.-L. *Anal. Lett.* **2011**, 44, 687-697.
- 3) Wang, X.; Ramstroem, O.; Yan, M. *Chem. Commun.* **2011**, 47, 4261-4263.
- 4) Qin, D.; He, X.; Wang, K.; Tan, W. *Biosens. Bioelectron.* **2008**, 24, 626-631.
- 5) Wang, Z.; Miu, T.; Xu, H.; Duan, N.; Ding, X.; Li, S. *J. Microbiol. Methods.* **2010**, 83, 179-184.
- 6) Zhang, X.; Song, C.; Chen, L.; Zhang, K.; Fu, A.; Jin, B.; Zhang, Z.; Yang, K. *Biosens. Bioelectron.* **2011**, 26, 3958-3961.
- 7) Fent, K.; Weisbrod, C. J.; Wirth-Heller, A.; Pieleles, U. *Aquat. Toxicol.* **2010**, 100, 218-228.
- 8) Ow, H.; Larson, D. R.; Srivastava, M.; Baird, B. A.; Webb, W. W.; Wiesner, U. *Nano Lett.* **2005**, 5, 113-117.
- 9) Sokolov, I.; Naik, S. *Small* **2008**, 4, 934-939.
- 10) Ha, S.-W.; Camalier, C. E.; Beck, G. R., Jr.; Lee, J.-K. *Chem. Commun.* **2009**, 2881-2883.
- 11) Herz, E.; Marchincin, T.; Connelly, L.; Bonner, D.; Burns, A.; Switalski, S.; Wiesner, U. *J. Fluoresc.* **2010**, 20, 67-72.
- 12) Roy, S.; Woolley, R.; MacCraith, B. D.; McDonagh, C. *Langmuir* **2010**, 26, 13741-13746.
- 13) Penn, S. G.; He, L.; Natan, M. J. *Curr. Opin. Chem. Biol.* **2003**, 7, 609-615.
- 14) Katz, E.; Willner, I. *Angew. Chem., Int. Ed.* **2004**, 43, 6042-6108.
- 15) Zhong, Wenwan. *Anal. Bioanal. Chem.* **2009**, 394, 47-59.

- 16) Langhals, H.; Esterbauer, A. J. *Chem. Eur. J.* **2009**, 15, 4793-4796.
- 17) Faisal, M.; Hong, Y.; Liu, J.; Yu, Y.; Lam, J. W. Y.; Qin, A.; Lu, P.; Tang, B. Z. *Chem. Eur. J.* **2010**, 16, 4266-4272.
- 18) Xie, C.; Yin, D.; Li, J.; Zhang, L.; Liu, B.; Wu, M. *Nano Biomed. Eng.* **2009**, 1, 39-47.
- 19) Burns, A.; Sengupta, P.; Zedayko, T.; Baird, B.; Wiesner, U. *Small* **2006**, 2, 723-726.
- 20) Verhaegh, N. A. M.; Blaaderen, A. V. *Langmuir* **1994**, 10, 1427-1438.
- 21) Montalti, M.; Prodi, L.; Zaccheroni, N.; Zattoni, A.; Reschiglian, P.; Falini, G. *Langmuir* **2004**, 20, 2989-2991.
- 22) Chen, X.-L.; Zou, J.-L.; Zhao, T.-T.; Li, Z.-B. *J. Fluoresc.* **2007**, 17, 235-241.
- 23) Folling, J.; Polyakova, S.; Belov, V.; van Blaaderen, A.; Bossi Mariano, L.; Hell Stefan, W. *Small* **2008**, 4, 134-142.
- 24) Moro, A. J.; Schmidt, J.; Doussineau, T.; Lapresta-Fernandez, A.; Wegener, J.; Mohr, G. *J. Chem. Commun.* **2011**, 47, 6066-6068.
- 25) Cho, Y.-S.; Yoon, T.-J.; Jang, E.-S.; Soo Hong, K.; Young Lee, S.; Ran Kim, O.; Park, C.; Kim, Y.-J.; Yi, G.-C.; Chang, K. *Cancer Lett.* **2010**, 299, 63-71.
- 26) Wang, Y.; Gildersleeve, J. C.; Basu, A.; Zimmt, M. B. *J. Phys. Chem. B* **2010**, 114, 14487-14494.
- 27) Langhals, H.; Esterbauer, A. J. *Chem. Eur. J.* **2009**, 15, 4793-4796.
- 28) Gao, X.; He, J.; Deng, L.; Cao, H. *Opt. Mater.* **2009**, 31, 1715-1719.
- 29) Yang, H.-H.; Qu, H.-Y.; Lin, P.; Li, S.-H.; Ding, M.-T.; Xu, J.-G. *Analyst* **2003**, 128, 462-466.

- 30) Santra, S.; Zhang, P.; Wang, K.; Tapeç, R.; Tan, W. *Anal. Chem.* **2001**, 73, 4988-4993.
- 31) Lebret, V.; Raehm, L.; Durand, J.-O.; Smaïhi, M.; Gerardin, C.; Nerambourg, N.; Werts, M. H. V.; Blanchard-Desce, M. *Chem. Mater.* **2008**, 20, 2174-2183.
- 32) Sokolov, I.; Kievsky, Y. Y.; Kaszpurenko, J. M. *Small* **2007**, 3, 419-423.
- 33) Godoy-Navajas, J.; Aguilar-Caballos, M.-P.; Gomez-Hens, A. *J. Fluoresc.* **2010**, 20, 171-180.
- 34) Yao, K. S.; Li, S. J.; Tzeng, K. C.; Cheng, T. C.; Chang, C. Y.; Chiu, C. Y.; Liao, C. Y.; Hsu, J. J.; Lin, Z. P. *Adv. Mater. Res.* **2009**, 513-516.
- 35) Cao, A.; Ye, Z.; Cai, Z.; Dong, E.; Yang, X.; Liu, G.; Deng, X.; Wang, Y.; Yang, S.-T.; Wang, H.; Wu, M.; Liu, Y. *Angew. Chem., Int. Ed.* **2010**, 49, 3022-3025.
- 36) Lee, K. G.; Kim, J. C.; Wi, R.; Min, J. S.; Ahn, J. K.; Kim, D. H. *J. Nanosci. Nanotechnol.* **2011**, 11, 686-690.
- 37) Lee, K. G.; Wi, R.; Park, T. J.; Yoon, S. H.; Lee, J.; Lee, S. J.; Kim, D. H. *Chem. Commun.* **2010**, 46, 6374-6376.
- 38) Fowler, C. E.; Mann, S.; Lebeau, B. *Chem. Commun.* **1998**, 1825-1826.
- 39) Lebeau, B.; Fowler, C. E.; Mann, S.; Farcet, C.; Charleux, B.; Sanchez, C. *J. Mater. Chem.* **2000**, 10, 2105-2108.
- 40) Lin, Y.-S.; Tsai, C.-P.; Huang, H.-Y.; Kuo, C.-T.; Hung, Y.; Huang, D.-M.; Chen, Y.-C.; Mou, C.-Y. *Chem. Mater.* **2005**, 17, 4570-4573.
- 41) Slowing, I.; Trewyn, B. G.; Lin, V. S. Y. *J. Am. Chem. Soc.* **2006**, 128, 14792-14793.
- 42) Chhabra, V.; Pillai, V.; Mishra, B. K.; Morrone, A.; Shah, D. O. *Langmuir* **1995**,



- 11, 3307-3311.
- 43) Rocha, L. A.; Caiut, J. M. A.; Messaddeq, Y.; Ribeiro, S. J. L.; Martines, M. A. U.; Freiria, J. d. C.; Dexpert-Ghys, J.; Verelst, M. *Nanotechnology* **2010**, 21, 155603.
  - 44) Kresge, C. T.; Leonowicz, M. E.; Roth, W. J.; Vartuli, J. C.; Beck, J. S. *Nature* **1992**, 359, 710-712.
  - 45) Firouzi, A.; Atef, F.; Oertli, A. G.; Stucky, G. D.; Chmelka, B. F. *J. Am. Chem. Soc.* **1997**, 119, 3596-3610.
  - 46) Nandiyanto, A. B. D.; Kim, S. G.; Iskandar, F.; Okuyama, K. *Micropor. and Mesopor. Mat.* **2009**, 120, 447-453.
  - 47) Muto, S.; Oaki, Y.; Imai, H. *Chem. Lett.* **2006**, 35, 880-881.
  - 48) Willner, I.; Katz, E. *Angew. Chem., Int. Ed.* **2000**, 39, 1181-1218.
  - 49) Katz, E.; Willner, I. *Angew. Chem. Int. Ed.* **2004**, 43, 6042-6108.
  - 50) Zhang, Q.; Huang, R. F.; Guo, L.-H. *Chin. Sci. Bull.* **2009**, 54, 2620-2626.
  - 51) Smith, P. K.; Krohn, R. I.; Hermanson, G. T.; Mallia, A. K.; Gartner, F. H.; Provenzano, M. D.; Fujimoto, E. K.; Goeke, N. M.; Olson, B. J.; Klenk, D. C. *Anal. Biochem.* **1985**, 150, 76-85.
  - 52) Wiechelman, K. J.; Braun, R. D.; Fitzpatrick, J. D. *Anal. Biochem.* **1988**, 175, 231-7.
  - 53) Silin, V.; Weetall, H.; Vanderah, D. J. *J. Colloid Interface Sci.* **1997**, 185, 94-103.
  - 54) Houseman, B. T.; Mrksich, M. *Chemistry and Biology.* **2002**, 9, 443-454.
  - 55) Wolcott, A.; Gerion, D.; Visconte, M.; Sun, J.; Schwartzberg, A.; Chen, S.;

- Zhang, J. Z. *J. Phys. Chem. B* **2006**, 110, 5779-5789.
- 56) Cho, Y.-S.; Yoon, T.-J.; Jang, E.-S.; Soo Hong, K.; Young Lee, S.; Ran Kim, O.;  
Park, C.; Kim, Y.-J.; Yi, G.-C.; Chang, K. *Cancer Lett.* **2010**, 299, 63-71.